# Numerical Methods for the Computation of Invariant Tori

by

Kossi Delali Edoh

M.Sc., Simon Fraser University, Canada, 1992

B.Sc.(Hons), University of Cape Coast, Ghana, 1986

Dip. in Education, University of Cape Coast, Ghana, 1986

A THESIS SUBMITTED IN PARTIAL FULFILLMENT

OF THE REQUIREMENTS FOR THE DEGREE OF

DOCTOR OF PHILOSOPHY

in the Department

of

Mathematics & Statistics



SIMON FRASER UNIVERSITY

August 1995

## APPROVAL

**Name:** Edoh Kossi Delali

**Degree:** Doctor of Philosophy

**Title of thesis:** Numerical Methods for the Computation of Invariant Tori

**Examining Committee:**

*Dr. G.A.C. Graham*
*Chair*

---

*Dr. R.D. Russell*
Senior Supervisor

---

*Dr. M.R. Trummer*

---

*Dr. Tang Tao*

---

*Dr. K. Promislow*

---

*Dr. C.J. Budd*
External Examiner
School of Mathematics
University Walk, Bristol, UK.

**Date Approved:** August 4, 1995

## PARTIAL COPYRIGHT LICENSE

I hereby grant to Simon Fraser University the right to lend my thesis, project or extended essay (the title of which is shown below) to users of the Simon Fraser University Library, and to make partial or single copies only for such users or in response to a request from the library of any other university, or other educational institution, on its own behalf or for one of its users. I further agree that permission for multiple copying of this work for scholarly purposes may be granted by me or the Dean of Graduate Studies. It is understood that copying or publication of this work for financial gain shall not be allowed without my written permission.

**Title of Thesis/Project/Extended Essay**

NUMERICAL METHODS FOR THE COMPUTATION OF INVARIANT TORI

**Author:** _____
(signature)

_____
(name)

JUNE 20, 1995
(date)

# Abstract

Low dimensional invariant manifolds of dynamical systems include fixed points, periodic solutions, connecting orbits and invariant tori. Considerable work has been done on the computation and bifurcation analysis of all these manifolds with the exception of the invariant tori. The importance of computing an invariant tori can be observed in the numerous dynamical systems including dissipative partial differential equations in which they occur. Tori appear mostly in the bifurcation sequence from a steady state to a chaotic solution. One is interested in following the torus to a breakdown and see what it bifurcates to. The results of this study can give us some insight into Ruelle Takens scenario of transition to turbulence in fluid dynamics. In this thesis we investigate the partial differential equation approach to compute invariant tori using orthogonal collocation discretization. We introduce an adaptive grid refinement scheme for several problems in order to study the breakdown of the torus. We also implement the Hadamard graph transform approach which is used in computing attracting invariant manifolds. We find the results of this method to be similar to that of the collocation method. Finally, we did some visualization work using computer graphics to enable us observe the geometry and the flow on the torus, as well as help us in the study of the breakdown.

# Acknowledgements

I want to take this opportunity to express my sincere appreciation to my senior supervisor Prof R.D. Russell for the wonderful help that he has given me and without whom I couldn't have survived this program. His encouragement and relentless support in all aspects of my life has made this possible. I want to thank him for this bold step that he took and wish him the best in his search for knowledge around the globe. I want to thank Dr Manfred Trummer for his concern and encouragement in my trouble times and Dr Weiwei Sun for helping me through part of this thesis.

Finally, my thanks go to Daryl Hepting, Gianne Derks, Maggie Fankboner, Sylvia Holmes, Ana, the department and the University, who in one way or the other helped me to complete this program.

# Dedication

*TO MY PARENTS*

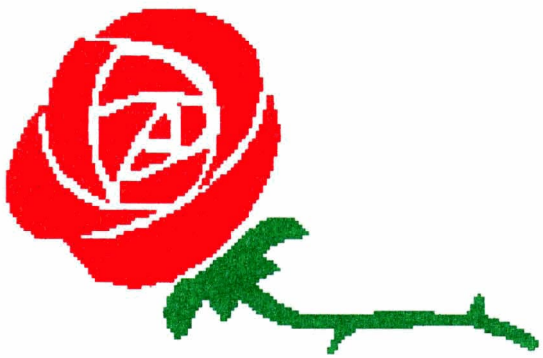

# Contents

# List of Tables

# List of Figures

# Chapter 1

# Introduction

While a relatively complete theory has been developed for linear ordinary differential equations, there is still a considerable work to be done for nonlinear systems of equations. One fairly successful method is the application of perturbation methods to weakly nonlinear problems. Poincaré, in the late 19th century showed that this method does not always yield correct results in all cases, since the series used in such calculations sometimes diverge[GH]. He introduced geometry into the analysis to help in the study of nonlinear differential equations. Until the mid-1970s the work has been mostly in the hands of pure mathematicians. Ruelle and Takens [RT] in 1971 introduced the importance of "strange attractors" in the study of turbulence. This then attracted the attention of scientists to this field of study. This geometric approach is now widely adopted in differential equations and has come to be known as *Dynamical Systems*.

In this thesis we focus on this geometric approach and study the invariant tori. The computation of these objects have received considerable attention in recent years due to diverse and numerous models in which they appear. Some of these models can be found in the models of chemical reactions, population dynamics, electric circuit theory, electrodynamics, fluid dynamics [MJ] etc. These models have dissipative properties and the evolution of their trajectories sometimes settle down to this finite dimensional invariant manifold.

One major unresolved problem in bifurcation theory is that of understanding the transition to chaos in dynamical systems (turbulence in fluids). One of the main sequence of bifurcation leading to chaos begins with one or more bifurcations of steady states, followed by a Hopf bifurcation to a periodic orbit, then a Naimark-Sacker torus bifurcation (or possibly a period doubling cascade), and finally the appearance of a strange attractor

representing a turbulent flow [LW]. By a torus we mean a non chaotic invariant set that is neither a steady state nor a periodic solution. Up to torus bifurcation in the sequence, the computation is straightforward and a fair amount of work has been done, and the sequence well understood. We concentrate on torus bifurcation. However, in completely integrable n-degree-of-freedom Hamiltonian systems, the Kolmogorov-Arnold-Moser(KAM) theorem explains the preservation of these n-frequency quasiperiodic motions under perturbations of the vector field. Various aspects of the collapse of KAM torus are clear enough. Only little has been understood of the collapse of a torus in dissipative non-Hamiltonian systems which leaves the transition to chaos still an important problem in nonlinear science.

Some known results are as follows [KK]:

- Bifurcation from a 2-torus
  (a) Phase instability inducing a phase locking of the torus to a periodic solution.
  (b) Amplitude instability bringing about an oscillatory behavior leading to a fractalization of the torus(chaotic attractor)
  (c) Doubling of the torus.

- Bifurcation from a 3-torus
  Phase locking to a 2-torus.

In most cases a 2-torus is known to have a generic property of phase locking to a periodic solution during its breakdown [T]. We conjecture that an invariant torus bifurcates at the point where one of its radial polar coordinates becomes zero.

There have been several methods for computing an invariant torus of which the two recent popular ones are: the partial differential equation approach and the Hadamard graph transform approach. In the former approach the torus is parameterized in terms of a subset of the variables of the original dynamical system. The condition that the torus must satisfy the original system leads to solving a system of first order hyperbolic partial differential equations with the same principal part and subject to periodic boundary conditions. The later is based on the Hadamard graph transform technique developed in [F]. This approach was implemented by Edoh and Russell [ER] to compute invariant circles for maps as well as the Poincaré of invariant tori.

The partial differential equation approach was introduced by Dieci, et al. [DLR1] in which there were some standard problems: the type of discretization to use, and how to solve the sparse matrix that is obtained after linearization and discretization. Dieci, et al.

used a leap-frog discretization scheme and showed second order convergence for the constant coefficient case. They used compactification to solve the linear system. Similarly, Dieci and Lorenz [DL] used the upwind discretization for the partial differential equation and showed stability and first order convergence for a model linear variable coefficient problem. Dieci and Bader [DB] used a first order discretization, specifically the upwind scheme and iterative methods to solve the linear system. They also used this iterative schemes as smoothers for their multigrid methods. With the multigrid methods, they use as many as $320 \times 320$ grid points for one of the numerical examples. The large number of mesh points used is due to the low order discretization scheme used to discretize the partial differential equations.

In this thesis we use an $O(h^4)$ collocation scheme to discretize the partial differential equations. We discretize our equations at Gauss points with cubic Hermite basis functions. For a model problem where the partial differential equation has constant coefficients, we prove the conditions for the existence, uniqueness and the accuracy of the numerical solution. Our collocation matrix has a sparse block structure, and we adopted the block LU and QR decomposition schemes by Wright [W] to solve the linear system and reduce the storage of our matrix considerably. In some of the numerical examples we introduced an adaptive grid refinement scheme in order to follow the torus breakdown. The results of this method show one successful use of collocation for hyperbolic PDEs.

Our aim of computing an invariant torus is to follow it to its breakdown and determine what it bifurcates to. We realize that in this process the torus naturally loses its smoothness and becomes harder to compute. In the next approach we used the fact that a torus can be defined implicitly from an invariant circle under a Poincaré map. Restricting the computations of the whole torus to this invariant circle will naturally reduce the difficulty in the computations.

In our second approach therefore we use a discrete version of the graph transform technique used in the analytical work of Fenichel [F]. We perform a finite sequence of graph transform iterations, where each graph transform itself requires the solution of finitely many ODE boundary value problems (BVP). Each BVP is independent of the others and thus, they can be solved concurrently. We restrict the Hadamard graph transform technique to the Poincaré cross-section of the torus. This technique has the advantage of been used to compute invariant circles of known discrete maps. We show how it relates to the Poincaré map approach of van Veldhuizen[VV1]. We sketch a prove for the convergence and the uniqueness of the computed solution of this scheme when our functions are smooth enough.

In solving the BVP we use simple and multiple shooting with Newton and bisection methods.

In the two schemes described above we used the method of simple continuation with a bifurcation parameter to follow the computation of the torus to its breakdown. In some problems one can determine the initial approximation of the torus at the point of its Naimark-Sacker torus bifurcation. From our experience, we have seen that the Hadamard graph transform method has a larger domain of convergence than the collocation method. The relative difference in the results of both methods is about 0.01%. Our collocation method has a higher order of accuracy and more expensive than the Hadamard graph transform method. The Hadamard graph transform iteration takes on the average one graph transform step to converge when the invariant circle is exponentially attracting.

In chapter two we state some properties of invariant manifolds and look at the bifurcation sequence

$$\textit{Steady State} \rightarrow \textit{periodic solution} \rightarrow \textit{invariant torus} \rightarrow \textit{chaos}.$$

We focus on the background theory of the formation, dynamics, breakdown and the computations of invariant tori. We study how to extend this idea to higher and infinite dimensions. We did computations on some properties of the torus like the Lyapunov exponents. In chapter three we describe the Hadamard graph transform approach, and give sketch of a convergence proof for this numerical scheme, then illustrate the efficiency of the scheme with some examples. In chapter four we talk about the collocation algorithm and give a convergence proof for a model problem. We apply the scheme to some examples. In chapter five we do a comparison between the HGT and the PDE approaches. We also give some description of the visualization tools that has been used in the study of the breakdown of the torus.

Finally, in chapter six we give some concluding remarks and our plans for future work.

# Chapter 2

# Background theory

In the theory of dynamical systems, many problems of interest require understanding the dynamical features that evolve over long-time periods. The dynamical systems we consider in this thesis have parameters which change the qualitative structure of their solution branches as the parameters are varied. These changes are called *bifurcations* and the parameter values at which they occur are called *bifurcation values*. Some of these dynamical systems are dissipative and their large time dynamics can exhibit a variety of behavior ranging from simple steady states, through moderately complex periodic or quasi-periodic behavior, to extremely complex chaotic behavior as the bifurcation parameter is varied. Thus, an accurate numerical approximation of evolution equations over long-time intervals is of importance. Much work has been been done on these long term steady states except the invariant torus and so our attention will be focussed on this steady state.

In this chapter, we give background theories related to the dynamics and the computation of invariant manifolds specifically invariant tori for finite and infinite dimensional systems. We study the stability of solution branches for maps and flows by looking at the center manifold and the normal form theorems. They form the essential components of bifurcation theory. These theorems provide two systematic methods of simplifying equations and are used to reduce the dimension of the system of equation and their forms. We also look at the computational methods for some dynamical properties of invariant tori such as the Lyapunov exponents. Most of this work is from the books of Guckenheimer and Holmes [GH], Marsden and McCracken [MM] and Wiggins [Wi].

## 2.1 Systems of ordinary differential equations

In this section we discuss invariant tori for finite dimensional maps and flows. Some of this material will be used for infinite dimension systems too. We start by considering a system of ordinary differential equations (ODEs) of the form

$$\frac{d\mathbf{x}}{dt} = f(\mathbf{x}), \tag{2.1}$$

where $t \in \mathbb{R}, \mathbf{x}, \in \mathbb{R}^n$ and $f : \mathbb{R}^n \to \mathbb{R}^n$. We also consider the discrete map

$$\mathbf{x}_{k+1} = F(\mathbf{x}_k), \qquad k \in \aleph, \tag{2.2}$$

where $\mathbf{x_k} \in \mathbb{R}^n$ and $F : \mathbb{R}^n \to \mathbb{R}^n$. It is assumed that the map $F : \mathbb{R}^n \to \mathbb{R}^n$ is a diffeomorphism. By diffeomorphism we mean:

**Definition 2.1.1** *Let $U \in \mathbb{R}^n$ and $V \in \mathbb{R}^n$. Then a smooth map $F : U \to V$ is a diffeomorphism if it is invertible and if the inverse map $F : V \to U$ is also smooth.*

The system (2.1) is called an autonomous system. If the vector field $f$ is time dependent, then (2.1) is called a non-autonomous system. The non-autonomous systems that we use in this thesis have vector fields that are time periodic with non-trivial period $T > 0$. They can always be converted to autonomous systems. Let $\mathbf{x}_0$ be in the open set $\Omega$ in the $\mathbb{R}^n$, then, there is a unique solution $\mathbf{x}(t)$ of (2.1) with $\mathbf{x}(0) = \mathbf{x}_0$ if $f$ is Lipshitz continuous at $\mathbf{x}_0$.

**Definition 2.1.2** *A flow on $\Omega$ is a collection of maps $\phi_t : \Omega \to \Omega$ defined for all $t \in \mathbb{R}$ such that*

1. *$\phi_0$ is the identity,*
2. *$\phi_{t+s} = \phi_t \circ \phi_s$ for all $t,\ s \in \mathbb{R}$,*
3. *$\frac{d}{dt}\phi_t(\mathbf{x}) = f(\phi_t(\mathbf{x}))$ for all $\mathbf{x} \in \Omega, t \in \mathbb{R}$.*

*A semiflow on $\Omega$ is a collection of maps $\phi_t : \Omega \to \Omega$ defined for all $t \geq 0$, and satisfying the 3 conditions above for $t, s \geq 0$.*

For a fixed $t_0$, the map $\phi_{t_0}$ is assumed to be a diffeomorphism if $f$ is smooth enough. For the map (2.2), the solution $\{\mathbf{x}_k, k = 1, \ldots, \infty\}$ is called its orbit.

### 2.1.1 Stability

In our computations we use a simple continuation method in a bifurcation parameter to follow the torus computations to its breakdown. In the process we perturb the bifurcation parameter variable in the vector field or the diffeomorphism and use the known computed torus to determine the unknown torus of the perturbed system. Let the initial and the boundary conditions be called the data for the system (2.1) or (2.2). In numerical computations the system and its data that is actually being simulated is a perturbed version of the system described in the state equation (2.1) or (2.2).

We are then interested in determining when changes in the data and perturbations in the vector field or the diffeomorphism do change the qualitative structure of the solution of equation (2.1) and (2.2). We give some definitions that determine when a solution is locally stable and a vector field $f$ (diffeomorphism $F$) is structurally stable. We also determine when a set is said to be invariant with respect to (2.1) or (2.2).

#### Stability of solutions

A solution is said to be stable if a nearby solution remains nearby under the dynamical system. They are the ones that can be easily observed experimentally. In that case a small perturbation in the data does not change the qualitative structure of the solution. In this section we try to examine the conditions under which a solution is said to be stable.

Suppose the initial condition is perturbed then, in a flow, the following definition suffices to show whether a solution is stable or not.

**Definition 2.1.3** *(Lyapunov Stability) The solution* $\bar{\mathbf{x}}(t)$ *of (2.1) is said to be stable (or Lyapunov stable) if, given* $\epsilon > 0$, *there exists a* $\delta = \delta(\epsilon) > 0$ *such that for any other solution* $\mathbf{y}(t)$ *of (2.1) satisfying* $||\bar{\mathbf{x}}(t_0) - \mathbf{y}(t_0)|| < \delta$, *then* $||\bar{\mathbf{x}}(t) - \mathbf{y}(t)|| < \epsilon$ *for* $t > t_0, t_0 \in \boldsymbol{R}$. *The solution* $\bar{\mathbf{x}}(t)$ *is said to be unstable if it is not stable. Moreover,* $\bar{\mathbf{x}}(t)$ *is asymptotically stable if it is stable and*

$$\lim_{t\to\infty} ||\bar{\mathbf{x}}(t) - \mathbf{y}(t)|| = 0. \tag{2.3}$$

Analogous definition for diffeomorphisms can be suitably defined by substituting $\bar{\mathbf{x}}^n, \bar{\mathbf{x}}^0$, $\mathbf{y}^n$ *and* $\mathbf{y}^0$ for $\bar{\mathbf{x}}(t), \bar{\mathbf{x}}(t_0), \mathbf{y}(t)$ *and* $\mathbf{y}(t_0)$ respectively.

### Stability of vector fields and diffeomorphisms

We now consider the stability of vector fields and diffeomorphisms. First we define what we mean by a perturbation of size $\epsilon$ of vector functions.

**Definition 2.1.4** *If $f \in C^r(\boldsymbol{R}^n), r, k$ are two positive integers, $k \leq r$ and $\epsilon > 0$, then $g$ is a $C^k$ perturbation of size $\epsilon$ if there is a compact set $K \subset \boldsymbol{R}^n$ such that $f = g$ on the set $\boldsymbol{R}^n - K$ and for all $(i_1, \ldots, i_n)$ with $i_1 + \cdots + i_n = i \leq k$ we have $|(\partial^i / \partial x_1^{i_1} \cdots \partial x_n^{i_n}(f-g)| < \epsilon$.*

If the conditions in the definition above are satisfied then the two vector fields or diffeomorphisms are said to be "close" to the other. The two properties that determine this "closeness" are topological equivalence and structural stability. The equivalence of two diffeomorphisms can be defined as follows:

**Definition 2.1.5** *Two $C^r$ maps $F$ and $G$ are $C^k$ equivalent or $C^k$ conjugate ($k \leq r$) if there exists a $C^k$ homeomorphism $h$ such that $h \circ F = G \circ h$. $C^0$ equivalence is called topological equivalence.*

This implies that $h$ takes an orbit $\{F^n(\mathbf{x})\}$ to an orbit $\{G^n(\mathbf{x})\}$ and the other way round. A similar definition is given below for vector fields.

**Definition 2.1.6** *Two $C^r$ vector fields, $f$, $g$ are said to be $C^k$ equivalent ($k \leq r$) if there exists a $C^k$ diffeomorphism $h$ which takes orbits $\phi_t^f(\mathbf{x})$ of $f$ to orbits $\phi_t^g(\mathbf{x})$ of $g$, preserving senses (orientation) but not necessarily parametrization by time. If $h$ does preserve parametrization by time, then it is called a conjugacy.*

The case where $h$ is a conjugacy, then for any $\mathbf{x}$ and $t_1$ there is a $t_2$ such that $h(\phi_{t_1}^f(\mathbf{x})) = \phi_{t_2}^g(h(\mathbf{x}))$. We now give the definition of structural stability:

**Definition 2.1.7** *A map $F \in C^r(\boldsymbol{R}^n)$ (vector field $f$) is structurally stable if there is an $\epsilon > 0$ such that all $C^1, \epsilon$-perturbations of $F$ ($f$) are topologically equivalent to $F$ ($f$).*

If a system is structurally stable, then any sufficiently close system has the same qualitative behavior. Structural stability is not a *generic property*, that is, we can find structural unstable system which remain unstable under small perturbations and even continually change their topological equivalence class as we perturb them [GH]. One may therefore define the structural stability for a class of systems one is dealing with. By that we mean

**Definition 2.1.8** *suppose the vector field $f_1 g, (F, G)$ belong to some topological space $B$. Then the flows $f$ and $g$ ($F$ and $G$) are said to be structurally stable if there is a neighborhood $N(f)$ of $f$ ($N(F)$ of $F$) in $B$ such that $f$ and $g$ ($F$ and $G$) are equivalent for every $g$ ($G$) in $N(f)$ ($N(F)$).*

### 2.1.2 Invariant sets

We are interested in the long term dynamics of equations (2.1) and (2.2). The long term solutions sometimes lie on invariant subsets like the invariant tori of $\mathbf{R}^n$. In this section we determine the properties that these invariant sets possess and give some examples.

The orbit $\eta(p)$ of (2.1) through p is defined as

$$\eta(p) := \{\mathbf{x} : \mathbf{x} = \phi_t(p), -\infty < t < \infty\}, \tag{2.4}$$

Note that if q belongs to $\eta(p)$ then $\eta(q) = \eta(p)$. The $\omega$-limit set of an orbit $\eta$ of (2.1) is the set of points in $\mathbf{R}^n$ which are approached along $\eta$ with increasing time. To be precise,

**Definition 2.1.9** *a point $q$ belongs to the $\omega$-limit set or positive limit set $\omega(\eta)$ of an orbit $\eta$ if there exists a sequence of real numbers $\{t_k\}, t_k \to \infty$ such that $\phi_{t_k}(p) \to q$ as $k \to \infty$. Or*

$$\omega(\eta) = \bigcap_{p \in \eta} \overline{\eta^+(p)} = \bigcap_{\tau \in (-\infty, \infty)} \overline{\bigcup_{t \geq \tau} \phi_t(p)}, \tag{2.5}$$

*where $\eta^+(p)$ is $\eta(p)$ for which $t$ is increasing in time and bar the denotes closure.*

*A point $q$ belongs to the $\alpha$- limit set or negative limit set $\alpha(\eta)$ if there is a sequence of real numbers $\{t_k\}$, $t_k \to -\infty$ as $k \to \infty$ such that $\phi_{t_k}(p) \to q$ as $k \to \infty$. So*

$$\alpha(\eta) = \bigcap_{p \in \eta} \overline{\eta^-(p)} = \bigcap_{\tau \in (-\infty, \infty)} \overline{\bigcup_{t \leq \tau} \phi_t(p)}. \tag{2.6}$$

*where $\eta^-(p)$ is $\eta(p)$ for which $t$ is decreasing in time.*

**Definition 2.1.10** *The set $M \subset \boldsymbol{R}^n$ is called an invariant set of (2.1) if for any $p \in M$, the solution $\phi_t(p)$ of (2.1) through $p$ belongs to $M$ for $t \in (-\infty, \infty)$. $M$ is called positively (negatively) invariant if for each $p \in M$, $\phi_t(p) \in M$ for $t \geq 0$ ($t \leq 0$). A similar definition for maps is as follows: An invariant set $M$ for a map (2.2) on $\boldsymbol{R}^n$ is a set $M \subset \boldsymbol{R}^n$ such that $F^k(\mathbf{x}) \in M$, for $\mathbf{x} \in M$ for all $k \geq 1$.*

A set $M \subset \mathbf{R}^n$ is called a *minimal* set of (2.1) if it is non-empty, closed and invariant and has no proper subset which possesses these properties. We are interested in the long-term behavior of the dynamics on the invariant sets, so we focus on nonwandering sets. A point $p$ is nonwandering for the flow $\phi_t$ (resp. the map $F$) if for any neighborhood $U$ of p, there exists arbitrarily large t (resp. $k > 0$) such that $\phi_t(U) \cap U \neq \emptyset$ (resp. $F^k(U) \cap U \neq \emptyset$). A nonwandering set $M$ is a collection of such points. A closed invariant set $M$ is said to be indecomposable if for every pair of points $\mathbf{x}, \mathbf{y}$ in $M$ and every $\epsilon > 0$, there are $\mathbf{x}, \mathbf{x_0}, \mathbf{x_1}, \ldots, \mathbf{x_k} = \mathbf{y}$ and $t_1, \ldots, t_k \geq 1$ such that the distance from $\phi_{t_i}(\mathbf{x}_{i-1})$ to $\mathbf{x}_i$ is smaller than $\epsilon$. Some examples of invariant sets are given below.

### Equilibrium Points

We define an equilibrium point $\mathbf{x}_{eq}$ of (2.1) as the constant solution

$$\mathbf{x}_{eq} = \phi_t(\mathbf{x}_{eq}) \tag{2.7}$$

for all $t$. At this point $f(\mathbf{x}_{eq}) = 0$. An equilibrium point is the simplest nonwandering set of a dynamical system (2.1). The local stability of a nonlinear problem can be determined from definition (2.1.2) if we take $\bar{\mathbf{x}}(t_0) = \mathbf{x}_{eq}$. A second approach to determine the stability of a fixed point is to consider the eigenvalues of the Jacobian matrix of $f$ at the equilibrium point $\mathbf{x}_{eq}$. If all the eigenvalues of the Jacobian at the equilibrium point, $Df(\mathbf{x}_{eq})$ have non-zero real part then the equilibrium point is said to be hyperbolic. Let the eigenvalues of $Df(\mathbf{x}_{eq})$ be given by $\lambda_i, \ \ i = 1, \ldots, n$. If $Re(\lambda_i) < 0$ for all $i$ then $\mathbf{x}_{eq}$ is asymptotically stable. If $Re(\lambda_i) > 0$ for some $i$ then $\mathbf{x}_{eq}$ is unstable.

For the map (2.2), an equivalent definition of a fixed point denoted by $\mathbf{x}^*$ is given by

$$\mathbf{x}^* = F(\mathbf{x}^*). \tag{2.8}$$

Denote the eigenvalues of $DF(\mathbf{x}^*)$ by $m_i, i = 1, \ldots, n$. The fixed point is said to be hyperbolic if $|m_i| \neq 1$ for all $i$. For hyperbolic fixed points, if $|m_i| < 1$ for all $i$ then $\mathbf{x}^*$ is asymptotically stable. If $|m_i| > 1$ for some $i$ then $\mathbf{x}^*$ is unstable. A necessary condition for flows or maps to be structurally stable is that all fixed points must be hyperbolic.

### Periodic Solutions

A solution of (2.1) through the point $\mathbf{x_0}$ is said to be periodic with period $T$ if

$$\phi_t(\mathbf{x_0}) = \phi_{t+T}(\mathbf{x_0}) \tag{2.9}$$

for all $t \in \mathbf{R}$. With exception of equilibrium points, periodic solutions are the simplest invariant sets. Denote the periodic solution by $\gamma$. The stability of a periodic solution is determined by its characteristic exponents or Floquet multipliers. Let $\gamma$ be a periodic solution of (2.1) which satisfies the condition $\phi_t(\mathbf{x}^*) = \phi_{t+T}(\mathbf{x}^*)$ for any point $\mathbf{x}$ on the orbit of $\gamma$. The linearized system around $\gamma$ is given by

$$\dot{\xi} = Df(\phi_t(\mathbf{x}^*))\xi, \qquad t \in \mathbf{R}, \tag{2.10}$$

where $Df(\phi_t(x^*))$ is the Jacobian matrix of $f$. The fundamental matrix solution of this $T$-periodic system can be written as

$$\Phi(t) = Z(t)e^{tR}, \qquad Z(t) = Z(t+T) \tag{2.11}$$

where $\Phi, Z$, and $R$ are $n \times n$ matrices. If $\Phi(0) = Z(0) = I$ then

$$\Phi(T) = Z(T)e^{TR} = Z(0)e^{TR} = e^{TR}.$$

The eigenvalues of the constant matrix $e^{TR}$ are called the Floquet multipliers and the eigenvalues of $R$ are called the characteristic exponents. The stability of the periodic solution can often be determined from the characteristic exponents or Floquet multipliers. A periodic solution is said to be stable if all the Floquet multipliers $\mu_i$ satisfy $\mu_i < 1$ except for one with value equal to 1. A periodic solution is unstable if there are some that have absolute value greater than 1. An important map associated with a periodic solution is the Poincaré map

### The Poincaré map

The Poincaré map is the discrete time system associated with an ordinary differential equation (ODE). The construction of which results in the elimination of at least one of the variables of the system and thereby reducing the study of the ODE to a lower dimensional system. Some of the advantages include: Numerically computed Poincaré maps in lower dimensional system (say dimension $n \leq 4$) provide insight to the global dynamics of the system [Wi]. Many concepts in ordinary differential equations can be easily stated in the associated Poincaré map. A simple case is the the orbital stability of a periodic orbit of an ODE which can be reduced to the stability of a fixed point of the Poincaré map.

The construction of the Poincaré map requires some knowledge of the geometric structure of the phase space of the ordinary differential equation. We are interested in the Poincaré

map of a system in which the phase space of the ODE includes periodic variables like in invariant tori.

### Poincaré map near a periodic orbit

Consider the system

$$\dot{\mathbf{x}} = f(\mathbf{x}) \qquad \mathbf{x} \in \mathbb{R}^n, \qquad f : V \to \mathbb{R}^n, \tag{2.12}$$

where $f$ is $C^\infty$. Let $\mathbf{x}_0 \in \mathbb{R}^n$ be a point on the periodic solution of (2.12) (with period $T$) and let $\sum$ be an $n-1$ dimensional surface transverse to the vector field at this point. By transverse we mean the vector dot product $f(\mathbf{x}).n(\mathbf{x}) \neq 0$ where $n(\mathbf{x})$ is the normal to $\sum$ at $\mathbf{x}$. Let $V \subset \sum$ with $\mathbf{x} \in V$. The Poincaré map denoted $P$ is given by

$$P : V \to \sum \tag{2.13}$$

with

$$\mathbf{x} \to \phi(\tau(\mathbf{x}), \mathbf{x}) \in \sum \tag{2.14}$$

where $\tau(\mathbf{x})$ is the time of first return such that $\tau(\mathbf{x}_0) = T$ and $P(\mathbf{x}_0) = \mathbf{x}_0$. If $f$ is time periodic and of a fixed period $2\pi/\omega = T$ then we have

$$\dot{\mathbf{x}} = f(\mathbf{x}, t) \tag{2.15}$$

which reduces to

$$\begin{aligned} \dot{\mathbf{x}} &= f(\mathbf{x}, \theta) \\ \dot{\theta} &= \omega. \end{aligned} \tag{2.16}$$

The Poincaré cross-section in this case is given by

$$\sum = \{(\mathbf{x}, \theta) \in \mathbb{R}^n \times S^1 | _{\theta=\theta_0}\}. \tag{2.17}$$

If one can find a corresponding Poincaré map $P$ associated with the periodic solution then the eigenvalues of $DP(\mathbf{x}^*)$ are the characteristic multipliers.

For the map (2.2) the orbit $\mathbf{x}^0 \in \mathbb{R}^n$ is said to be periodic of period $k > 0$ if $F^k(\mathbf{x}^0) = \mathbf{x}^0$.

### Invariant Tori

A quasi-periodic solution can be expressed as a sum of periodic functions

$$\mathbf{x}(t) = \sum_{i=1}^{n} \phi_i(t) \tag{2.18}$$

where $\phi_i$ has minimum period $T_i$ and base frequency $f_i := 1/T_i$.

**Example 2.1.1**

$$x(t) = cos(2\pi t) + cos(2\pi\sqrt{2}t).$$

A quasi-periodic solution with $p$ base frequencies is called $p$-periodic where $p$ is an integer. The solution can be considered to lie on a p-torus. To determine the nature of a flow on say a 2-torus we can use the concept of rotation numbers.

In biological science this phenomenom arises in the study of suspensions of cells, each of which is oscillatory, with cell-cell communication occuring indirectly via release of substances into the surrounding medium. As a second example, consider a system of two pendulums of lengths $l_1 = l_2 = 1$ and masses $m_1 = m_2 = 1$ in a gravitational field with acceleration due to gravity $g = 1$. Suppose the masses are connected by a weightless spring whose length equal to the distance between the points of suspension. Using Newton's law on the coupled nonlinear oscillators, we arrive at

$$\ddot{q_1} = -q_1 + \frac{(q_1)^3}{6} + \delta(q_2 - q_1)$$

$$\ddot{q_2} = -q_2 + \frac{(q_2)^3}{6} + \delta(q_1 - q_2).$$

Making the substitution $c_1^i = q_i,\ c_2^i = \dot{q}_i,\ i = 1, 2.$ we get the system of equations

$$\begin{pmatrix} \dot{c}_1^1 \\ \dot{c}_2^1 \\ \dot{c}_1^2 \\ \dot{c}_2^2 \end{pmatrix} = \begin{pmatrix} c_2^1 \\ -c_1^1 + \frac{(c_1^1)^3}{6} + \delta(c_1^2 - c_1^1) \\ c_2^2 \\ -c_1^2 + \frac{(c_1^2)^3}{6} + \delta(c_1^1 - c_1^2) \end{pmatrix}.$$

Using a change of variables (see [ADO] for details), we arrive at a special case ($\alpha = 0, \beta = 1$) of the canonical nonlinear oscillator with coupling

$$\begin{aligned} \dot{x_1} &= \alpha_1 x_1 + \beta_1 y_1 - (x_1^2 + y_1^2)x_1 - \delta(x_1 + y_1 - x_2 - y_2) \\ \dot{y_1} &= \alpha_1 y_1 - \beta_1 x_1 - (x_1^2 + y_1^2)y_1 - \delta(x_1 + y_1 - x_2 - y_2) \\ \dot{x_2} &= \alpha_2 x_2 + \beta_2 y_2 - (x_2^2 + y_2^2)x_2 + \delta(x_1 + y_1 - x_2 - y_2) \\ \dot{y_2} &= \alpha_2 y_2 - \beta_2 x_2 - (x_2^2 + y_2^2)y_2 + \delta(x_1 + y_1 - x_2 - y_2) \end{aligned}$$

where $\alpha$ and $\beta$ are constants. To determine the nature of a flow on say a 2-torus we can use the concept of rotation numbers.

**Rotation Numbers**

A rotation number determines a typical orbit structure on an invariant circle. We will focus

on the Poincaré map of a two-torus for a $C^2$ vector field. In this case it characterizes the qualitative features of a sufficiently differentiable flow on the torus. It is the average rotation of a point $\mathbf{x}_0$ on the invariant circle under the iterates of the Poincaré map of the torus.

**Definition 2.1.11** *Let $P$ be the Poincaré map of $\dot{\boldsymbol{\theta}} = f(\theta_1, \theta_2)$ for which $f(\theta_1, \theta_2)$ is $2\pi$-periodic in both $\theta_1, \theta_2$ and defined by $P(\bar{\theta}_2) := \phi_T(0, \bar{\theta}_2)$. The rotation number of $P$, denoted by $\rho(P)$ is defined as*

$$\rho(P) := \lim_{|n| \to +\infty} P^n(\theta_2)$$

*where $n$ is an integer.*

**Theorem 2.1.1** *If the rotation number $\rho(P)$ is well-defined, that is if the limit exists and is independent of the initial point $\theta_2$ and furthermore, if $P$ is a $C^2$ map, then*

- *$\rho(P)$ is rational if and only if $P$ has a periodic orbit of some period.*
- *$\rho(P)$ is irrational if and only if every orbit of $P$ is dense on $S^1$.*

In general let $P_\lambda : S^1 \to S^1$ be the Poincaré map of

$$\dot{\mathbf{x}} = f(\lambda, \mathbf{x}), \ \lambda \in \mathbf{R}, \ \mathbf{x} \in \mathbf{R}^n \tag{2.19}$$

where $f$ is a $C^2$ 2-periodic vector field.

**Theorem 2.1.2** *The rotation number $\rho(P_\lambda)$ is a continuous function of the parameter $\lambda$.*

Rotation numbers can also be used to determine the structural stability of a torus.

**Theorem 2.1.3** *Consider the flow on the torus of a $C^2$ differential equation (2.19) that is 2-periodic in $\mathbf{x}$, where $\lambda$ is a (vector) parameter. For a fixed value $\lambda = \bar{\lambda}$, the differential equation*

$$\dot{\mathbf{x}} = f(\bar{\lambda}, \mathbf{x})$$

*is structurally stable if and only if it has rational rotation number and all of its periodic orbits are hyperbolic.*

### Strange Attractor

A bounded steady state behavior that is not an equilibrium point, periodic solution, or a quasi-periodic solution is called a strange attractor, specifically,

**Definition 2.1.12** *A strange attractor is a geometrical object in the state space to which trajectories are attracted.*

An attractor for a flow $\phi_t$ for PDEs is a subset $X$ (generally assumed compact) of the state space with the following properties:

- X is invariant: $\phi_t(X) = X$.
- X has a shrinking neighborhood $V$, i.e., there is an open set $V \supset X$ with $\phi_t(V) \subset V$ for $t > 0$ and such that $\phi_t(V)$ shrinks down to $X$ as $t \longrightarrow \infty$.
- The flow $\phi_t$ on $X$ is recurrent (no part of $X$ is transient) and indecomposable (cannot be split into two closed nonoverlapping invariant pieces).
- $\phi_t$ admits a finite number $X_1, X_2, \ldots, X_n$ of attractors, each of which is closed, bounded, and of zero volume.
- The set of initial states of $\mathbf{x}$ which are not in the basin of attraction of any one of the $X$'s has zero volume.
- the set of initial states $\mathbf{x}$ which are in the basin of attraction of any one of the $X_i$'s has volume zero.

The result is that there are finitely many attractors whose basins of attraction fill up essentially all of the state space for a well behaved $\phi_t$.

### Lyapunov Exponents

Lyapunov exponents are generalizations of characteristic multipliers, and they can be used to determine the stability of the invariant sets discussed so far. For a continuous-time system, the definition is as follows:

**Definition 2.1.13** *Let $\mathbf{x}_0 \in \boldsymbol{R}^n$ and $m_1(t), m_2(t), \ldots, m_n(t)$ be the eigenvalues of $\Phi_t(x_0)$, the fundamental solution matrix of (2.1). The Lyapunov exponents of $\mathbf{x}_0$ are*

$$\lambda_i := \lim_{t \to \infty} \frac{1}{t} ln|m_i(t)|, \qquad i = 1, \ldots, n. \tag{2.20}$$

*whenever the limit exists.*

For discrete systems, we have the following equivalent definition:

**Definition 2.1.14** *Let $\{\mathbf{x}_k\}_{k=0}^{\infty}$ be the orbit of an n-dimensional, discrete system (2.2). If $m_1(k), \ldots, m_n(k)$ are the eigenvalues of $DF^k(\mathbf{x}_0)$ then the Lyapunov numbers of $\mathbf{x}_0$ are*

$$m_i := \lim_{k \to \infty} |m_i(k)|^{1/k}, \qquad i = 1, \ldots, n, \tag{2.21}$$

*whenever the limit exists.*

Let $\lambda_1, \lambda_2, \ldots, \lambda_n$ be the Lyapunov exponents of the system (2.1). An equilibrium point $\mathbf{x}_0$ of (2.1) is stable if its Lyapunov exponents satisfy the condition $\lambda_n \leq \lambda_{n-1} \leq, \ldots, \leq \lambda_1 < 0$. A periodic solution is stable if $\lambda_1 = 0$ and $\lambda_n \leq, \ldots \leq \lambda_2 < 0$ and a $k$-periodic solution is stable if $\lambda_1, \ldots, \lambda_k = 0$ and $\lambda_n, \leq \ldots, \leq \lambda_{k+1} < 0$. Finally, a chaotic attractor has at least one of its Lyapunov exponents equal zero and satisfies $\sum_{i=1}^{n} \lambda_i < 0$.

### Computing Lyapunov exponents

In this section we give a modified version of a method essentially due to Karlheinz et al. [KUW] to compute the Lyapunov exponents of a continuous dynamical systems. This scheme is formulated in terms of the singular value decomposition (SVD) of matrices. Consider the nonlinear equation (2.1) with the variational equation

$$\dot{\Phi} = J\Phi \tag{2.22}$$

where $J = Df(\mathbf{x})$. Let the SVD matrix decomposition of $\Phi$ be

$$\Phi = U\Lambda V^T. \tag{2.23}$$

To avoid exponentially increasing and decreasing diagonal elements of $\Lambda$ define

$$E := \ln(\Lambda) = diag(\varepsilon_1, \varepsilon_2, \ldots, \varepsilon_n) \tag{2.24}$$

where $\varepsilon_i = ln(\sigma_i)$, and $\sigma_i$'s are the singular values of $\Phi$. Taking the derivative of (2.24) we get

$$\dot{E} = \Lambda^{-1}\dot{\Lambda} = \Lambda^{-1}\dot{U}^T U\Lambda + \Lambda^{-1}U^T JU\Lambda + V^T\dot{V}. \tag{2.25}$$

Since V is orthogonal

$$V^T\dot{V} + \dot{V}^T V = 0$$

and to eliminate it in equation (2.25) we compute the sum

$$\begin{aligned} 2\dot{E} &= \dot{E} + \dot{E}^T \\ &= \Lambda^{-1}\dot{U}^T U\Lambda + \Lambda U^T \dot{U}\Lambda^{-1} + \Lambda^{-1}U^T JU\Lambda + \Lambda U^T JU\Lambda^{-1} + V^T\dot{V} + \dot{V}V^T \\ &= \Lambda^{-1}\dot{U}^T U\Lambda + \Lambda U^T \dot{U}\Lambda^{-1} + \Lambda^{-1}U^T JU\Lambda + \Lambda U^T JU\Lambda^{-1}. \end{aligned} \tag{2.26}$$

Now let

$$\begin{cases} W := U^T\dot{U} = -\dot{U}^T U & \text{since U is orthogonal, then W is skew symmetric,} \\ X := -\Lambda^{-1}W\Lambda & \Longrightarrow X_{ij} = -W_{ij}\frac{\sigma_j}{\sigma_i},\ W_{ii} = X_{ii} = 0, \\ Y := U^T JU, & \\ Z := \Lambda^{-1}Y\Lambda & \Longrightarrow Z_{ij} = Y_{ij}\frac{\sigma_j}{\sigma_i}. \end{cases} \tag{2.27}$$

Equation (2.26) then reduces to

$$2\dot{E} = X + X^T + Z + Z^T. \tag{2.28}$$

The diagonal elements of (2.28) satisfy

$$\dot{e}_i = Y_{ii}, \tag{2.29}$$

while the off diagonal elements of (2.28) satisfy

$$\begin{aligned} 0 &= X_{ij} + X_{ji} + Z_{ij} + Z_{ji} \\ &= -W_{ij}\frac{\sigma_j}{\sigma_i} - W_{ji}\frac{\sigma_i}{\sigma_j} + Y_{ij}\frac{\sigma_j}{\sigma_i} + Y_{ji}\frac{\sigma_i}{\sigma_j} \qquad i > j. \end{aligned} \tag{2.30}$$

In order to reduce exponentially growing quantities in equation (2.30), we multiply through by $\frac{\sigma_i}{\sigma_j}$ and replace the critical terms $(\frac{\sigma_i}{\sigma_j})^2$ by $h_{ij} = exp(2(\varepsilon_i - \varepsilon_j))$, $(1 \le i, j \le n, i \ne j)$ to get

$$A = \begin{cases} \frac{C_{ji}+C_{ij}h_{ji}}{h_{ji}-1}, & i < j, \\ 0 & i = j, \\ \frac{C_{ij}+C_{ji}h_{ij}}{1-h_{ji}}, & i > j. \end{cases} \tag{2.31}$$

The differential equation for $U$ is given by

$$\dot{U} = UA. \tag{2.32}$$

To get the values $\varepsilon_i$ we solve the ODE system of equations

$$\begin{cases} \dot{\mathbf{x}} = f(\mathbf{x}) \\ \dot{\varepsilon} = C_{ii} \\ \dot{U} = UA \end{cases} \tag{2.33}$$

with the initial values $\mathbf{x}(0), \varepsilon(0), U(0)$. These conditions are chosen such that

| $\delta$ | *lyapunov1* | *lyapunov2* | *lyapunov3* | *lyapunov4* |
|---|---|---|---|---|
| 0.00 | 0.000100 | -1.999800 | -0.003930 | -2.001679 |
| 0.10 | -0.000109 | -2.000281 | -0.192574 | -2.208840 |
| 0.20 | -0.000124 | -2.000381 | -0.370761 | -2.430562 |
| 0.25 | -0.000130 | -2.000421 | -0.455481 | -2.545806 |
| 0.255 | 0.076127 | -1.926750 | -0.406823 | -2.497818 |
| 0.260 | 0.077678 | -1.925419 | -0.414101 | -2.508424 |
| 0.262 | 0.078300 | -1.924886 | -0.417007 | -2.512671 |

Table 2.1: The results for different values of $\delta$ at t = 10000.

1. $\mathbf{x}(0)$ is not an equilibrium point.

2. the matrix $U(0) = I$.

3. $\varepsilon_i(0) \neq \varepsilon_j(0), i \neq, n.$

The system (2.33) is solved from $t = 0$ to $t = t_{out}$ for several times such that $t_{out} \leq 0.1$. The matrix $U$ is reorthogonalize each time. The integration is done to a total time of about $T = 10000$ depending on the problem. The Lyapunov exponents are then given by

$$\lambda_i := \lim_{t\to\infty} \frac{ln(\sigma_i)}{t} = \lim_{t\to\infty} \frac{\varepsilon_i}{t}. \tag{2.34}$$

The scheme was applied to the example below.

**Example 2.1.2** *A system of two-coupled oscillators,*

$$\begin{pmatrix} \dot{x_1} \\ \dot{y_1} \\ \dot{x_2} \\ \dot{y_2} \end{pmatrix} = \begin{pmatrix} \alpha_1 x_1 + \beta_1 y_1 - (x_1^2 + y_1^2)x_1 - \delta(x_1 + y_1 - x_2 - y_2) \\ \alpha_1 y_1 - \beta_1 x_1 - (x_1^2 + y_1^2)y_1 - \delta(x_1 + y_1 - x_2 - y_2) \\ \alpha_2 x_2 + \beta_2 y_2 - (x_2^2 + y_2^2)x_2 + \delta(x_1 + y_1 - x_2 - y_2) \\ \alpha_2 y_2 - \beta_2 x_2 - (x_2^2 + y_2^2)y_2 + \delta(x_1 + y_1 - x_2 - y_2) \end{pmatrix}, \tag{2.35}$$

In table (2.1) the two zero and two negative Lyapunov exponents of the system when $\delta < 0.1$ indicates the existence of an attracting invariant torus in this region. As $\delta$ increases

one of the zero Lyapunov exponents becomes less than zero. This shows the existence of an attracting periodic solution among the solution of the system and possibly the disappearance of the invariant 2-torus.

### Dimension of limit sets

In some cases the torus been computed may bifurcate to a strange attractor during the continuation process. One then needs reliable methods to determine when this happens. To distinguish between a chaotic attractor and other limit sets we introduce the concept of fractal dimension. A fractal dimension is that dimension that allows non-integer values. A set that has a non-integer dimension is called a fractal. A strange attractor has almost always a non-integer dimension while the dimension of a non-chaotic attractor is always an integer.

In differential topology, the dimension of a manifold is the dimension of the Euclidean space that the manifold resembles locally. Let $N(\delta)$ be the minimum number of volume elements needed to cover $A$ where each volume element is of diameter $\delta$. Now we are ready to define the dimension of $A$.

The **Capacity dimension** of $A$ which is defined by

$$D_{cap} := \lim_{\delta \to 0} \frac{\ln N(\delta)}{\ln(1/\delta)} \tag{2.36}$$

Another common dimension is the

**Lyapunov dimension** of $A$ given as follows:

Let $\lambda_i, i = 1, \ldots, n$ be the Lyapunov exponents of an attractor $A$ with $\lambda_1 \geq \lambda_2, \geq, \cdots, \geq \lambda_n$ and $j$ be the largest integer such that $\lambda_1 + \cdots + \lambda_{j+1} \geq 0$, then

$$D_L := j + \frac{\lambda_1 + \cdots + \lambda_j}{|\lambda_{j+1}|}. \tag{2.37}$$

If no such $j$ exists, $D_L$ is defined to be 0. For a 3-dimensional system with chaotics attractor with Lyapunov exponents $\lambda_+ > 0 > \lambda_-$, $D_L = 2 + \frac{\lambda_+}{|\lambda_-|}$. In this case $D_L$ satisfies the condition $2 < D_L < 3$.

## 2.1.3 Integral manifolds

We define an integral manifold as follows:

**Definition 2.1.15** *A manifold $S$ in $(\mathbf{x},t)-$'space of a system of ODEs*

$$\dot{\mathbf{x}} = f(\mathbf{x},t)$$

*is an integral manifold if for any point $P$ in $S$ the solution $\mathbf{x}(t)$ of the equation through $P$ is such that $(\mathbf{x}(t),t)$ is in $S$ for all $t$ in the domain of definition of the solution $\mathbf{x}(t)$.*

There has been some early attempts to represent an invariant torus as an integral manifold [HJ] and [CH]. In this section, we present some fundamentals results of the integral representation of an invariant torus. We describe three methods to determine integral manifolds two of which have been numerically investigated in chapters three and four.

The idea here is that we have an invariant $\omega_0$-periodic solution $\mathbf{u}(t)$ given by

$$\Gamma = \{\mathbf{x} \in \mathbf{R}^n : \mathbf{x} = \mathbf{u}(\theta), \qquad 0 \leq \theta \leq \omega\}$$

for the system

$$\dot{\mathbf{x}} = f(\mathbf{x}). \tag{2.38}$$

We want to determine the integral manifold for a perturbed equation

$$\dot{\mathbf{x}} = f(\mathbf{x}) + f^*(\mathbf{x},t) \tag{2.39}$$

where $f^*(\mathbf{x},t)$ is periodic in $t$. Let's assume that $n-1$ of the characteristic exponents of the linear variational equation of (2.38) given by

$$\dot{\mathbf{y}} = \frac{\partial f(\mathbf{u}(t))}{\partial x}\mathbf{y} \tag{2.40}$$

have negative real parts.

The integral manifold of (2.38), given by

$$S = \{(t,\mathbf{x}) : \mathbf{x} = u(\theta),\ 0 \leq \theta \leq \omega_0,\ -\infty < t < \infty\}, \tag{2.41}$$

in the $(t,\mathbf{x})$-space is asymptotically stable. Introducing the coordinate transformation [HJ]

$$\mathbf{x} = \mathbf{u}(\theta) + Z(\theta)\rho \tag{2.42}$$

where $\mathbf{x} \in \mathbf{R}^n$ and $\rho \in \mathbf{R}^{n-1}$, we have in the neighborhood of S the solutions of (2.38) given by

$$\begin{pmatrix} \dot{\theta} \\ \dot{\rho} \end{pmatrix} = \begin{pmatrix} 1 + \Theta(\theta,\rho) \\ A(\theta)\rho + R(\theta,\rho) \end{pmatrix} \tag{2.43}$$

where $\Theta(\theta,\rho) = O(|\theta|)$, $R(\theta,\rho) = O(|\rho|^2)$ as $|\rho| \to 0$. From Floquet theory, a fundamental system of solutions of the linear equation is of the form

$$P(\theta)e^{B\theta}, \qquad \text{with} \qquad P(\theta+\omega_0) = P(\theta). \tag{2.44}$$

If we let $\rho(t) = P(\theta)bfz(t)$ with $\dot{\theta} = 1 + O(|\rho|)$ we get an equivalent system

$$\begin{pmatrix} \dot{\theta} \\ \dot{\mathbf{z}} \end{pmatrix} = \begin{pmatrix} 1+\Theta_1(\theta,z) \\ B\mathbf{z} + R(\theta,\mathbf{z}) \end{pmatrix} \tag{2.45}$$

where $\Theta_1(\theta,\mathbf{z}) = O(|\mathbf{z}|)$, $Z(\theta,\mathbf{z}) = O(|\mathbf{z}|^2)$ as $|\mathbf{z}| \to 0$ with the eigenvalues of $B$ having negative real parts. From [H] there is a positive definite matrix $C = \int_0^\infty e^{B't}e^{Bt}dt$ such that any solution of the linear system

$$\dot{\mathbf{z}} = B\mathbf{z} \tag{2.46}$$

with initial value on the ellipsoid $\mathbf{z}'C\mathbf{z} > 0$ must enter the ellipsoid as $t \to \infty$. For $c_0 > 0$ sufficiently small, such that any solution of (2.46) with initial value on the set

$$U_s(c) = \{(t,\mathbf{x}) : \mathbf{x} = \mathbf{u}(\theta) + Z(\theta)P(\theta)\mathbf{z},\ 0 \le \theta \le \omega_0,\ \mathbf{z}'C\mathbf{z} = c\ \ , -\infty < t < \infty\}, \tag{2.47}$$

and $0 < c \le c_0$ must enter this set for $t \to \infty$.

Consider the perturbed system

$$\dot{\mathbf{x}} = f(\mathbf{x}) + \epsilon f^*(t,\mathbf{x}) \tag{2.48}$$

where $f^*(t,\mathbf{x})$ is bounded in the neighborhood of $S$ then for a given $c > 0$ and $\epsilon$ sufficiently small, the solution will still enter $U_s(c)$ as time increases and we will expect some kind of integral surface inside $U_s(c)$. We describe three methods essentially due to Hale [H], two of which we have implemented in chapters three and four.

**Method 1 (Levinson-Deliberto)**

If the perturbation term is $\omega_1$-periodic in $t$, then we can define an annulus map as follows: Let $U_{s\tau}(c) := U_s(c) \cap \{t = \tau\}$ be the cross section $U_s(c)$ at $t = \tau$. If $\mathbf{x}(t,\mathbf{x}_0)$ is the solution of the perturbed equation (2.48), then the Poincaré map $\mathbf{x}(\tau,.)$ is a map of $U_{s0}(c)$ into the interior of

$$U_{s\tau}(c) = U_{s0}(c). \tag{2.49}$$

With the strong stability properties of the curve $\Gamma$, one would expect that $\exists$ a curve $\Gamma_{\epsilon\tau}$ such that $\mathbf{x}(\tau,\Gamma_{\epsilon\tau}) = \Gamma_{\epsilon\tau}$ is an invariant curve with $\Gamma_{0\tau} = \Gamma$. If $\tau = \omega_0$ then $\mathbf{x}(k\omega_1,\Gamma_{\epsilon\omega_1})$

gives an invariant torus. This idea has been developed further in chapter three with the idea of Hadamard graph transform to compute invariant circles and tori.

**Method 2 (Sacker)**

In his approach he considered the equation

$$\begin{aligned} \dot{\theta} &= \omega(0) + \Theta(\theta, \mathbf{x}) \\ \dot{\mathbf{x}} &= A(\theta)\mathbf{x} + F(\theta, \mathbf{x}) \end{aligned} \tag{2.50}$$

where $\theta \in \mathbb{R}^p, \mathbf{x} \in \mathbb{R}^q$ and all functions are periodic in $\theta$ of period $\omega$. If

$$S = \{(\theta, \mathbf{x}) : \mathbf{x} = R(\theta),\ \ R(\theta + \omega) = R(\theta),\ \theta \in \mathbb{R}^p\} \tag{2.51}$$

is to be an integral manifold of (2.50) then $R$ must satisfy the PDE

$$\frac{\partial R}{\partial \theta}[\omega(\theta), \Theta(\theta, R)] - A(\theta)R = F(\theta, R), \qquad R(\theta + \omega) = R(\theta). \tag{2.52}$$

In the case where $\omega, A$ are independent of $\theta$, one can integrate along characteristics to compute an invariant torus of (2.50). When $\omega(\theta) = 0$, then the solution will not in general be as smooth as the coefficients in the equation. Since the usual iteration procedures involve a loss of derivatives, Sacker [S] introduces a Laplacian term and solves

$$\mu \triangle_\theta R + \frac{\partial R}{\partial \theta}[\omega(\theta) + \Theta(\theta, R)] - A(\theta)R = F(\theta, R), \qquad R(\theta + \omega) = R(\theta) \tag{2.53}$$

for $\mu$ small and where $\triangle_\theta$ is the Laplacian operator. The solutions thus have as many derivatives as possible. In chapter four we solve the PDE (2.52) using collocation discretization but did not introduce the Laplacian term in (2.53).

**Method 3 (Krylov-Bogoliubou-Mitropolski)**

Krylov et al. defined a mapping of cylinders to cylinders such that the fixed points are the integral manifolds of (2.38), which for $\epsilon = 0$ reduce to $S$. These methods do not use any perturbation properties of the dependence of the perturbation terms upon $t$.

Consider the equations

$$\begin{aligned} \dot{\theta} &= 1 + \Theta(t, \theta, \rho, \epsilon) \\ \dot{\rho} &= A\rho + R(t, \theta, \rho, \epsilon) \end{aligned} \tag{2.54}$$

where $A$ is an $\in \mathbb{R}^{n \times n}$ constant matrix, $\Theta(t, \theta, 0, 0) = R(t, \theta, 0, 0) = \frac{\partial R(t,\theta,0,0)}{\partial \rho} = 0$. We seek integral manifolds of (2.54) of the form $\rho = f(t, \theta, \epsilon)$ with $f(t, \theta, \epsilon)$ lying in a small neighborhood of $\rho = 0$ for $\epsilon$ small.

If $\theta(t, t_0, \theta_0, f)$ is the solution of the equation

$$\dot{\theta} = 1 + \Theta(t, \theta, f(t, \theta, \epsilon), \epsilon), \qquad \theta(t_0, t_0, \theta_0, f) = \theta_0 \tag{2.55}$$

and using the variation of constants formula, and the fact that $e^{A(t-t_0)} \to 0$ for $t \to \infty$ we have

$$\rho = f(t_0, \theta_0, \epsilon) = \int_{-\infty}^{t_0} e^{A(t_0-s)} R(s, \theta(s, t_0, \theta_0, f), f(s, \theta(s, t_0, \theta_0, f), \epsilon) ds \ [H]. \tag{2.56}$$

The integral manifolds are the fixed points of the RHS of equation (2.56) above for a given $f$.

### 2.1.4 Center manifolds

The center manifold theorem provides a means for systematically reducing the dimension of the state space of a system without losing any information about the stability of a specific solution of the system. The center manifold theorem can be used to analyze a bifurcation of a given type.

**Theorem 2.1.4** *(Center Manifold Theorem for Flows). Let $f$ be a $C^r$ vector field on $R^n$ vanishing at the origin ($f(0) = 0$) and let $A = Df(0)$. Divide the spectrum of $A$ into three parts, $\sigma_s, \sigma_c, \sigma_u$ with*

$$Re\lambda \begin{cases} < 0 & if \ \lambda \in \sigma_s, \\ = 0 & if \ \lambda \in \sigma_c, \\ > 0 & if \ \lambda \in \sigma_u. \end{cases} \tag{2.57}$$

*Let the(generalized) eigenspaces of $\sigma_s, \sigma_c$, and $\sigma_u$ be $E^s, E^c$, and $E^u$, respectively. Then there exist $C^r$ stable and unstable invariant manifolds $W^u$ and $W^s$ tangent to $E^u$and $E^s$ at 0 and a $C^{r-1}$ center manifold $W^c$ tangent to $E^c$ at 0. The manifolds $W^u, W^s$ and $W^c$are all invariant for the flow of $f$. The stable and unstable manifolds are unique, but $W^c$ need not be [GH].*

Assume that the unstable manifold of the system (2.1) is empty and let the system be transformed to the form:

$$\begin{pmatrix} \dot{\mathbf{x}} \\ \dot{\mathbf{y}} \end{pmatrix} = \begin{pmatrix} B\mathbf{x} + f(\mathbf{x}, \mathbf{y}) \\ C\mathbf{y} + g(\mathbf{x}, \mathbf{y}) \end{pmatrix} \tag{2.58}$$

$$(\mathbf{x}, \mathbf{y}) \in \mathbf{R}^c \times \mathbf{R}^s.$$

Assume that the matrices $B$ and $C$ have eigenvalues with zero and negative real parts respectively and that $f, g, Df$ and $Dg$ vanish at the origin. The following is the definition of the center manifold.

**Definition 2.1.16** *An invariant manifold is called a center manifold for (2.58) at* $\mathbf{0}$ *if it can locally be represented as follows:*

$$W^c(0) = \{(\mathbf{x}, \mathbf{y}) \in \boldsymbol{R}^c \times \boldsymbol{R}^s \,|\mathbf{y} = h(\mathbf{x}),\ |\mathbf{x}| < \delta,\ h(0) = Dh(0) = 0\} \tag{2.59}$$

*for* $\delta$ *sufficiently small.*

The solution to

$$\dot{\mathbf{u}} = B\mathbf{u} + f(\mathbf{u}, h(\mathbf{u})) \tag{2.60}$$

provides a good approximation to the flow (2.58) close to the origin. The next theorem illustrates the relationship between the flow (2.58) and (2.60).

**Theorem 2.1.5** *(1) Suppose the zero solution of (2.60) is stable (asymptotically stable) (unstable); then the zero solution of (2.58) is also stable (asymptotically stable) (unstable). (2) Suppose the zero solution of (2.60) is stable. Then if* $(\mathbf{x}(t), \mathbf{y}(t))$ *is a solution of (2.58) with* $(\mathbf{x}(0), \mathbf{y}(0))$ *sufficiently small, there is a solution* $\mathbf{u}(t)$ *of (2.60) such that as* $t \longrightarrow \infty$

$$\begin{aligned} \mathbf{x}(t) &= \mathbf{u}(t) + O(e^{-\gamma t}), \\ \mathbf{y}(t) &= h(\mathbf{u}(t)) + O(e^{-\gamma t}), \end{aligned} \tag{2.61}$$

*where* $\gamma > 0$ *is a constant.*

To determine $h(\mathbf{x})$, we substitute it into the equation

$$\dot{\mathbf{y}} = C\mathbf{y} + g(\mathbf{x}, \mathbf{y}) \tag{2.62}$$

to get

$$\dot{\mathbf{y}} = Dh(\mathbf{x})[B\mathbf{x} + f(\mathbf{x}, h(\mathbf{x}))] = Ch(\mathbf{x}) + g(\mathbf{x}, h(\mathbf{x})). \tag{2.63}$$

We then solve the quasi-linear partial differential equation

$$N(h(\mathbf{x})) = D \qquad\qquad h(\mathbf{x})[B\mathbf{x} + f(\mathbf{x}, h(\mathbf{x})] - Ch(\mathbf{x}) - g(\mathbf{x}, h(\mathbf{x})) = 0 \tag{2.64}$$

with the initial conditions $h(0) = Dh(0) = 0$ for $h(\mathbf{x})$. The problem (2.64) may be difficult to solve for $h(\mathbf{x})$ so we approximate it to a desired accuracy by using its power series expansion. In this thesis we try two numerical methods to approximate the center manifold when it is a 2-torus.

Since most of the systems we deal with contain a bifurcation parameter, we will extend the determination of center manifolds to these type of systems. We consider the extension of the system (2.58) to the form

$$\begin{pmatrix} \dot{\mathbf{x}} \\ \dot{\mathbf{y}} \\ \dot{\lambda} \end{pmatrix} = \begin{pmatrix} B_\lambda \mathbf{x} + f(\lambda, \mathbf{x}, \mathbf{y}) \\ C_\lambda \mathbf{y} + g(\lambda, \mathbf{x}, \mathbf{y}) \\ 0 \end{pmatrix} \qquad \text{where } \lambda \in \mathbf{R}^p \tag{2.65}$$

The center manifold of such a system is given by

$$\begin{aligned} W^c_{loc}(0) = \{(\lambda, \mathbf{x}, \mathbf{y}) \in \mathbf{R}^p \times \mathbf{R}^c \times \mathbf{R}^s \,|y = h(\lambda, \mathbf{x}),\ |\mathbf{x}| < \delta, \\ |\lambda| < \bar{\delta}, \qquad h(0,0) = Dh(0,0) = 0\} \end{aligned} \tag{2.66}$$

for $\delta$ and $\bar{\delta}$ sufficiently small. Similarly the center manifold $h(\lambda, x)$ can be determined from the quasi-linear PDE

$$\begin{aligned} N(h(\lambda, \mathbf{x})) = D_{\mathbf{x}} h(\lambda, \mathbf{x})[B\mathbf{x} + f(\lambda, \mathbf{x}, h(\lambda, \mathbf{x}))] \\ -Ch(\lambda, \mathbf{x}) - g(\lambda, \mathbf{x}, h(\lambda, \mathbf{x})) = 0 \end{aligned} \tag{2.67}$$

The last case we consider is when our system includes an unstable manifold. Consider the equation

$$\begin{pmatrix} \dot{\mathbf{x}} \\ \dot{\mathbf{y}} \\ \dot{\mathbf{z}} \end{pmatrix} = \begin{pmatrix} B_\lambda \mathbf{x} + f(\lambda, \mathbf{x}, \mathbf{y}, \mathbf{z}) \\ C_\lambda \mathbf{y} + g(\lambda, \mathbf{x}, \mathbf{y}, \mathbf{z}) \\ E_\lambda \mathbf{z} + h(\lambda, \mathbf{x}, \mathbf{y}, \mathbf{z}) \end{pmatrix} \qquad z \in R^{\mathbf{u}} \tag{2.68}$$

where

$$f,\ g,\ h,\ Df,\ Dg, \text{ and } Dh$$

vanish at the origin. The matrix $E$ has eigenvalues with positive real parts. The local center manifold can be represented by

$$\begin{aligned} W^c(0) = \{(\mathbf{x}, \mathbf{y}, \mathbf{z}) \in \mathbf{R}^c \times \mathbf{R}^s \times \mathbf{R}^u \ |\mathbf{y} = h_1(\mathbf{x}), \mathbf{z} = h_2(\mathbf{x}), \\ h_i(0) = 0,\ \ Dh_i(0) = 0, i = 1, 2\} \end{aligned} \tag{2.69}$$

for $\mathbf{x}$ sufficiently small. The vector field restricted to the center manifold is given by

$$\dot{\mathbf{u}} = B\mathbf{u} + f(\mathbf{u}, h_1(\mathbf{u}), h_2(\mathbf{u})), \qquad \mathbf{u} \in \mathbf{R}^c \tag{2.70}$$

The center manifolds $h_1(\mathbf{x}), h_2(\mathbf{x})$ can be determined from the system of quasi-linear partial differential equations

$$\begin{aligned} N_1(h(\mathbf{x})) &= Dh(\mathbf{x})[C\mathbf{x} + f(\mathbf{x}, h(\mathbf{x})] - Eh(\mathbf{x}) - g(\mathbf{x}, h(\mathbf{x})) = 0. \\ N_2(h(\mathbf{x})) &= Dh(\mathbf{x})[C\mathbf{x} + f(\mathbf{x}, h(\mathbf{x})] - Eh(\mathbf{x}) - g(\mathbf{x}, h(\mathbf{x})) = 0. \end{aligned} \tag{2.71}$$

Similar results exists for maps.

### 2.1.5 Normal forms

A normal form is one of the tools that provides a basis for the study of the qualitative properties of flows near a bifurcation point. At this point on the center manifold one can find coordinate transformations which simplify the analytic expression of the vector field. The normal form is a way of eliminating the nonlinearity in a system. The resulting vector fields are called the normal forms. The dimension of an infinite system can be reduced using the center manifold theory and the resulting system simplified using the normal form theorem. For example an invariant torus in an infinite dimension can be determined using this idea of reducing the dimension with center manifold theory and simplifying the resulting system using the normal form theorem. We start with the normal forms at a fixed point and do a coordinate transformation in the neighborhood of this fixed point. Note that if the fixed point is not at the origin a translation can be done to translate it to the origin. Consider the vector field

$$\dot{\mathbf{x}} = f(\mathbf{x}), \qquad \mathbf{x} \in \mathbb{R}^n \tag{2.72}$$

with $f \in C^r$, $r \geq 4$ and with a fixed point at the origin. Linearize (2.72) about the fixed point to get

$$\dot{\mathbf{x}} = Df(0)\mathbf{x} + \tilde{F}(\mathbf{x}) \tag{2.73}$$

and then make the transformation

$$\mathbf{x} = T\mathbf{v} \tag{2.74}$$

to convert $Df(0)$ to the Jordan canonical form $J$. Using this transformation equation (2.73) becomes

$$\dot{\mathbf{v}} = J\mathbf{v} + F(\mathbf{v}). \tag{2.75}$$

Expanding the non-linear term $F(\mathbf{v})$ in (2.75) we get

$$\dot{\mathbf{v}} = J\mathbf{v} + F_2(\mathbf{v}) + F_3(\mathbf{v}) + F_4(\mathbf{v}) + \cdots + F_{r-1}(\mathbf{v}) + O(|\mathbf{v}|^r) \tag{2.76}$$

where $F_i(\mathbf{v})$ represents the *ith* order term. To simplify the term $F_2(\mathbf{v})$ we introduce the transformation

$$\mathbf{v} = \mathbf{y} + h_2(\mathbf{y}) \tag{2.77}$$

where $h_2(\mathbf{y})$ is second order in $\mathbf{y}$. Equation (2.76) then reduces to

$$\begin{aligned}\dot{\mathbf{v}} &= (I + Dh_2(\mathbf{y}))\dot{\mathbf{y}} \\ &= J\mathbf{y} + Jh_2(\mathbf{y}) + F_2(\mathbf{y} + h_2(\mathbf{y})) + F_3(\mathbf{y} + h_2(\mathbf{y})) + \cdots \\ &+F_{r-1}(\mathbf{y} + h_2(\mathbf{y})) + O(|\mathbf{y}|^r).\end{aligned} \tag{2.78}$$

Each nonlinear term

$$F_k(\mathbf{y} + h_2(\mathbf{y})) \qquad 2 \leq k \leq r-1$$

can be expressed in the form

$$F_k(\mathbf{y} + h_2(\mathbf{y})) = F_k(\mathbf{y}) + O(|\mathbf{y}|^{k+1}) + \cdots + O(|\mathbf{y}|^{2k}). \tag{2.79}$$

Equation (2.78) becomes

$$(I + Dh_2(\mathbf{y}))\dot{\mathbf{y}} = J\mathbf{y} + Jh_2(\mathbf{y}) + F_2(\mathbf{y}) + \tilde{F}_3(\mathbf{y}) + \cdots + \tilde{F}_{r-1}(\mathbf{y}) + O(|\mathbf{y}|^r), \tag{2.80}$$

where $\tilde{F}_i(\mathbf{x})$ are the modified order $O(|\mathbf{y}|^k)$ terms. For small $\mathbf{y}$ the matrix $(I + Dh_2(\mathbf{y}))^{-1}$ exists and can be represented in a series expansion

$$(I + Dh_2(\mathbf{y}))^{-1} = I - Dh_2(\mathbf{y}) + O(|\mathbf{y}|^2). \tag{2.81}$$

Substituting this in (2.79) we get

$$\begin{aligned}\dot{\mathbf{y}} &= J\mathbf{y} + Jh_2(\mathbf{y}) - Dh_2(\mathbf{y})J\mathbf{y} + F_2(\mathbf{y}) \\ &+\tilde{F}_3(\mathbf{y}) + \cdots + \tilde{F}_{r-1}(\mathbf{y}) + O(|\mathbf{y}|^r).\end{aligned} \tag{2.82}$$

We simplify equation (2.82) by looking for $h_2(\mathbf{y})$ such that

$$Dh_2(\mathbf{y})J\mathbf{y} - Jh_2(\mathbf{y}) = F_2(\mathbf{y}).$$

One can solve this by choosing an appropriate linear vector space with a linear operator defined on it [W]. We describe the new problem in this linear space. Define the basis of the linear vector space as $(\mathbf{x}_1, \mathbf{x}_2, \ldots, \mathbf{x}_n) \in \mathbf{R}^n$. Let $(\mathbf{y}_1, \mathbf{y}_2, \ldots, \mathbf{y}_n)$ be the coordinates with respect to this basis and let the coefficients of this basis be monomials of degree $k$.

$$(\mathbf{y}_1^{m_1}\mathbf{y}_2^{m_2}\cdots\mathbf{y}_n^{m_n})x_i \qquad \sum_{j=1}^{n} m_j = k \tag{2.83}$$

Denote the set of vector-valued monomials of degree $k$ by $H_k$. Define the linear operator

$$L_J(h_k(\mathbf{y})) \equiv [h_k(\mathbf{y}), J\mathbf{y}] = -(Dh_k(\mathbf{y})J\mathbf{y} - Jh_k(\mathbf{y})). \tag{2.84}$$

We choose a complement $G_k$ for $L_J(h_k(\mathbf{y}))$ in $H_k$ so that

$$H_k = L_J(H_k) \otimes G_k. \tag{2.85}$$

**Theorem 2.1.6** *Normal Form Theorem.*

*By a sequence of analytic coordinate changes, equation (2.76) can be transformed into*

$$\dot{\mathbf{y}} = J\mathbf{y} + F_2^r(\mathbf{y}) + \cdots + F_{r-1}^r(\mathbf{y}) + O(|y|^r), \tag{2.86}$$

*where $F_k^r(\mathbf{y}) \in G_k$, $2 \leq k \leq r-1$, and $G_k$ is a space complimentary to $L_J(H_k)$. Equation (2.86) is said to be in a normal form*

**Example 2.1.3** *Let*

$$J = \begin{pmatrix} 1 & 1 \\ 0 & 1 \end{pmatrix},$$

*and a standard basis in $\mathbf{R}^2$ given by*

$$\begin{pmatrix} 1 \\ 0 \end{pmatrix}, \begin{pmatrix} 0 \\ 1 \end{pmatrix}.$$

*Let*

$$H_2(y) = span\left\{ \begin{pmatrix} x^2 \\ 0 \end{pmatrix}, \begin{pmatrix} xy \\ 0 \end{pmatrix}, \begin{pmatrix} y^2 \\ 0 \end{pmatrix}, \begin{pmatrix} 0 \\ x^2 \end{pmatrix}, \begin{pmatrix} 0 \\ xy \end{pmatrix}, \begin{pmatrix} 0 \\ y^2 \end{pmatrix} \right\} \tag{2.87}$$

*and*

$$L_J(H_2) = span\left\{ \begin{pmatrix} -x^2 - 2xy \\ 0 \end{pmatrix}, \begin{pmatrix} -y^2 - xy \\ 0 \end{pmatrix}, \begin{pmatrix} -y^2 \\ 0 \end{pmatrix}, \begin{pmatrix} x^2 \\ -x^2 - 2xy \end{pmatrix}, \begin{pmatrix} xy \\ -y^2 - xy \end{pmatrix}, \begin{pmatrix} y^2 \\ -y^2 \end{pmatrix} \right\}. \tag{2.88}$$

*The matrix associated with $L_J$ is*

$$\begin{pmatrix} -1 & 0 & 0 & 1 & 0 & 0 \\ -2 & -1 & 0 & 0 & 1 & 0 \\ 0 & -1 & -1 & 0 & 0 & 1 \\ 0 & 0 & 0 & -1 & 0 & 0 \\ 0 & 0 & 0 & -2 & -1 & 0 \\ 0 & 0 & 1 & 0 & -1 & -1 \end{pmatrix}. \tag{2.89}$$

*Finding two vectors that are orthogonal to the columns vectors above, one can then determine the normal form.*

The normal forms for vector fields with parameters and also maps can be determined in a similar way.

### 2.1.6 Local bifurcations

We have seen in the introductory chapter that one of the main sequence of bifurcations leading to an invariant torus begins with one or more bifurcations of steady states, followed by a Hopf bifurcation to periodic orbit, then a Naimark-Sacker torus bifurcation. ie.

$$\textit{Steady State} \rightarrow \textit{periodic solution} \rightarrow \textit{invariant torus.}$$

In this section we analyze the Hopf bifurcation theorem which plays a major role in this bifurcation sequence for both flows and maps.

If the Jacobian $Df$ of (2.1) at the point $\mathbf{x}_0$ has eigenvalues with zero real parts then it is said to be nonhyperbolic. Let equation

$$\dot{\mathbf{x}} = f(\mathbf{x}, \lambda) \tag{2.90}$$

have a hyperbolic equilibrium point for $\lambda = 0$ at $\mathbf{x}_0 = 0$. As $\lambda$ varies the implicit function theorem can be used to determine the flow near this point as a smooth function of $\lambda$.

A term that is used to describe bifurcation is co-dimension. The co-dimension of an $l-$dimensional submanifold of $n$-space is $(n - l)$. A transversal intersection of manifolds in $n-$dimensional space is one for which the tangent spaces of the intersecting manifolds span $n-$dimensional space. Let $\sum_1$ and $\sum_2$ be two submanifolds. Then the co-dimension of $\sum_1 \cap \sum_2$ is the sum of the co-dimensions of $\sum_1$ and $\sum_2$ if their intersection is transversal. The co-dimension of a bifurcation is the smallest dimension of a parameter space which contains the bifurcation in a persistent way (It is the number of degenerate conditions that are satisfied at a particular bifurcation). Below are some examples of the normal forms of co-dimension one bifurcations of equilibrium points.

#### Saddle-node bifurcation

$$f(x, \lambda) = \lambda - x^2.$$

**Transcritical bifurcation**

$$f(x,\lambda) = \lambda x - x^2.$$

**Pitchfork bifurcation**

$$f(x,\lambda) = \lambda x - x^3.$$

**Hopf bifurcation**

Let $a, b, c, d$ and $\omega$ be some constants. Then the normal form of a Hopf bifurcation is given by

$$f(x,y,\lambda) = \begin{pmatrix} (d\lambda + a(x^2+y^2))x - (\omega + c\lambda + b(x^2+y^2))y \\ (\omega + c\lambda + b(x^2+y^2))x + (d\lambda + a(x^2+y^2))y \end{pmatrix}. \tag{2.91}$$

In polar coordinates this reduces to

$$\begin{aligned} \dot{r} &= (d\lambda + ar^2)r \\ \dot{\theta} &= (\omega + c\lambda + br^2). \end{aligned} \tag{2.92}$$

**Theorem 2.1.7** *Hopf bifurcation for flows*

*Suppose that the system* $\dot{\mathbf{x}} = f(\mathbf{x},\lambda)$, $\mathbf{x} \in \boldsymbol{R}^n$, $\lambda \in \boldsymbol{R}$ *has an equilibrium* $(\mathbf{x}_0, \lambda_0)$ *at which the following properties are satisfied:*

- *(a)* $D_{\mathbf{x}} f(\mathbf{x}_0, \lambda_0,)$ *has a simple pair of pure imaginary eigenvalues and no other eigenvalues with zero real parts.*

*Then (a) implies that there is a smooth curve of equilibra* $(\mathbf{x}(\lambda),\lambda)$ *with* $\mathbf{x}(\lambda_0) = \mathbf{x}_0$. *The eigenvalues* $\mu(\lambda)$, $\bar{\mu}(\lambda)$ *of* $D_{\mathbf{x}} f(\mathbf{x}(\lambda),\lambda_0)$ *which are imaginary at* $\lambda = \lambda_0$ *vary smoothly with* $\lambda$. *If, moreover,*

$$\frac{d}{d\lambda}(\boldsymbol{R}e\mu(\lambda))|_{\lambda=\lambda_0} = d \neq 0. \tag{2.93}$$

*then there is a unique three-dimensional center manifold passing through* $(\mathbf{x}_0, \lambda_0)$ *in* $\boldsymbol{R}^n \times \boldsymbol{R}$ *and a smooth system of coordinates (preserving the planes* $\lambda$ = *constant) for which the Taylor expansion of degree 3 on the center manifold is given by (2.91). If* $a \neq 0$, *there is a surface of periodic solutions in the center manifold which has quadratic tangency with the eigenspace of* $\mu(\lambda_0), \bar{\mu}(\lambda_0)$ *agreeing to second order with the paraboloid*

$$\lambda = -(a/d)(x^2+y^2). \tag{2.94}$$

*If $a < 0$, then these periodic solutions are stable limit cycles, while if $a > 0$, the periodic solutions are repelling.*

The Hopf bifurcation of a periodic solution to an invariant torus in a flow can be considered as the Hopf bifurcation of a fixed point to a periodic solution under a Poincaré map. Below is the corresponding Hopf bifurcation theorem for maps.

**Theorem 2.1.8** *Hopf bifurcation for maps*

*Let $f_\lambda : \boldsymbol{R}^2 \to \boldsymbol{R}^2$ be a one-parameter family of mappings which has a smooth family of fixed points $\mathbf{x}(\lambda)$ at which the eigenvalues are complex conjugates $\mu(\lambda), \bar{\mu}(\lambda)$. Assume*

- *(a) $|\mu(\lambda_0)| = 1 \qquad$ but $\mu^j(\lambda_0) \neq 1 \qquad$ for $j = 1, 2, 3, 4$.*
- *(b) $\frac{d}{d\lambda}(|\mu(\lambda_0)|) = d \neq 0$.*

*Then there is a smooth change of coordinates $h$ so that the expression of $hf_\lambda h^{-1}$ in polar coordinates has the form*

$$hf_\lambda h^{-1}(r, \theta) = (r(1 + d(\lambda - \lambda_0) + ar^2), \theta + c + br^2) + \textit{ higher order terms.} \tag{2.95}$$

*(Note: $\mu$ complex and (b) imply $|arg(\mu)| = c$ and $d$ are non-zero.) If, in addition,*

$$a \neq 0, \tag{2.96}$$

*then there is a two-dimensional surface $\sum$ (not necessarily infinitely differentiable) in $\boldsymbol{R}^2 \times \boldsymbol{R}$ having quadratic tangency with the plane $\boldsymbol{R}^2 \times \{\lambda_0\}$ which is invariant for $f$. If $\sum \cap (\boldsymbol{R}^2 \times \{\lambda\})$ is larger than a point, then it is a simple closed curve.*

In the Hopf bifurcation theorems above the signs of the coefficients $a$ and $d$ determine the direction and the stability of the bifurcating periodic orbits and $c$ and $b$ give asymptotic information on rotation numbers.

## 2.2 Systems of partial differential equations

We hope to extend the numerical algorithms developed in this thesis for computing an invariant torus to those that arise in infinite systems. By an infinite dimension we mean a system that corresponds to a PDE written in terms of Fourier or eigen modes. In this section we discuss some background theory and some extension of the theory discussed in finite dimensional systems to PDEs.

The field of dynamical systems generated by PDEs has in recent years grown rapidly. The notions from the theory of finite-dimensional dynamical systems have penetrated deeply into the theory of infinite-dimensional systems and partial differential equations. The evolution equations of these PDEs are now been investigated from the standpoint of the theory of dynamical systems. These equations include the Navier-Stokes equation (NVS), Magneto-hydrodynamics equations and reaction-diffusion equations. One common feature is the theory of turbulence arising in a dynamical system approach to identify turbulence with the long time dynamics of the solutions of the Navier Stokes equations. Among the latest achievements, it has been established that in the case of two-dimensional Navier Stokes equations there is a global attractor which has a finite dimension. Further examples constructed in the 2-dimensional Navier Stokes equation indicate that, under suitable conditions, the dimension of the attractor can be arbitrarily large. This indicates that the long-time dynamics of the Navier Stokes equations may involve many different degrees of dynamical complexity. It has been shown that the invariant sets and attractors are bounded in 3-dimensional Navier-Stokes equations and have finite Hausdorff (and fractal) dimension[TR].

The bifurcation in partial differential equation has been observed in the Navier-Stokes equations, chemical reactions Kopell-Howard [KH] and population dynamics. Some early works of Ruelle Takens indicate that under some smoothness assumptions on the vector fields the bifurcations yielding, periodic solutions and invariant tori in ODEs can be applied to some dissipative PDEs. Further bifurcations to higher dimensional stable tori can also be observed leading to a strange attractor which is abundant on $k - tori$ $(k \geq 4)$.

### 2.2.1 Bifurcation theorems for partial differential equations

In application to partial differential equations, the key assumption is that the semi-flow defined by the equations be smooth in all variables for $t > 0$. One determines that for partial differential equations the vector fields generating the flows are usually not smooth

functions on any reasonable Banach space. However, for certain parabolic type of PDEs some of the Hopf bifurcation theorems for ODEs can be pushed through [IO]. We will see that if the spectral condition of Hopf's theorem are fulfilled, then indeed a periodic solution will develop. One hypothesis needed is analyticity of the solution in t. In this section we look at some other conditions necessary for the bifurcation to periodic solutions.

Consider a system of evolution equations of the general form

$$\frac{d\mathbf{x}}{dt} = X_\lambda(\mathbf{x}) \qquad \text{with} \quad \mathbf{x}(0) \quad \textit{given} \tag{2.97}$$

and $X_\lambda$ a densely defined nonlinear operator on a Banach space B, which depends on a parameter $\lambda$. We want the flow $\phi_t$ for each fixed t and $\lambda$ to be a $C^\infty$ mapping on the Banach space B (note that $\phi_t$ is only locally defined in general). We assume the following properties are valid for the flow:

- $\phi_t$ is defined on an open subset of $\mathbf{R}^+ \times B$, $\qquad \mathbf{R}^+ = \{t \in \mathbf{R} \mid t \geq 0\}$;
- $\phi_{t+s} = \phi_t \circ \phi_s$ (where defined);
- $\phi_t(\mathbf{x})$ is separately continuous in (t,x) $\in \mathbf{R}^+ \times B$.

Two assumptions that the flow must satisfy are:

**Assumption 2.2.1** *(Smoothness)*
*Assume that for each fixed t, $\phi_t$ is a $C^\infty$ map of (an open set in) B to B.*

With these conditions and the assumption for the flow, $\phi(t)$ can be defined as a smooth semigroup. We can expect smoothness in $\lambda$ and t for $t > 0$. This is the nonlinear analogue of "analytic semigroups" and holds for "parabolic type" equations.

**Assumption 2.2.2** *(Continuation)*
*Let $\phi_t(\mathbf{x})$ for fixed $\mathbf{x}$ lie in a bounded set in B for all t for which $\phi_t(\mathbf{x})$ is defined. Then $\phi_t(\mathbf{x})$ is defined for all $t \geq 0$.*

This guarantees that the only way an orbit can fail to be defined is if it tends to infinity in a finite time.

Let us assume that the origin $\mathbf{0}$ is a fixed point of $\phi_t$ ie. $\phi_t(\mathbf{0}) = \mathbf{0}$ for all $t \geq 0$. Let $\Phi_t = D\phi_t(\mathbf{0})$ denote the Fréchet derivative of $\phi_t$ for a fixed $t$ at $\mathbf{x} = \mathbf{0}$ with generator $DX(\mathbf{0})$. The linear semi-group $G_t$ under suitable conditions is the exponential of the spectrum of $DX(\mathbf{0})$. The spectrum therefore determines the stability type of (2.97).

**Hypotheses 2.2.1** *(On the spectrum)*

*Assume we have a family $\phi_t^\lambda$ of smooth nonlinear semigroups defined for $\lambda$ in an interval about $\mathbf{0} \in \boldsymbol{R}$. Suppose $\phi_t^\lambda(\mathbf{x})$ is jointly smooth in t,x, $\lambda$, for $t > 0$. Assume:*

1. *$\mathbf{0}$ is a fixed point for $\phi_t^\lambda(\mathbf{x})$;*
2. *for $\lambda < 0$, the spectrum of $\Phi_t^\lambda(\mathbf{x})$ is contained in $D = \{z \text{ is Complex} : |z| < 1\}$, where $\Phi_t^\lambda = D_x\phi_t^\lambda(\mathbf{x})|_{\mathbf{x}=\mathbf{0}}$;*
3. *for $\lambda = 0$ (resp. $\lambda > 0$) the spectrum of $\Phi_t^\lambda(\mathbf{x})$ at the origin has two isolated simple eigenvalues $\mu(\lambda)$ and $\overline{\mu(\lambda)}$ with $|\mu(\lambda)| = 1$ (resp. $\mu(\lambda) > 1$) and the rest of the spectrum is in D and remains bounded away from the unit circle.*
4. *$(\frac{d}{dt})|\mu(\lambda)||_{\lambda=0} > 0$ (the eigenvalues move steadily across the unit circle).*

Under these conditions we have the bifurcation to periodic orbits, the stability of which is determined from Marsden [MM].

**Theorem 2.2.1** *Under the above hypotheses, there is a fixed neighborhood U of $\mathbf{0}$ in B and an $\epsilon > 0$ such that $\phi_t^\lambda(\mathbf{x})$ is defined for all $t \geq 0$ for $\lambda \in [-\epsilon, \epsilon]$ and $\mathbf{x} \in V$. There is a one-parameter family of closed orbits for $\phi_t^\lambda(\mathbf{x})$ for $\lambda > 0$, one for each $\lambda > 0$ varying continuously with $\lambda$. They are locally attracting and hence stable . Solutions near them are defined for all $t \geq 0$. There is a neighborhood U of the origin such that any closed orbit in U is one of the above orbits.*

One can generalize the theorem to the case where the system depends on many parameters with multiple eigenvalues crossing or to a system with symmetry. It can also be extended to the bifurcation to an invariant torus. If $\phi_t^\lambda(\mathbf{x})$ is smooth in $t, \lambda, \mathbf{x}$ for $t > 0$ then the Poincaré map for the closed orbit will be well defined and smooth and after we reduce to finite dimensions via the center manifold theorem.

Ruelle Takens theory of turbulence has related the qualitative theory of differential equations to turbulence in fluids. The theory is based on some concrete mathematical conjectures about the Navier Stokes equations which are only supported by indirect evidence [SG]. And to apply the theorem above to this problem all we need to do is to show that the semiflow of the Navier Stokes equation is smooth. In Marsden and McCracken [MM] it is shown that the Navier-Stokes equations in dimension 2 and 3 define a smooth local semiflow on Sobolev space.

There is a unique correspondence between a given boundary and internal forcing data and the predicted motion, when the Reynolds number is small. Also at small Reynolds number, there exists a unique solution, determined by the data after the initial conditions have died away.

### 2.2.2 Projections

The results obtained so far are in infinite dimension and in order to reduce them to a lower dimension, we consider the following methods of reduction,

1. the use of the center manifold theory to reduce the problem to the center manifold [C], [MM], [HKW];
2. the use of inertial manifolds;
3. a discretization method such as the Galerkin method where one expands the solution in an eigenfunction, then truncate the expansion and substitute it into the PDE to get a system of ODEs for the coefficients.

## 2.3 Strange Attractors and Turbulence

> The mathematical object which accounts for turbulence is an attractor or a few attractors, of reasonably small dimension, embedded in the very-large dimensional state-space of the fluid system. Motion on the attractor depends sensitively on the initial conditions, and this sensitive dependence accounts for the apparently stochastic time dependence of the fluid. [SG]

This approach assumes that turbulence is to be understood within the framework of Navier-Stokes equations. There is no global existence theorem for solution of the initial value problem for Navier-Stokes equations. The fluid system is regarded as a mechanical system with friction and mathematically, its motion is viewed as governed by a first-order in time differential equation on a state space. The phenomenon understanding turbulence is finite dimensional though the state space for the fluid is infinite dimensional.

Some stability properties in $R^3$ of the Navier-Stokes equations are in [MM].

| *Model* | *Mechanism* | | | | | | | | | |
|---|---|---|---|---|---|---|---|---|---|---|
| Landau | stationary point | → Hopf | singly periodic orbit | → Hopf | Doubly periodic orbit | → Hopf | triply periodic orbit | → ... → Hopf | turbulent motion |
| Ruelle Takens-Newhouse | stationary point | → Hopf | singly periodic orbit | → Hopf | doubly periodic orbit | → | strange attractor | | |
| Feigenbaum | stationary point | → Hopf | singly periodic orbit period T | → pitchfork | singly periodic orbit period 2T | → pitchfork | singly periodic orbit period 4T | → ... → pitchfork | strange attractor |
| Pomeau-Manneville | stationary point | → Hopf | singly periodic orbit | → reverse tangent bifurcation | intermittent chaotic motion | | | | |

Table 2.2: Models of the transition to turbulence

# Chapter 3

# The ODE methods

In this chapter we present a numerical method to compute invariant circles for maps and differential equations. It is an application of the Hadamard graph transform (HGT) for computing attracting invariant manifolds. We perform a sequence of graph transforms, where each transform requires the solution of finitely many ODE boundary value problems in the differential equation case. The HGT iteration is seen to converge after one iteration when the invariant circle is exponentially attracting. We give a convergence proof for our algorithm and apply it to three problems.

We start by giving some basic theories related to our computations. As we have seen in the introductory chapter, the computation of nonwandering sets or manifolds have been a major concern in the area of dynamical systems. One such important low dimensional manifold is the invariant torus, which can be defined implicitly from an invariant circle under the Poincaré map. In bifurcation analysis, one is frequently interested in following a torus to its breakdown. During the process of its computations, the torus naturally loses its smoothness and become harder to compute as we vary a bifurcation parameter. Instead, computing an invariant circle of the torus one can thereby reduce the complexity of the computation of the torus.

In [ACHM], a direct iteration was used to compute the invariant circles of discrete maps. One of the recent methods used to compute invariant circle for maps and differential equations is the Poincaré map approach of van Veldhuizen[VV1] and Kevrekidis et al.[KASP]. The method of van Veldhuizen uses a polygon to approximate the invariant circle. His algorithms then require the use of a large number of mesh points. The algorithm of Kevrekidis uses the Newton-Raphson method to find a fixed point of a nonlinear mapping in a finite

dimensional space that results from the discretization of the problem. The algorithm suffers from the undesirable convergence properties of Newton's method but can work well provided the Jacobian exits.

In the Hadamard graph transform approach each transform step involves solving a number of ode boundary value problems. One advantage of this approach is that each boundary value problem is independent of the others, and they can be solved concurrently. The Hadamard graph transform technique as implemented in this work bears some similarities to the Poincaré map approach.

## 3.1 The Shooting method for BVPs

This is an initial value method for solving boundary value problems (BVP). It is relatively an easy method for solving two-point boundary value problems but has stability problems. These problems are alleviated by methods like multiple shooting, the stabilized march and the Riccati methods [AMR].

### 3.1.1 Simple shooting for linear problems

In this section we describe the shooting method for the general linear two-point BVP of the form

$$\begin{aligned} &\mathbf{u}' = A(x)\mathbf{u} + q(x), \qquad a < x < b, \qquad \mathbf{u} \in \mathbf{R}^n \\ &B_a\mathbf{u}(a) + B_b\mathbf{u}(b) = \beta \end{aligned} \tag{3.1}$$

with general solution

$$\mathbf{u}(x) = \mathbf{U}(x)\mathbf{s} + \mathbf{v}(x), \qquad a \leq x \leq b \tag{3.2}$$

where $\mathbf{U}(x) := \mathbf{U}(x;a)$ is a fundamental matrix solution, $\mathbf{s} \in \mathbf{R}^n$ a parameter vector and $\mathbf{v}(t)$ a particular solution. The particular solution $\mathbf{v}(x)$ satisfies

$$\mathbf{v}' = A(x)\mathbf{v} + q(x) \tag{3.3}$$

with the initial condition

$$\mathbf{v}(a) = \alpha$$

for some $\alpha \in \mathbf{R}^n$. The $n$ columns of the fundamental matrix solution can be determined from the variational equation

$$\begin{aligned} &\mathbf{U}' = A(x)\mathbf{U} \qquad a < x < b \\ &U(a) = I. \end{aligned} \tag{3.4}$$

We determine the parameters $\mathbf{s}$ by substituting (3.2) into the boundary conditions of equation (3.1) to obtain

$$\beta = B_a[\mathbf{U}(a)s + \mathbf{v}(a)] + B_b[\mathbf{U}(b)s + \mathbf{v}(b)] = [B_a + B_b\mathbf{U}(b)]s + B_a\mathbf{v}(a) + B_b\mathbf{v}(b) \quad (3.5)$$

which can be written as

$$Q\mathbf{s} = \hat{\beta} \quad (3.6)$$

$$\text{where} \quad \hat{\beta} = \beta - \beta_a\mathbf{v}(a) - B_b\mathbf{v}(b) \qquad Q := B_a + B_b\mathbf{v}(b).$$

If BVP (3.1) has a unique solution then $Q$ is nonsingular, and $\mathbf{s}$ is well defined by (3.5). The solution obtained by this method depends on the discretization and the roundoff errors. The discretization error is bounded by

$$|\mathbf{u}(x_i) - u_i| \leq K\ Tol \| \int_a^b G(x_i, t)dt \| \simeq K\ Tol\ \kappa. \quad (3.7)$$

where $Tol$ is the tolerance given to the IVP integration routine which controls the local error in the solution $\mathbf{v}(t)$ and $\mathbf{U}(t)K \approx 1$. The shooting method will in general give appropriate global discretization errors if the BVP is well-conditioned ie. when $\kappa$ is not too large.

### Simple shooting for nonlinear systems

Consider the nonlinear differential equation

$$\mathbf{u}' = f(x, \mathbf{u}), \qquad a < x < b, \quad (3.8)$$

subject to the boundary conditions

$$g(\mathbf{u}(a), \mathbf{u}(b)) = 0.$$

Denote the solution of (3.8) by $\mathbf{u}(x, \mathbf{s})$ which satisfies the initial condition

$$\mathbf{u}(a, \mathbf{s}) = \mathbf{s}.$$

Our problem then reduces to that of finding $\mathbf{s}^*$ which solves the nonlinear algebraic equations

$$g(\mathbf{s}, \mathbf{u}(b, \mathbf{s})) = \mathbf{0}. \quad (3.9)$$

Below we describe a Newton's method to solve the algebraic equations for $\mathbf{s}^*$. Let

$$F(\mathbf{s}) := g(\mathbf{s}, \mathbf{u}(b; \mathbf{s})) = 0. \quad (3.10)$$

and the fundamental matrix solution of (3.8) be given by

$$U(x) \equiv \frac{\partial \mathbf{u}(x;s)}{\partial s}. \tag{3.11}$$

$U(x)$ can be determined from

$$\begin{aligned} \dot{U} &= A(x)U \qquad a < x < b \\ U(a) &= I \end{aligned} \tag{3.12}$$

where

$$A(x) = A(x,\mathbf{s}) \equiv \frac{\partial f}{\partial \mathbf{u}}(x, \mathbf{u}(x;\mathbf{s})).$$

If $\mathbf{s}^0$ is the initial guess, then the sequence $\mathbf{s}^1, \mathbf{s}^2, \ldots$ is obtained from

$$\mathbf{s}^{m+1} := \mathbf{s}^m + \psi$$

where $\psi$ solves the linear system

$$G'(\mathbf{s}^m)\psi = -F(\mathbf{s}^m) \tag{3.13}$$

with $G'$ defined by

$$G'(\mathbf{s}) := \frac{\partial G(\mathbf{s})}{\partial \mathbf{s}} = B_a + B_b U(b)$$

where

$$B_a = \frac{\partial g(\mathbf{w},\mathbf{v})}{\partial \mathbf{w}}, \qquad B_b = \frac{\partial g(\mathbf{w},\mathbf{v})}{\partial \mathbf{v}} \qquad \text{at } \mathbf{w} = \mathbf{s},\ \mathbf{v} = U(b;\mathbf{s}) \tag{3.14}$$

As mentioned earlier, the simple shooting method is not very robust and its numerical results cannot always be trusted. Some of the reasons are as follows:

(1) The IVPs integrated in the process could be unstable, even when the BVP is well-conditioned ie.

(a) There could be a propagation of roundoff errors by the initial value integrator. A rough estimate for the bound on this error is of order $\epsilon_M e^{L(b-a)}$ where $L = \max_x \|A(x)\|$ and $\epsilon_M$ is the machine precision.

(b) There could be discretization errors.

(2) For non-linear problems a problem arises when shooting with initial values for which the exact solution does not exist on the whole interval [a,b].

### 3.1.2 Multiple shooting for nonlinear problems

For a description of multiple shooting algorithm for linear problems see [AMR]. A basic solution to the problems above is to reduce the length of the integration interval $[a, b]$. We divide the interval to form the mesh

$$\Pi = \{a = x_1 < x_2 < \cdots < x_{N+1} = b\}. \tag{3.15}$$

Consider equation (3.8) in the subinterval $(x_i, x_{i+1})$, $i = 1, \ldots, N$ with the initial condition

$$\mathbf{u}(x_i) = s_i$$

and solution denoted by

$$\mathbf{u}(x) := \mathbf{u}_i(x; \mathbf{s}). \tag{3.16}$$

Let

$$\mathbf{u}_i(x_{i+1} : \mathbf{s}_i) = \mathbf{s}_{i+1} \qquad 1 \le i \le N$$

and $g(\mathbf{s}_1, \mathbf{u}_N(b, \mathbf{s}_N)) = 0$. We define

$$F(\mathbf{s}) := \begin{bmatrix} \mathbf{s}_2 - \mathbf{u}_1(x_2; \mathbf{s}_1) \\ \mathbf{s}_3 - \mathbf{u}_2(x_3; \mathbf{s}_2) \\ \vdots \\ \mathbf{s}_N - \mathbf{u}_{N-1}(x_N; \mathbf{s}_{N-1}) \\ g(\mathbf{s}_1, \mathbf{u}_N(b; \mathbf{s}_N)) \end{bmatrix} \tag{3.17}$$

and solve a set of $nN$ nonlinear algebraic equations $F(\mathbf{s}) = 0$ for $\mathbf{s}^*$. Let

$$F'(\mathbf{s}) = \begin{bmatrix} -U_1(x_2) & I & & & \\ & -U_2(x_3) & I & & \\ & & \ddots & \ddots & \\ & & & -U_{N-1}(x_N) & I \\ B_a & & & & B_b U_N(b) \end{bmatrix} \tag{3.18}$$

where $U_i(x) = U_i(x; x_i, \mathbf{s}_i)$ is the $n \times n$ fundamental solution defined by

$$\begin{aligned} U_i'(x) &= A(x) U_i \qquad x_i < x < x_{i+1} \\ U_i(x_i) &= I \qquad 1 \le i \le N \end{aligned} \tag{3.19}$$

with $A(x) = A(x; \mathbf{s}), B_a = B_a(\mathbf{s})$ and $B_b = B_b(\mathbf{s})$ defined as in simple shooting. The rest of the process is the same as in single shooting for nonlinear problems using the Newton's method.

## 3.2 Numerical Formulation

The basic dynamical system we consider is that of the form

$$\dot{\mathbf{x}} = f(\mathbf{x}), \qquad \mathbf{x}(t_0) = \mathbf{x}_0, \tag{3.20}$$

where $f : R^n \longrightarrow R^n$, and has a solution denoted by $\phi_t(\mathbf{x}_0)$. Assume (3.20) has a periodic solution and $\mathbf{x}_0$ a point on it with period $T$. Let $\sum$ be an $n-1$ dimensional surface transverse to the vector field at $\mathbf{x}_0$ with an open set $V \subset \sum$ and $\mathbf{x} \in V$. The Poincaré map denoted $P : V \to \sum$ is defined by $P(\mathbf{x}) := \phi(\tau(\mathbf{x}), \mathbf{x}) \in \sum$ where $\tau(\mathbf{x})$ is the time of first return such that $\tau(\mathbf{x}_0) = T$ and $P(\mathbf{x}_0) = \mathbf{x}_0$[W]. If $f$ is time periodic and of a fixed period $T = 2\pi/\omega$ then (3.20) can be written as

$$\dot{\mathbf{x}} = f(\mathbf{x}, t) \tag{3.21}$$

which can be reduced to

$$\begin{aligned} \dot{\mathbf{x}} &= f(\mathbf{x}, \theta) \\ \dot{\theta} &= \omega. \end{aligned} \tag{3.22}$$

In this case, the $n-1$ dimensional surface is given by $\sum := \{(\mathbf{x}, \theta) \in \mathbf{R}^n \times S^1|_{\theta=\theta_0}\}$. The set $\{P^k(\mathbf{x}) = \phi_{t_0+kT}(\mathbf{x}, t_0), \quad k = 1, 2, ...\}$ is the corresponding orbit. We assume that $P$ is homeomorphic. A fixed point of the Poincaré map corresponds to a $T$-periodic solution of the ODE system. When the solution of (1.2) is two-periodic, then the Poincaré map possesses an invariant curve, ie., an invariant curve $\gamma$ in $R^n$ such that $P\gamma \subset \gamma$. Note that the flow $\phi_t(\mathbf{x}, t_0)$ of (3.21) with $\mathbf{x} \in \gamma$ and $t \in (0, T]$ determines its invariant 2-torus of (3.21). The solutions of the differential equation lying on the torus correspond to solutions of the Poincaré map on the invariant circle.

When considering the Hopf bifurcation of an ordinary differential system from a periodic solution to an invariant torus, under the Poincaré map, one can reduce it to a simpler bifurcation problem from a fixed point to an invariant circle. At the point of Hopf bifurcation, the plane $\Pi$ containing the invariant curve can be determined from the eigenvectors of the two eigenvalues that cross the unit circle. At the bifurcation point, the plane $\Pi$ is then the center manifold. The essential action of the system (3.21) takes place in this plane which actually gives a detailed asymptotic information about the plane. Perturbation techniques can be used to compute the Euclidean projection of such invariant circles in this plane close to the Hopf bifurcation point in the parameter space. Below, we assume there is a nonlinear

coordinate transformation such that the plane $\Pi$, is spanned by the first two coordinates in $\mathbf{R}^n$. For some $\mathbf{x}_c \in \mathbf{R}^n$ there exists such a nonlinear coordinate transformation as follows:

**Assumption 1.1 (Radial coordinates)**[vv2]

In the annular neighborhood of the curve $\gamma$ the nonlinear coordinate transformation

$$(\theta, \rho, \nu) \longrightarrow \mathbf{x}_c + (r(\theta) + \rho)(cos(\theta), sin(\theta), \mathbf{0})^T + (0, 0, \psi(\theta) + \nu)^T, \tag{3.23}$$

is a smooth invertible map, with $r(\theta) > 0, \nu \in R^{n-2}$, and $\theta \in S^1$. In particular, the Jacobian matrix of the transforming map should be invertible with uniformly bounded inverse along $\gamma$. The curve $\gamma$ can then be described by

$$\gamma : \theta \in [0, 2\pi) \longrightarrow \gamma(\theta) = \mathbf{x}_c + (r(\theta)cos(\theta), r(\theta)sin(\theta), \psi(\theta))^T. \tag{3.24}$$

We assume that the projection of the invariant curve $\gamma$

$$\gamma : \theta \in [0, 2\pi) \longrightarrow \gamma(\theta) = \mathbf{x}_c + (r(\theta)cos(\theta), r(\theta)sin(\theta), \psi^0)^T. \tag{3.25}$$

in the plane $\Pi$ looks like a curve. We define the radial distance $d_r(x, \gamma) = |(\rho, \nu)|$ as the Euclidean length of $(\rho, \nu)$.

We can also generalize this transformation to the case where we have a Hopf bifurcation to $\gamma = (\gamma_1 \mathbf{r} U \gamma_2 U \ldots U \gamma_q)$ invariant circles. Let the corresponding planes be denoted by $\mathbf{\Pi} = (\mathbf{\Pi_1 U \Pi_2 U \ldots U \Pi_q})$. In the new coordinate system, equation (2.26) becomes

$$\begin{pmatrix} \dot{\theta} \\ \dot{\mathbf{r}} \\ \dot{\psi} \end{pmatrix} = \begin{pmatrix} f(\theta, \mathbf{r}, \psi) \\ g(\theta, \mathbf{r}, \psi) \\ h(\theta, \mathbf{r}, \psi) \end{pmatrix} \qquad 0 \leq t \leq \tau \tag{3.26}$$

$$\theta \in S^1, \qquad \mathbf{r} \in \mathbf{R}^q, \text{and} \qquad \psi \in \mathbf{R}^{n-q-1}$$

### 3.2.1 The Hadamard graph transform approach

In this section we outline a new approach to compute the invariant circle for maps and differential equations. This method is an application of the graph transform method developed in Fenichel [F]. It is a tool for obtaining a (locally) attracting invariant manifold. The approach then works for attractive and repellent curves but not for those with mixed attractivity. One performs a sequence of graph transforms (iterations), where each graph

transform itself requires the solution of finitely many (BVP) for each point $\theta \in S^1$. We assume that the projection of the invariant curve $\gamma$ in the plane $\Pi$ can be parameterized by

$$\gamma : \theta \longrightarrow \mathbf{R}(\theta), \qquad \theta \in [0, 2\pi] \qquad \mathbf{R} = \{R^1, R^2, \ldots, R^q\}. \tag{3.27}$$

We choose a mesh

$$\Omega_h := \{0 = \theta_1 \leq \theta_2 \leq \ldots \leq \theta_N\} = 2\pi\} \tag{3.28}$$

Define $\mathbf{R}_i := \mathbf{R}(\theta_i)$, $i = 1, \ldots, N$ and $\mathbf{R}^{old}(\theta)$ the initial approximation to $\gamma$. Let $\{P\mathbf{R}_i^{old}\}_{i=1}^N$ be the image of the points $\{\mathbf{R}_i^{old}\}_{i=1}^N$ under the Poincaré map $P$. If the curve $\gamma$ is attracting(repelling) then the sequence of points $P^n\mathbf{R}_i$, $n = 1, ..., \infty(-\infty)$ for $i$=1, 2,...,N gets closer to the curve $\gamma$. However, they will converge to a single point on $\gamma$ if it contains a fixed point of the Poincaré map. In the Poincaré map approach the points are equi-distributed after each map of $\{\mathbf{R}_{i=1}^N\}$. The basic algorithm consists of 2 parts:

- compute the images of the old mesh points.
- project the old mesh onto $\{P\mathbf{R}_i^{old}\}_{i=1}^N$ to get the new mesh points.

If $K$ is defined as the composition of the Poincaré map $P$ and the projection map then this approach results in solving the set of equations

$$\mathbf{R}_i^{new} = K\mathbf{R}_i^{old}, \qquad i = 1, \ldots, N. \tag{3.29}$$

Van Veldhuizen[VVH1] solves (3.29) using simple iteration with piecewise polynomial interpolation projection whiles Kevrekidis et al.[KASP] use the Newton-Raphson iteration with spline and finite element interpolation. In the Hadamard graph transform approach we introduce the HGT step $H$ which is similar to $K$ and solve (3.29) using simple iteration.

We start by defining the projection operators $U$, $V$ and $W$ by

$$U(\theta, r, \psi) := \theta \qquad V(\theta, r, \psi) := r \qquad W(\theta, r, \psi) := \psi. \tag{3.30}$$

We see that they project the state space $S^1 \times \mathbf{R}^q \times \mathbf{R}^{n-q-1}$ onto $S^1$, $\mathbf{R}^q$ and $\mathbf{R}^{n-q-1}$ respectively. Define the Poincaré map $P$ by

$$P(\theta^0, r^0, \psi^0) := \phi_\tau(\theta^0, r^0, \psi^0) = (\tilde{\theta}, \tilde{r}, \psi^0) \tag{3.31}$$

where $\tau > 0$ and $\psi = \psi^0$ is the Poincaré cross-section. Assume that the manifold $\gamma$ is locally attracting in positive time. ie. if the flow $\phi_t(\theta, r, \psi)$ is sufficiently close to $\gamma$ then the

distance of $\phi_t(\theta, r, \psi)$ to $\gamma$ tends to zero as $t \longrightarrow \infty$. Let $r(t) = R(\theta(t))$, with $r(0) = R^{old}$ and if $\gamma$ is globally attracting then the longterm behavior of (3.26) is given by

$$\begin{cases} \dot{\theta} = f(\theta, R(\theta), \psi) \\ r(t) = R(\theta(t)). \end{cases} \tag{3.32}$$

We solve the boundary value problem $BVP(\bar{\theta}, R^{old})$

$$\begin{cases} \begin{pmatrix} \dot{\theta} \\ \dot{r} \\ \dot{\psi} \end{pmatrix} = \begin{pmatrix} f(\theta, r, \psi) \\ g(\theta, r, \psi) \\ h(\theta, r, \psi) \end{pmatrix} \qquad 0 \le t \le \tau \\ r(0) = R^{old}, \ \ \theta(\tau) = \bar{\theta}, \ \ \psi(0) = \psi^0 = \psi(\tau) \end{cases} \tag{3.33}$$

to determine $\alpha$ and $R^{new}(\bar{\theta})$ such that

$$U(\phi_\tau(\alpha, R^{old}(\alpha), \psi^0) = \bar{\theta} \tag{3.34}$$

$$V(\phi_0(\alpha, R^{old}(\alpha), \psi^0)) = R^{old}(\alpha). \tag{3.35}$$

The Hadamard operator $H^\tau$ applied to $\mathbf{R}^{old}$ is defined by

$$(H^\tau \mathbf{R}^{old})(\bar{\theta}) := V(\phi_\tau(\alpha, \mathbf{R}^{old}(\alpha), \psi^0) = \mathbf{R}^{old}((\bar{\theta}), \tau). \tag{3.36}$$

Let $\mathbf{R}^{new} := H^\tau \mathbf{R}^{old}$ be the new approximation to $\mathbf{R}$ and $H^\tau$ be one Hadamard iteration. Under appropriate assumptions, the iteration $\mathbf{R}^{n+1} = H^\tau \mathbf{R}^n$ converges linearly to the fixed point $\mathbf{R}$. In the case where one component of $\psi \in S^1$, say $\psi_1 \in S^1$ we get an invariant torus and $\tau$ can be chosen as $2\pi$. This is illustrated in the numerical example 4. The BVP$(\bar{\theta}, R^{old})$ for the $\bar{\theta}_j$ values in the discrete mesh $\bar{\theta}_j \in \Omega_h \subset S^1$ are independent of each other at each point $\alpha$. This allows us to parallelize our code. We can assign N $BVP(\bar{\theta}, R^{old})s$ to N processors. No communication is necessary provided the functions $f, g, h$ and $R^{old}$ are available locally. We solved the $BVP(\bar{\theta}, R^{old})$ using simple and multiple shooting with bisection and Newton's method. The algorithm is as follows:

1. Choose

   (a) initial values $\{R_i^{old}\}_{i=1}^N$. The mesh is distributed such that $\{\theta_i\}$ are equi-distributed with respect to arclength,

   (b) a tolerance $\delta$,

   (c) maximum number of iterations $M_{max}$.

2. Build the interpolant $(I\{R_i^{old}\}_{i=1}^N)$ using e.g. a periodic cubic spline.

3. Compute the Poincaré map $P\phi_\tau(\theta_i(0), R^{old}(\theta_i(0)), \psi^0) = (\tilde{\theta}_i, \bar{\tau}, \psi^0)$ $i = 1, \ldots, N$ by integrating the differential equation in the $BVP(\bar{\theta}, R^{old})$ (3.33) (using say a standard integrator like RKF45 or ODE).

4. For each $\theta_j$, $1 \leq j \leq N$ find $\tilde{\theta}_k$ and $\tilde{\theta}_{k+1}$ such that $\tilde{\theta}_k \leq \theta_j \leq \tilde{\theta}_{k+1}$. Identify $\theta_1$ with $\theta_{N+1}$.

5. Solve the $BVP(\bar{\theta}, R^{old})$ using bisection for the first Hadamard iteration and Newton's method for subsequent iterations to determine $(H^\tau R^{old})(\theta_j)$, $\quad j = 1, \ldots, N$.

6. If Number of iterations $> M_{max}$ or $\max_{i=1,\ldots,N} |R^{new} - R^{old}| \leq tol$ update $R^{old}$ and exit; else go to 2.

### 3.2.2 Convergence analysis

In this section we prove the convergence of the Hadamard graph transform algorithm. The results of which are for attractive invariant curves and are from the work of Hale [H] and van Veldhuizen [VV2]. To determine $\gamma$ in principle, we have to perform an infinite sequence of graph transforms (iterations) where each graph transform itself requires the solution of infinitely many BVPs of each point in $\theta \in S$. Our algorithm performs a finite number of iterations (HGT) and solves finitely many BVPs. This introduces an error in our numerical approximation scheme for the invariant curve $\gamma$. We give the convergence rate for our algorithm and the conditions for a unique solution. If the HGT contracts then we can indeed obtain an attracting invariant manifold which does persists under small perturbations. In the case of differential equations the error in computing the Poincaé map is assume negligible.

The convergence analysis is done in the coordinate system described below. Let the invariant curve $\gamma$ be defined by

$$\gamma := \{\mathbf{x} \in \mathbb{R}^n : \mathbf{x} = \mathbf{u}(\theta), \qquad 0 \leq \theta \leq 2\pi\}. \tag{3.37}$$

Hale has proved rigorously that for a simple curve $\gamma$ there always exist a vector not in the set of all tangents vectors to $\gamma$. In the neighborhood of $\gamma$ one can generalize this to the following coordinate system around $\gamma$ and define

$$\{e_1(\theta), e_2(\theta), \ldots, e_n(\theta)\} \quad \in \mathbf{R}^n \tag{3.38}$$

as an orthonormal coordinate system for each $\theta \in [0, 2\pi]$ along the invariant curve $\gamma$. Let the coordinates be periodic in $\theta$ of period $2\pi$ with $\frac{du(\theta)}{d\theta} \neq 0$, $0 \leq \theta \leq 2\pi$ and one of the $e_j(\theta)$'s equal to

$$v(\theta) = \left[\frac{du(\theta)}{d\theta} / \left|\frac{du(\theta)}{d\theta}\right|\right]. \tag{3.39}$$

The orthogonal coordinate system (3.38) becomes $(v, \psi_1, \psi_2, \ldots, \psi_{n-1})$. We do a coordinate transformation $x \rightarrow (\theta, \rho)$, where $\rho = col(\rho_1, \rho_2, \ldots, \rho^{n-1})$ given by

$$x = u(\theta) + Z(\theta)\rho, \tag{3.40}$$

and $Z(\theta)$ an $n$ x $(n-1)$ matrix with orthonormal column vectors $\{\psi_1, \psi_2, \ldots, \psi_{n-1}\}$. This transformation is well defined. In addition, all columns of $Z(\theta)$ are orthogonal to the vector $\frac{du}{d\theta}(\theta)$. With the new coordinate transformation the invariant curve is given by $\theta \longrightarrow (\theta, 0)$. In $R^2$ the matrix $Z$ reduces to the normal vector to the curve $\gamma$. The distance $d_t(\mathbf{x}; \gamma)$ of the vector $\mathbf{x}$ *to* $\gamma$ is given by the Euclidean norm $||\rho||$. Now we give some conditions under which the $BVP(\bar{\theta}, R^{old}$ gives a unique solution.

**Lemma 3.2.1** *The $(BVP)(\bar{\theta}, R^{old})$ (3.33) has a unique solution iff the system (3.34) has a unique solution.*

**Proof** : Suppose $\alpha = \alpha(\bar{\theta})$ is the unique solution of (3.34) and let

$$\alpha = U(\theta_0, R(\theta_0), \nu^0). \tag{3.41}$$

This implies

$$\begin{aligned}(H^\tau R)\bar{\theta} &= V\phi_\tau(\alpha, R(\alpha), \nu^0) \\ &= R(\theta(\tau))\bullet\end{aligned} \tag{3.42}$$

The converse has been proved in [DLR2].

Assume that the mapping $\alpha = \alpha(\bar{\theta})$ defined in (3.34) is orientation preserving (ie. one-to-one and onto) and suppose that $H^\tau R = R$. The manifold

$$M = \{\theta, R(\theta) : \theta \in S\} \tag{3.43}$$

is invariant under $\phi$ [DLR22].

If the invariant curve $\gamma$ is attracting in the forward time then there exists a constant $0 \leq \chi < 1$ such that for all $\mathbf{x}$ in the neighborhood of $\gamma$

$$d_t(P\mathbf{x}; \gamma) \leq \chi d_t(\mathbf{x}; \gamma) \tag{3.44}$$

and a constant $C_d \geq 1$ such that the following relation hold

$$d_t(\mathbf{x}, \gamma) \leq d_r(\mathbf{x}, \gamma) \leq C_d d_t(\mathbf{x}, \gamma) \, [VV2]. \tag{3.45}$$

Let $I$ be an interpolation operator in the Banach space of continuous functions on $[0, 2\pi)$ with the norm $\|I\|$. The norm $\|.\|$ is the supremum norm of functions. Unlike in the case of [VV2], the norm of $I$ is considered over only a fixed grid. The approximation $I\{H\mathbf{x}_i\}_{i=1}^N$ to $\gamma$ is done by interpolating with abscissae as $\theta$. We let $I$ be a piecewise polynomial interpolation operator. If $I\gamma = \gamma^*$ then the operator $I$ converges as follows: $I\{H^n\mathbf{x}_i\}_{i=1}^N \longrightarrow \gamma^*$ as $n \longrightarrow \infty$. Define the interpolation error as $\|I\gamma^* - \gamma\|$. Let $\{R_i^*\}_{i=1}^N$ be the fixed point of the set of equations

$$\{R_i\}_{i=1}^N = \{H R_i\}_{i=1}^N. \tag{3.46}$$

Assume the points on the polygon are well ordered and close to $\gamma$, with $\mathbf{x}_c$ in the interior. Assume that the restriction of P to $\gamma$ is a homeomorphism so the images $P\mathbf{x}_i$ are nicely ordered along $\gamma$. Then this implies that for vertices close to $\gamma$ their images are close to $\gamma$.

**Lemma 4.2:** For $\{\mathbf{x_i}\}_{\mathbf{i=1}}^{\mathbf{N}}$ close enough to $\gamma$

$$d_r(H\mathbf{x}_i, \gamma) \leq \chi C_d \|I\| \max_{i=1,\ldots,N} d_t(\mathbf{x}_i, \gamma) + \|I\gamma - \gamma\|. \tag{3.47}$$

**Proof:** The radial distance between $H\mathbf{x}_i$ and $\gamma$ can be estimated as follows:

$$\begin{aligned} d_r(H\mathbf{x}_i, \gamma) &\leq \|I\{P\mathbf{x}_i\}_{i=1}^N - I\gamma\| + \|I\gamma - \gamma\| \\ &\leq \|I\| \max_{i=1,\ldots,N} d_r(P\mathbf{x}_i, \gamma) + \|I\gamma - \gamma\| \\ &\leq \|I\| C_d \max_{i=1,\ldots,N} d_t(P\mathbf{x}_i, \gamma) + \|I\gamma - \gamma\| \text{ from (3.45)} \\ &\leq \|I\| \chi C_d \max_{i=1,\ldots,N} d_t(\mathbf{x}_i, \gamma) + \|I\gamma - \gamma\| \text{ from (3.44)} \end{aligned} \tag{3.48}$$

In [VV2], van Velhuizen showed that if $H$ is a convex set map and if the radial distance of $I\{\mathbf{x}_i\}_{i=1}^N$ from $\gamma$ is at most $\delta$ then the iterates of $I\{\mathbf{x}_i\}_{i=1}^N$ under $H$ satisfy this property. And from lemma 4.2 we have the following condition

$$\delta < \chi C_d |\psi| \delta + |\psi\gamma - \gamma|. \tag{3.49}$$

**Theorem 3.2.1** *If $\chi\|I\|C_d < 1$ and if the interpolation error is sufficiently small, then the radial distance from points in this neighborhood to $\gamma$ is bounded by*

$$\delta = \frac{\|I\gamma - \gamma\|}{1 - \chi C_d \|I\|}. \tag{3.50}$$

*And if $I$ is a piecewise linear interpolation operator then the Hadamard graph transform iteration converges to $I\gamma$ with a convergence factor $\leq \bar{k}$, where $C_d\chi < \bar{k} < 1$.*

For the proof see [VV2].

We used a classical periodic cubic spline operator. In view of this theorem (3.2.1) the error in this method is $O(|\theta_{i+1} - \theta_i|^4)$. Since we don't need a nonuniform mesh, higher order piecewise interpolation schemes can be used without much problems.

## 3.3 Numerical examples

While we apply our numerical scheme to four low dimensional problems to illustrate its robustness. The algorithm can be extended to problems in higher dimension. The first example is a simple rigid map which is used to show the accuracy of the method with two different piecewise polynomial interpolation operators. The second example is the delayed logistic map and the last two are the van-der Pol equation and a system of two-coupled oscillators. In the last two examples the Poincaré map is not known explicitly and has to be determined during the process. The computations were done on a SUN SPARC 20 workstations and the 3-dimensional pictures produced on a Silicon Graphics Iris Indigo 2 Extreme.

### 3.3.1 Simple problem

This example is used to illustrate the accuracy of the method with respect to different piecewise interpolation operators. We chose a simple map $F$ given by

$$F(r, \theta) = (1 + \kappa(r - 1), \theta + \alpha) \tag{3.51}$$

with $0 \leq \kappa < 1$ and $\alpha \in (0, 2\pi]$. The invariant circle in this case is a unit circle and is

| *Number of points* | *Piecewise linear inter* | *Cubic spline* |
|---|---|---|
| 10 | 2.1555E-03 | 2.0157E-05 |
| 20 | 5.3888E-04 | 1.2045E-06 |
| 40 | 1.3472E-04 | 7.5382E-08 |
| 80 | 3.3048E-05 | 4.7274E-09 |
| 160 | 8.2601E-06 | 2.9874E-10 |
| 320 | 2.0653E-06 | 1.8631E-11 |

Table 3.1: The comparison of the accuracy of the cubic spline interpolation and the piecewise linear interpolation

attractive. The circle map $F|_\gamma$ is a rigid rotation over the angle $\alpha$ and with a rotation number $\alpha/2\pi$.

The results indicate that the order of accuracy for cubic spline interpolation is $O(h^4)$ while that for piecewise linear interpolation is $O(h^2)$. The aim of this work is show that these results agree with the theoretical results indicated in theorem (3.2.1). And we are yet to show that is the case. The error estimates depends on how one choses the center $x_c$ and the accuracies given above are about optimal.

### 3.3.2 Delayed logistic map

This is a population model that has been investigated in great details by Aronson et al.[ACHM]. If we let $N_n$ be the population density in the $n^{th}$ generation and let $a$ be a parameter reflecting the growth rate then the model is given by

$$N_{n+1} = aN_n(1.0 - N_{n-1}). \tag{3.52}$$

Set $x_n = N_{n-1}$, $y_n = N_n$, to get

$$F_a(x_n, y_n) = (x_{n+1}, y_{n+1}) = (y_n, ay_n(1.0 - x_n)). \tag{3.53}$$

The map $F_a$ has fixed points $(x^*, y^*) = (0,0)$ and $\frac{a-1}{a}(1,1)$. The linearise map at the origin has eigenvalues 0 and $a$ thus for values of $a > 1$ it is a saddle. The eigenvalues of the linearised map at $\frac{a-1}{a}(1,1)$ are $\lambda_{1,2} = \frac{1}{2}(1 \pm \sqrt{5-4a})$ and the fixed point $\frac{a-1}{a}(1,1)$ is stable for $1 < a \leq 2$. For $a \geq \frac{5}{4}$ the eigenvalues are complex conjugates. At $a = 2$, $\lambda\bar{\lambda} = 1$ with $\frac{d}{da}|\lambda(a)|_{a=2} = 1$ and the condition (2.96) of theorem (2.1.8) is satisfied. Thus at $a = 2$, the fixed point losses its stability and spawns an invariant circle via a Hopf bifurcation. It is known that for values of $a > 2.177$ the invariant curves are topologically circles but no longer differentiable [vv1]. We were able to follow the circle up to $a = 2.270$ using a simple continuation in $a$. Since the origin is a saddle, the outer most figure shows that we are approaching a homoclinic orbit. The first initial guess for this problem is not that difficult since we know the point of Hopf bifurcation. Van Veldhuizen computes invariant curves up to $a = 2.18$ and requires 1044 points to be able to compute the invariant circle at $a = 2.18$, whereas our method required 50 points to get similar results. The results of the HGT method is shown in figure 1.

### 3.3.3 The van der Pol oscillator

This equation serves as a simple mathematical model of a self-excited system. The unforced oscillator consists of a periodic motion which varies from sinusoidal to nearly discontinuous as a bifurcation parameter is varied. We are interested in the forced oscillator in which the motion is quasiperiodic. It has been used to model electric circuit with a triode valve and in math biology. The equation is given by

$$\ddot{x} + \alpha(x^2 - 1)\dot{x} + x = \beta cos(\omega t). \tag{3.54}$$

Under the transformations [GH] $p(x) = x^3/3 - x \qquad y = \dot{x} + \alpha p(x)$, we get

$$\begin{aligned} \dot{x} &= y - \alpha p(x) \\ \dot{y} &= -x + \beta cos(\omega t). \end{aligned} \tag{3.55}$$

We use bisection and later Newton's iteration in our computations. The Hadamard graph transform is used to compute a torus that is obtained as result of a Hopf bifurcation. Let $\kappa = \beta/2\alpha$ and $\sigma = (1-\omega^2)/\alpha$. The invariant curves for the $\kappa$ values 0.38, 0.385, 0.387, 0.389 and 0.390 with $\sigma = 0.55$ and $\alpha = 0.4$ are shown in figure (3.2). See [GH] for the importance of these parameters. These results indicate how the radius of the invariant circles grows from zero.

### 3.3.4 Coupled oscillators

In this example we look at the dynamics of 2-coupled planar oscillators which give rise to a system of ordinary differential equations in $R^4$. For the uncoupled system each oscillator has a unique periodic solution that is attracting and the coupled product system has a unique invariant torus that is also attracting. The torus persists for weak coupling and contains 2-periodic solutions when the coupling is linear and conservative. However, the torus disappears for strong coupling. Our desire is to understand the phenomenon of its disappearance.

The differential system is given by

$$\begin{aligned} \dot{x_1} &= \alpha_1 x_1 + \beta_1 y_1 - (x_1^2 + y_1^2)x_1 - \delta(x_1 + y_1 - x_2 - y_2) \\ \dot{y_1} &= \alpha_1 y_1 - \beta_1 x_1 - (x_1^2 + y_1^2)y_1 - \delta(x_1 + y_1 - x_2 - y_2) \\ \dot{x_2} &= \alpha_2 x_2 + \beta_2 y_2 - (x_2^2 + y_2^2)x_2 + \delta(x_1 + y_1 - x_2 - y_2) \\ \dot{y_2} &= \alpha_2 y_2 - \beta_2 x_2 - (x_2^2 + y_2^2)y_2 + \delta(x_1 + y_1 - x_2 - y_2). \end{aligned} \tag{3.56}$$

With the parameterization $x_i = r_i cos(\theta_i)$ and $y_i = -r_i sin(\theta_i)$, $i = 1, 2$ and $A = r_1[sin(\theta_1 + \theta_2) - cos(\theta_1 - \theta_2)]$ we get

$$\begin{aligned}
\dot{\theta_1} &= f_1(\theta_1, \theta_2, r_1, r_2) = \beta_1 + \delta\{cos2\theta_1 - \tfrac{r_2}{r_1}[sin(\theta_1 - \theta_2) + cos(\theta_1 + \theta_2)]\} \\
\dot{\theta_2} &= f_2(\theta_1, \theta_2, r_1, r_2) = \beta_2 + \delta\{cos2\theta_2 - \tfrac{r_1}{r_2}[sin(\theta_2 - \theta_1) + cos(\theta_1 + \theta_2)]\} \\
\dot{r_1} &= g_1(\theta_1, \theta_2, r_1, r_2) = r_1(\alpha_1 - r_1^2) - \delta\{r_1(1 - sin2(\theta_1)) + A\} \\
\dot{r_2} &= g_2(\theta_1, \theta_2, r_1, r_2) = r_2(\alpha_1 - r_2^2) - \delta\{r_2(1 - sin2(\theta_2)) + A\}
\end{aligned} \tag{3.57}$$

Let $\alpha_1 = \alpha_2 = 1.0, \beta_1 = \beta_2 = 0.55$ and the coupling parameter $\delta$ be our bifurcation parameter. The attracting limit circles of the uncoupled system is given by $x_i^2 + y_i^2 = \alpha_i$. If we define the invariant torus $M$ by $M := (\theta_1, \theta_2, r(\theta_1, \theta_2), r_2(\theta_1, \theta_2))$. then for the uncoupled system we have $M = (\theta_1, \theta_2, 1, 1)$.

The differential equations in (3.57) can be converted to the form

$$\begin{pmatrix} d\theta_2/d\theta_1 \\ dt/d\theta_1 \\ dr_1/d\theta_1 \\ dr_2/d\theta_1 \end{pmatrix} = \begin{pmatrix} f_2(\theta_1, \theta_2, r_1, r_2)/f_1(\theta_1, \theta_2, r_1, r_2) \\ 1.0/f_1(\theta_1, \theta_2, r_1, r_2) \\ g_1(r, \theta)/f_1(r, \theta_1)/f_1(\theta_1, \theta_2, r_1, r_2) \\ g_2(r, \theta)/f_1(r, \theta_1)/f_1(\theta_1, \theta_2, r_1, r_2) \end{pmatrix} \qquad 0 \le t \le \tau. \tag{3.58}$$

The value of $\tau$ is $2\pi$ in this example. The torus has two period solutions, one of which is stable and the other unstable. A simulation with the bifurcation program AUTO shows that for $\delta \approx 0.2605$ there is a saddle-node like bifurcation of the unstable orbit on the torus [HDER2].

From $\delta = 0$ to $\delta = 0.2600$ we use the initial guess $r_1 = 1, r_2 = 1$. We also use a simple continuation in $\delta$ with $\triangle\delta = 0.001$ from $\delta = 0.2600$ to $\delta = 0.2604$. The results compares favorably with those of the pde approach of Edoh et al.[ERS] but differ with Deici et al.[DB] for values of $\delta > 0.25$(about). The Hadamard graph transform

- is more robust,
- use less mesh points,
- use less CPU time,
- has results which are much further in the direction of the breakdown of the torus,

Some results are shown in figures 3,4,5,6 when we use 50 mesh points on each invariant circle. We realised that the results are similar to those when we use a higher number of mesh points.

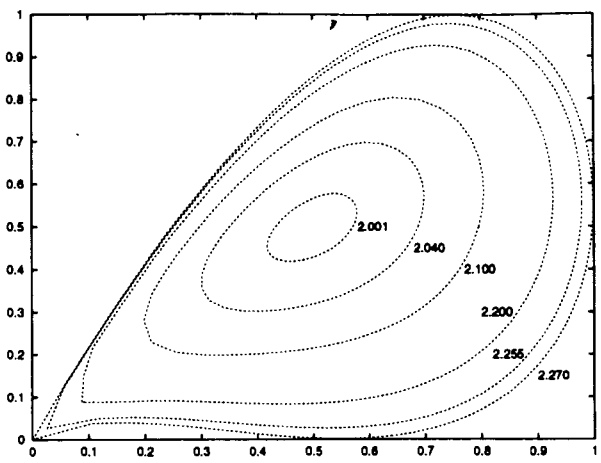


Figure 3.1: The invariant curves for the delayed logistic map for the values of $a$ as shown above.

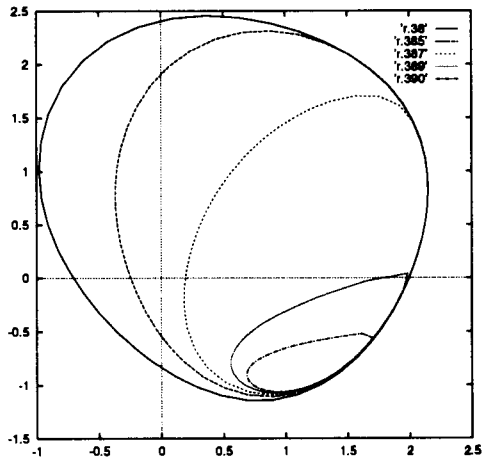


Figure 3.2: The invariant curves of the van der Pol oscillator for values of $\beta$ as shown above.

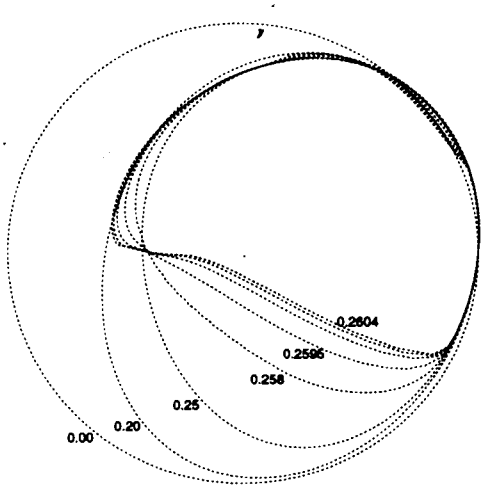


Figure 3.3: The cross-section of the torus $r_1(0, \theta_2)$ and $r_2(\theta_1, 0)$ with $\delta$ as shown above for $\beta_1 = \beta_2 = 0.55$ and $\alpha_1 = \alpha_2 = 1.0$.

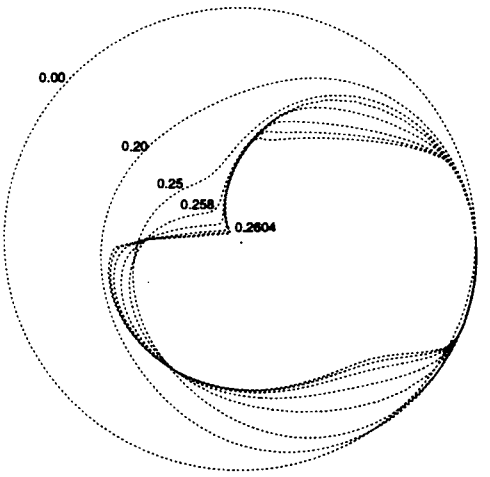


Figure 3.4: The cross-section of the torus $r_2(0, \theta_2)$ and $r_1(\theta_1, 0)$ with $\delta$ as shown above for $\beta_1 = \beta_2 = 0.55$ and $\alpha_1 = \alpha_2 = 1.0$.

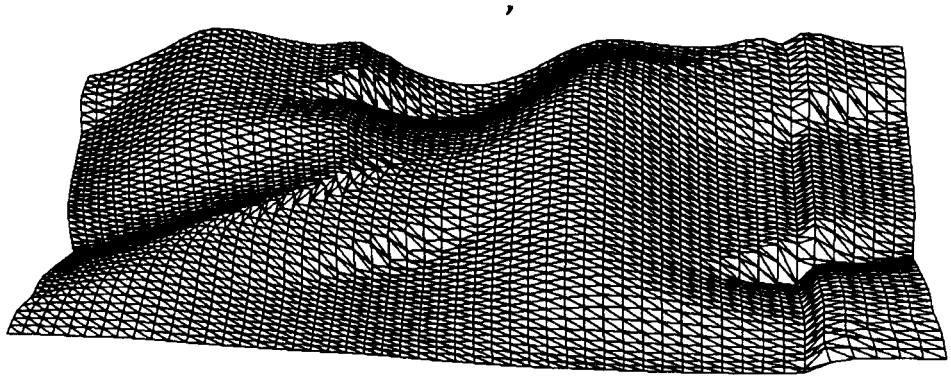

Figure 3.5: The flat surface of the torus $r_1(\theta_1, \theta_2)$ for $\delta = 0.2601$, $\beta_1 = \beta_2 = 0.55$. and $\alpha_1 = \alpha_2 = 1.0$ where $\theta_1$ is in the horizontal direction and $\theta_2$ in the vetical direction.

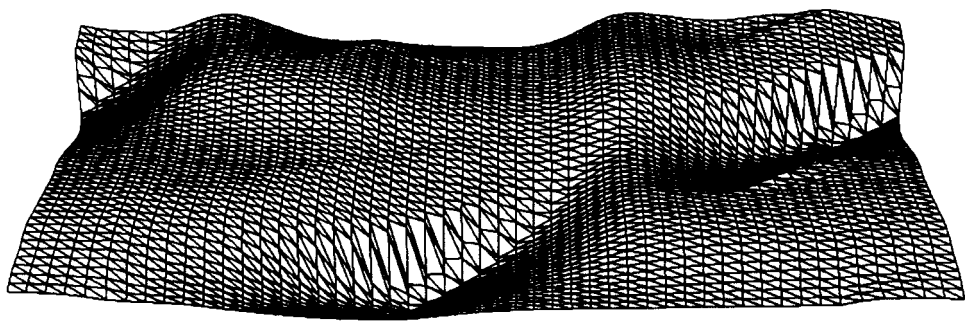

Figure 3.6: The flat surface of the torus $r_2(\theta_1, \theta_2)$ for $\delta = 0.2601$, $\beta_1 = \beta_2 = 0.55$. and $\alpha_1 = \alpha_2 = 1.0$ where $\theta_1$ is in the horizontal direction and $\theta_2$ in the vetical direction.

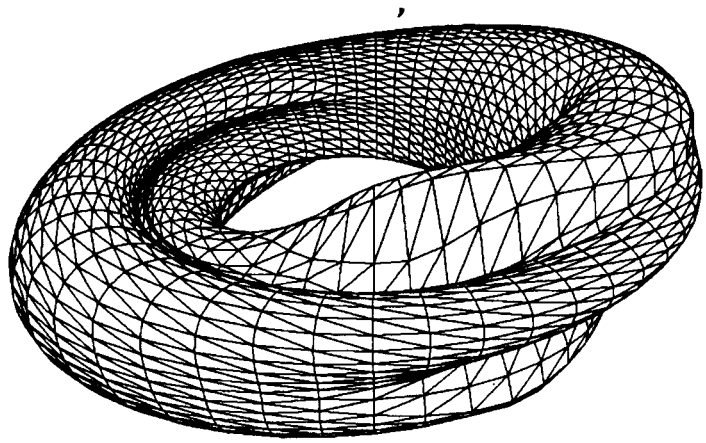

Figure 3.7: The torus $r_1(\theta_1, \theta_2)$ for $\delta = 0.2601$, $\beta_1 = \beta_2 = 0.55$. and $\alpha_1 = \alpha_2 = 1.0$

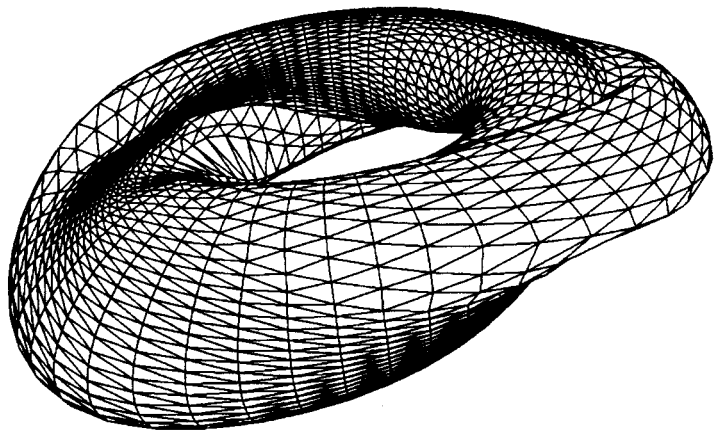

Figure 3.8: The torus $r_2(\theta_1, \theta_2)$ for $\delta = 0.2601$, $\beta_1 = \beta_2 = 0.55$. and $\alpha_1 = \alpha_2 = 1.0$

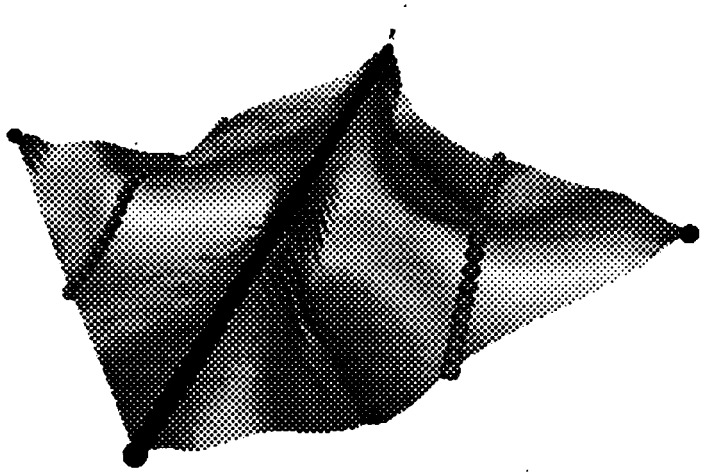

Figure 3.9: The flat surface of the torus $r_1(\theta_1, \theta_2)$ for $\delta = 0.2601$, $\beta_1 = \beta_2 = 0.55$. and $\alpha_1 = \alpha_2 = 1.0$ where $\theta_1$ is in the horizontal direction and $\theta_2$ in the vetical direction. The darker dots are the stable solution and the lighter dots are the unstable solution.

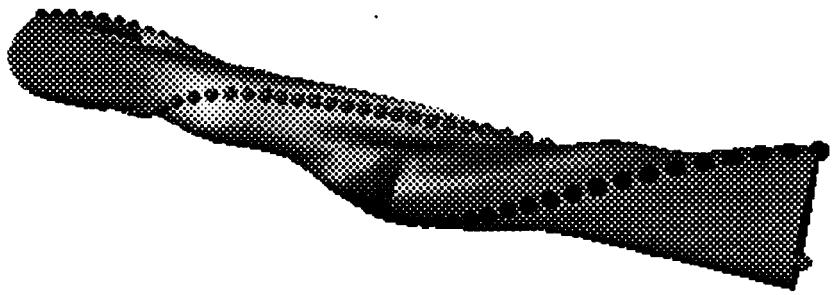

Figure 3.10: The cylindrical view of the torus $r_1(\theta_1, \theta_2)$ for $\delta = 0.2601$, $\beta_1 = \beta_2 = 0.55$. and $\alpha_1 = \alpha_2 = 1.0$. The darker dots are the stable solution and the lighter dots are the unstable solution.

# Chapter 4

# The PDE formulation

A partial differential equation approach has been used recently in various contexts for computing invariant tori for systems of ordinary differential equations. We present an $O(h^4)$ collocation method for solving these resulting nonlinear hyperbolic partial differential equations with periodic boundary conditions. A convergence proof is given and numerical results for the method contrasted with those of some previously tested methods. We also introduce an adaptive grid refinement scheme and use it to study the torus breakdown.

The purpose of this work is two fold. First, we consider a collocation discretization scheme for solving PDEs". Orthogonal collocation has been a popular method in areas such as chemical engineering ([F1],[LP]), where it has primarily been used to solve elliptic and parabolic partial differential equations (e.g.,[PR],PW]). Here we consider it for hyperbolic PDEs with periodic boundary conditions. In particular, we show $O(h^4)$ convergence and stability of the algorithm for a class of linear model problems. We adapt a block LU decomposition scheme of Wright [W] which takes the sparse block structure of the resulting collocation matrices into consideration and reduces the storage. The numerical scheme is tested on two problems. The first is a simple first order linear partial differential equation for which we show that the collocation scheme has the predicted accuracy. The second involves the computation of an invariant torus and issues related to the computation of such tori comprise the second major purpose of this paper. Here we propose the Hermite collocation method as a high order alternative for solving this problems. In particular we use a continuation in a bifurcation parameter to follow the torus for a coupled oscillator as it loses its smoothness. The results of our numerical scheme are compared with previous results for other numerical schemes. We show how to determine the cusp which characterizes

the loss of smoothness in the torus near breakdown and how to refine the mesh around it using an adaptive scheme.

We present the torus as a graph and parameterized it in terms of a subset of the variables of the original system. The condition that the torus is an invariant set for the original system leads to the solution of an equivalent system of first order PDEs with the same principal part and subject to periodic boundary conditions. This approach is used numerically in [DL1] where a leap-frog discretization scheme is selected and showed to be second order convergent for a constant coefficient problem. In [DL1], an upwind discretization for the partial differential equation is used and shown to be stable and first order convergent for the linear variable coefficient problem. In [DB] Dieci and Bader use a first order upwind scheme and iterative methods to solve the linear systems. They also use iterative schemes for smoothing with their multigrid methods, using as many as $320 \times 320$ grid points numerically. The large number of mesh points is necessary due to the low order convergence of the discretization scheme and because the torus becomes difficult to compute (see below).

## 4.1 Spline approximation

The basic tool that we need in this chapter is spline approximation to PDEs. We start with some definitions for splines approximation for ODEs and later extend some of these ideas to PDEs with periodic boundary conditions. Most of this work is from the books of Schumaker [Sc] and Archer et al. [AMR].

### 4.1.1 Spline approximation to ODEs

Define the space of **polynomials of order** $m$ by

$$P_m := \{p(x) : p(x) = \sum_{i=1}^{m} c_i x^{i-1}\}, \qquad c_1, \ldots, c_m, x \in \mathbf{R}. \tag{4.1}$$

For a given interval $[a, b]$, let

$$\Pi = \{a = x_0 < x_1 < x_2 < \cdots < x_N < x_{N+1} = b\} \tag{4.2}$$

be its partition and

$$I = \{I_i = [x_i, x_{i+1}),\ \ i = 0, \ldots, N-1 \cup I_N = [x_N, x_{N+1}]\}$$

the $N+1$ subintervals of the partition. For a given positive integer $m$, define $P_m^p(\Pi)$ the space of **piecewise polynomials of order** $m$ with knots $x_1, x_2, \ldots, x_N$ by

**Definition 4.1.1**

$$P_m^p(\Pi) = \begin{cases} f : \textit{there exists polynomials } p_0, p_1, \ldots, p_N \in P_m \\ \textit{with } f(x) = p_i(x) \textit{ for } x \in I_i, i = 0, \ldots, N. \end{cases} \tag{4.3}$$

If we let

$$S_m(\Pi) = P_m^p(\Pi) \cap C^{m-2}[a,b],$$

then we call $S_m(\Pi)$ the space of **polynomial splines of order m** with simple knots at the points $x_1, x_2, \ldots, x_N$.

Let $m$ be a positive integer and $\Lambda = (m_1, m_2, \ldots, m_N)$ a vector of integers with $1 \leq m_i \leq m$, $i = 1, 2, \ldots, N$. We call the space

$$S(P_m; \Lambda; \Pi) = \begin{cases} s : \textit{there exits polynomials } s_0, s_1, \ldots, s_N \textit{ in } P_m \\ \textit{such that } s(x) = s_i(x) \textit{ on } I_i, \quad i = 0, 1, \ldots, N, \textit{and} \\ D^j s_{i-1}(x_i) = D^{j-1} s_i(x_i), \; j = 0, \ldots, m-1-m_i \\ i = 1, 2, \ldots, N. \end{cases} \tag{4.4}$$

the space of **polynomial splines of order** $m$ with knots $x_1, x_2, \ldots, x_N$ of multiplicities $m_1, m_2, \ldots, m_N$. The vector of integers $\Lambda$ controls the smoothness of the splines at the knots.

- a) $m = m_i$ there may be no relationship between $s_{i-1}$ and $s_i$ at the knot $x_i$ and possibly even a jump discontinuity at $x_i$.
- b) $m_i < m$ the spline $s$ and its first $m - 1 - m_i$ derivatives are all continuous across the knot $x_i$.

The space defined above is a Sobolev space. We define a Sobolev space as follows: let the classical Lebesgue space be defined by

**Definition 4.1.2**

$$L_p[I] = \{f : f \textit{ is measurable on } I \textit{ and } \|f\|_p < \infty\} \tag{4.5}$$

*where*

$$\|f\|_p = \left[\int_a^b |f(x)|^p dx\right]^{1/p} \qquad 1 \leq p \leq \infty \tag{4.6}$$

$$\|f\|_\infty = ess\ sup_{x\in I}|f(x)|, \qquad p = \infty.$$

The Lebesgue space $L_p[I]$ is a Banach space for each $1 \le p \le \infty$ where $I$ is an interval. For a positive integer $r$ and a given $1 \le p \le \infty$, we define the space of **Sobolev space** $L_p^r[I]$ by

**Definition 4.1.3**

$$L_p^r[I] = \{f : D^{r-1}f \in AC[I] \qquad and \qquad D^r f \in L_p[I]\}, \tag{4.7}$$

with norm

$$\|f\|_{L_p^r[I]} = \sum_{j=0}^{r} \|D^j f\|_{L_p[I]}. \tag{4.8}$$

where $AC[I]$ is the space of absolutely continuous functions.

### Periodic Splines

We use periodic spline functions in our numerical approximations and most discussions will be on these type functions. Most of the properties discussed above carry over to the periodic case as well with some minor changes.

We now define $S(P_m, \Lambda, \Pi)$ the space of **periodic polynomial splines of order** $m$ **with knots at** $x_1, \ldots, x_N$ **of multiplicity** $m_1, m_2, \ldots, m_N$ by

$$S_p(P_m; \Lambda, \Pi) = \begin{cases} s : \textit{there exits polynomials } s_1, s_2, \ldots, s_N \textit{ of order m so} \\ \textit{that } s(x) = s_i(x) \textit{ on } I_i, i = 1, 2\ldots, N \textit{ and} \\ D^{j-1}s_{i-1}(x_i) = D^{j-1}s_i(x_i), j = 1, \ldots, m - m_i \\ i = 1, 2, \ldots, N, \textit{ where we take } s_0 = s_N \end{cases} \tag{4.9}$$

$$\textit{Periodic splines } S_p(P_m; \Lambda; \Pi) = \begin{cases} s \in S(P_m; \Lambda, \Pi) : s^j(b) = s^j(a) \\ j = 0, 1, \ldots, m-1 \end{cases} \tag{4.10}$$

### Tensor product splines

The idea here is to use spline functions to approximate the solutions to PDEs. We construct a space of multi-dimensional splines by taking the tensor-product of a one-dimensional space of polynomial splines.

If $\mathbf{x} \in \mathbf{R}^p$, then for each $i = 1, \ldots, p$, define the interval $[a_i, b_i]$, a positive $m_i$ and the partition

$$\Pi_i = \{a_i = \mathbf{x}_i^0 < \mathbf{x}_i^1 < \ldots < \mathbf{x}_i^{N_i+1} = b_i\} \tag{4.11}$$

of $[a_i, b_i]$ such that

$$\Lambda_i = (m_{i,1}, m_{i,2}, \ldots, m_{i,N_i}), \qquad 1 \le m_{i,j} \le m_i \qquad j = 1, 2, \ldots, N_i. \tag{4.12}$$

We define

**Definition 4.1.4** *The space of* **tensor-product polynomial splines** *by*

$$S = \otimes_{i=1}^{p} S(P_{m_i}; \Lambda_i; \Pi_i) = span\{\phi^{i_1}(\mathbf{x}_1), \cdots, \phi^{i_p}(\mathbf{x}_p)\}_{i_1=1, i_2=1, \ldots, i_p=1}^{m_1+K_1, m_2+K_2, \ldots m_p+K_p}. \tag{4.13}$$

The space $S$ is a linear space of dimension $\prod_{i=1}^{p}(m_i + K_i)$. Each spline $s$ in $S$ is a function defined on the set

$$H = \otimes_{i=1}^{d}[a_i, b_i] = \{\mathbf{x} = (x_1, x_2, \ldots, x_p) : a_i \le x_i \le b_i, \qquad i = 1, \ldots, p\} \tag{4.14}$$

The partition $\Pi = \Pi_1 \otimes \Pi_2 \otimes \ldots \otimes \Pi_p$ divides $H$ into smaller rectangles

$$H_{i_1 \cdots i_p} = \{\mathbf{x} : \mathbf{x}_j^{i_j} \le x_j \le \mathbf{x}_j^{i_j+1}, \qquad j = 1, 2, \ldots, p\}. \tag{4.15}$$

The theorem below shows that the tensor-product spline

$$s(x_1, \ldots, x_p) = \sum_{i_1=1}^{m_1+k_1} \cdots \sum_{i_d=1}^{m_d+k_d} c_{i_1 \cdots i_p} \phi^{i_1}(x_1) \cdots \phi^{i_p}(x_p) \tag{4.16}$$

for any $s \subset S$ is a smooth piecewise polynomial.

**Theorem 4.1.1** *If $s \in S$, then for each $i = 1, \ldots, p$ and any fixed $a_j \le x_j \le b_j$, $j = 1, 2, \ldots, i-1, i+1, \ldots, p$,*

$$s(x_1, \ldots, x_{i-1}, \cdot, x_{i+1}, \ldots, x_p) \in S(P_{m_i}; \Lambda_i; \Pi_i). \tag{4.17}$$

*Moreover, for all $0 \le i_j \le k_j$, $j = 1, \ldots, p$*

$$S|_{H_{i_1 \cdots i_d}} \in P_m,$$

*where*

$$P_m = \otimes_{i=1}^{p} P_{m_i} = span\{x_1^{\nu_1 - 1} \cdots x_d^{\nu_p - 1}\}_{\nu_1=1, \ldots, \nu_d=1}^{m_1, \ldots, m_p} \tag{4.18}$$

*is the space of tensor-product polynomials of order* $\mathbf{m} = (m_1, m_2, \ldots, m_p)$.

The exact smoothness of the splines $s \in S$ can be deduced from (4.16) since the partial derivatives

$$D_{x_1}^{\alpha_1} \cdots D_{x_p}^{\alpha_p} s(\mathbf{x}) = \sum_{i_1=1}^{m_1+K_1} \cdots \sum_{i_p=1}^{m_p+K_p} c_{i_1 \cdots i_d} D_{x_1}^{\alpha_1} \phi^{i_1}(x_1) \cdots D_{x_p}^{\alpha_p} \phi^{i_p}(x_p). \tag{4.19}$$

exist and are continuous inside the subrectangles. The smoothness across the faces between two such subrectangles is controlled by the multiplicity vectors $\Lambda_1, \Lambda_2, \ldots, \Lambda_p$.

### 4.1.2 Spline collocation for ODE boundary value problems

In this section we show how one can use the method of collocation to solve boundary value ODEs. Let X be a linear subspace of $L_r[D]$, $1 \leq r \leq \infty$, the space of square integrable functions on $D$, where $D$ is some subset of the real line $\mathbf{R}$ or the real plane $\mathbf{R} \times \mathbf{R}$. Let $L : X_{N+1} \to X_{N+1}$ be a linear operator on the $(N+1)$-dimensional subspace

$$X_{N+1} = span\{\phi_1, \phi_2, \ldots, \phi_{N+1}\} \tag{4.20}$$

of $X$, where the $\phi_i$'s are linearly independent functions. Consider the linear equation

$$Lu = b(u), \tag{4.21}$$

where $b$ is a given function in $X$ and let $u_c$ be the collocation approximation of (4.21) defined by

$$u_c(x) = \sum_{j=1}^{N+1} c_j \phi_j(x) \qquad a \leq x \leq b. \tag{4.22}$$

The parameters $c_j$ are determined by requiring $u_c(x)$ to satisfy $N+1$ conditions. These conditions include the boundary conditions and satisfying the ODE (4.21) at some points (the collocation points) in the interval $[a, b]$. This results in solving an $(N+1) \times (N+1)$ linear system of equations obtained from

$$Lu_c(x_i) = \sum_{j=1}^{N+1} c_j L\phi_j(x_i) = b(x_i), \qquad 1 \leq i \leq N+1. \tag{4.23}$$

The function $u_c(x)$, if it exists, is said to collocate $b(x)$ at the points $x_1, x_2, \ldots, x_{N+1}$ and is said to be the approximate solution obtained by the **method of collocation**.

**Example 4.1.1** *Consider the boundary value problem*

$$\begin{cases} Lu(x) = u'' + 2u' = 3, \\ u(0) = u(1) = 0. \end{cases} \tag{4.24}$$

*Let* $\phi_1(x) = x(x-1)$ *and* $\phi_2(x) = x^2(x-1)$ *then*

$$\begin{aligned} L\phi_1(0) &= 2, \\ L\phi_2(0) &= -2, \\ L\phi_1(1) &= 2, \\ L\phi_2(1) &= 4 \end{aligned} \tag{4.25}$$

*Let the collocation approximate solution be given by*

$$u_c(x) = a_1\phi_1(x) + a_2\phi_2(x). \tag{4.26}$$

*To determine $a_1$ and $a_2$ we collocate the right-hand side of the first equation in (4.24) at $x_1 = 0$ and $x_2 = 1$ to get the linear system*

$$\begin{pmatrix} 2 & 2 \\ -2 & 4 \end{pmatrix} \begin{pmatrix} a_1 \\ a_2 \end{pmatrix} = \begin{pmatrix} 1 \\ 1 \end{pmatrix}. \tag{4.27}$$

*Solving we get $a_1 = 1/6$, $a_2 = 1/3$, and equation (4.26) becomes*

$$u_c(x) = 1/6x(x-1) + 1/3x^2(x-1). \tag{4.28}$$

Two questions that we have to deal with when we want to improve on our results are:

- a) **how to chose the functions** $\phi_1, \phi_2, \ldots, \phi_{N+1}$

A good choice of the $\phi$'s are the spline functions. We will focus our analysis on the space of polynomial splines $S(P_k, \Lambda, \Pi)$ with the elements of $\Lambda$ satisfying the condition

$$m_1 = m_2 = \cdots = m_N = k.$$

For some knots $0 \leq \rho_1 \leq \rho_2 \leq, \ldots, \leq \rho_k \leq 1$, define the distinct points

$$x_{ij} = x_i + (x_{i+1} - x_i)\rho_j \qquad 1 \leq j \leq k \qquad 0 \leq i \leq N+1. \tag{4.29}$$

- b) **how to chose the knots** $\rho_i$, $i = 1, \ldots, k$

The answer to this question will be given shortly.

Consider a general (BVP)

$$\begin{aligned} &Nu \equiv u^{(q)} - f(x, u, u', \ldots, u^{(q-1)}) = 0, \qquad a < x < b \\ &g(\mathbf{u}(a), \mathbf{u}(b)) = 0 \end{aligned} \tag{4.30}$$

and define $\mathbf{u} := (u, u', \ldots, u^{q-1})$ where $\mathbf{u} \in \mathbf{R}^q$ and define its collocation approximation $u_c$ on the mesh $\Pi$. Each polynomial piece of $u_c$ defined on the interval $[x_i, x_{i+1}]$ has $k+q$ parameters to be determined and satisfies $q$ marching constraints for $\mathbf{u}_c$ across each mesh point, i.e. each polynomial piece in $[x_i, x_{i+1}]$

- a) satisfies $q$ boundary conditions

- b) satisfies the ODE (4.30) at $k$ points in each of the $N+1$ subintervals of the mesh $\Pi$.

The total number of conditions to be satisfied in all the intervals is given by

$$(N+1)(k+q) - Nq = (N+1)k + q. \tag{4.31}$$

The collocation method then determines an approximate solution defined on $[a,b]$ such that

$$u_c(x) \in C[a,b]; \qquad u_c(x) \in S(P_m, \Lambda, \Pi) \tag{4.32}$$

$$g(\mathbf{u}_c(a), \mathbf{u}_c(b)) = 0$$

$$Nu_c(x_{ij}) \equiv u_c' - f(x_{ij}, \mathbf{u}_c(x_{ij})) = 0 \qquad 1 \le j \le k, \qquad 1 \le i \le N+1. \tag{4.33}$$

Normally the spline functions used are Hermite-type or B-splines basis functions. The basis functions in such cases have local support and satisfy the continuity conditions on $u_c$ while the collocation equations are satisfied later. With such basis functions, the linear system resulting from equation (4.33) and the boundary condition has a block banded matrix of the form,

$$\begin{bmatrix} V_1 & & & \\ & V_2 & & \\ & & \ddots & \\ & & & V_{N+1} \\ W_1 & & & W_2 \end{bmatrix}, \tag{4.34}$$

where $V_1, V_2, \cdots, V_N \in \mathbf{R}^{k\times(k+q)}$ and $W_1, W_2 \in \mathbf{R}^{m\times(k+q)}$.

The collocation scheme has $O(h^2)$ convergence and when $f$ is smooth enough one can get $0(h^3)$ convergence. Moreover, collocating at Gaussian knots using a basis of piecewise cubic Hermite polynomials gives an $O(h^4)$ order of convergence for a second-order boundary value problem.

### 4.1.3 Spline collocation for periodic PDEs

The existence theorems for the collocation approximations to partial differential equations are some what harder to come by than for the collocation solutions to ordinary differential

equations. This happens because one does not usually recognize the image of the approximate $\mathbf{u}_c$ under the linear operator $L$ or the non-linear operator $N$ even in the simplest case

$$L = -\triangle. \tag{4.35}$$

Thus the interpolatory capacities of $\triangle \mathbf{u}_c$ are not readily apparent in contrast to the ODE case.

Consider the linear PDE

$$L\mathbf{u}(\mathbf{x}) = b(\mathbf{x}), \tag{4.36}$$

with $\mathbf{x} \in S^p$, $p \geq 2$, $\mathbf{u} \in \mathbf{R}^q$ and the intervals $[a_i, b_i]$ with the mesh

$$\Pi_i = \{a_i = \mathbf{x}_{i0} < \mathbf{x}_{i1} < \ldots < \mathbf{x}_{iN_i} = b_i\} \tag{4.37}$$

for $i = 1, \ldots, p$. Define the vectors

$$\Lambda_i = (m_{i1}, m_{i2}, \ldots, m_{iN_i}) \qquad i = 1, \ldots, p \tag{4.38}$$

such that all the $m_{ij} = k$. The periodic spline space $S_p(P_{m_i}; \Lambda_i; \Pi_i)$ is an $M_i$- dimensional linear space, where

$$M_i = \sum_{j=1}^{N_i} m_{ij} \tag{4.39}$$

and

$$S_p(P_m; \Lambda_i; \Pi_i) = span\{\phi_{ij}(x_i)\}_{j=1}^{M_i}. \tag{4.40}$$

We define the space of tensor-product polynomial splines by

$$S := \otimes_{i=1}^{p} S_p(P_{m_i}; \Lambda_i; \Pi_i) = span\{\phi^{i_1}(x_1), \cdots, \phi^{i_p}(x_p)\}_{i_1=1,\ldots,i_p=1}^{K_i, K_2, \ldots K_p} \tag{4.41}$$

where $S$ is a linear space of dimension

$$M = \prod_{i=1}^{p} M_i. \tag{4.42}$$

Let $\mathbf{u}_c$ be a smooth spline piecewise polynomial defined by

$$\mathbf{u}_c(x_1, \ldots, x_p) := \sum_{i_1=1}^{M_1} \cdots \sum_{i_p=1}^{M_p} c_{i_1 \cdots i_p} \phi^{i_1}(x_1) \cdots \phi^{i_p}(x_p) \tag{4.43}$$

on the set

$$H = \otimes_{i=1}^{p} [a_i, b_i] = \{\mathbf{x} = (x_1, x_2, \ldots, x_p) : a_i \leq x_i \leq b_i,\ i = 1, \ldots, p\}. \tag{4.44}$$

The partition $\Pi = \Pi_1 \otimes \Pi_2 \otimes \ldots \otimes \Pi_p$ subdivides $H$ into smaller rectangles

$$H_{i_1 \cdots i_d} = \{\mathbf{x} = x_{ji_j} \leq x_j < x_{ji_j+1}, i = 1, 2, \ldots, d\}. \tag{4.45}$$

The partial derivatives

$$D_{x_1}^{\alpha_1} \cdots D_{x_p}^{\alpha_p} \mathbf{u}_c(\mathbf{x}) = \sum_{i_1=1}^{M_1} \cdots \sum_{i_d=1}^{M_p} c_{i_1 \cdots i_d} D_{x_1}^{\alpha_1} \phi_{i_1}(x_1) \cdots D_{x_d}^{\alpha_p} \phi_{i_d}(x_p) \tag{4.46}$$

exist and are continuous inside the subrectangles and the smoothness across the faces between two such subrectangles is controlled by the multiplicity vectors $\Lambda_1, \Lambda_2, \ldots, \Lambda_p$.

Substituting $\mathbf{u}_c$ into (4.36) at the points $\mathbf{x}_{ij}$ we get the collocation system

$$L\mathbf{u}(\mathbf{x}_{ij}) = b(\mathbf{x}_{ij}). \tag{4.47}$$

If we let $q = 1$ and $N_1 = N_2 = \cdots = N_p = N$, then equation (4.47) plus the boundary conditions has an associated collocation matrix of the form

$$A = \begin{bmatrix} V_1 & & & \\ & V_2 & & \\ & & \ddots & \\ & & & V_N \\ W_1 & & & W_2 \end{bmatrix}, \tag{4.48}$$

where $A \in \mathbf{R}^{M \times M}$.

## 4.2 Numerical formulation

The basic dynamical system we consider is the autonomous system of equations

$$\dot{\mathbf{x}} = F(x, \lambda), \quad x \in \mathbf{R}^n, \quad \lambda \in \mathbf{R}^1, \tag{4.49}$$

where $\mathbf{x} := (x_1, x_2, ..., x_n)$. We assume for simplicity that a suitable re-parametrization can be found such that the system (4.49) can be rewritten as

$$\begin{pmatrix} \dot{\theta} \\ \dot{\mathbf{r}} \end{pmatrix} = \begin{pmatrix} f(\mathbf{r}, \theta) \\ g(\mathbf{r}, \theta) \end{pmatrix} \qquad \mathbf{r} \in V \subset \mathbf{R}^q, \qquad \theta \in U \subset S^p, \tag{4.50}$$

where $V$ and $U$ are open sets in $\mathbf{R}^q$ and
$S^p = \{\theta = (\theta_1, \theta_2, ..., \theta_p) | \theta_j \in (\mathbf{R} \, mod \, 2\pi), \; j = 1, \ldots, p\}$, respectively, $f : S^p \times \mathbf{R}^q \longrightarrow \mathbf{R}^p$

and $g : S^p \times \mathbf{R}^q \longrightarrow \mathbf{R}^p$ are smooth functions. A treatment of a general parametrization is given in [DL2]. Suppose further that the torus denoted by the manifold

$$M = \{(\theta, \mathbf{r}(\theta)) | \theta \in S^p\},$$

is invariant under the flow (4.50), implying that $\mathbf{r}(\theta) : U \longrightarrow V$ solves the PDE

$$\sum_{j=1}^{p} f_j(\theta, \mathbf{r}(\theta)) \partial r_i(\theta)/\partial\theta_j = g(\theta, \mathbf{r}(\theta)), \quad i = 1, ..., q, \tag{4.51}$$

with periodic boundary conditions

$$r_i(\theta_1, ..., \theta_{j-1}, 0, \theta_{j+1}, ..., \theta_p) = r_i(\theta_1, ..., \theta_{j-1}, 2\pi, \theta_{j+1}, ..., \theta_p), \tag{4.52}$$

$i = 1, ..., q, \quad j = 1, ..., p$ [S].

This system of nonlinear hyperbolic equations can be solved using Newton method. If $\mathbf{r}^0$ denotes an initial approximation to
$\mathbf{r}(\theta) = (r_1(\theta), r_2(\theta), ..., r_q(\theta))^T$, then the next Newton iterate $\mathbf{r}^1$ (implicitly satisfying the boundary conditions (4.52)) satisfies

$$\sum_{j=1}^{p} f_j^0 \frac{\partial \mathbf{r}^1}{\partial \theta_j} + \left\{ \sum_{j=1}^{p} \frac{\partial \mathbf{r}^0}{\partial \theta_j} \bigtriangledown f_j^0 \right\} (\mathbf{r}^1 - \mathbf{r}^0) = g^0 + G^0(\mathbf{r}^1 - \mathbf{r}^0), \tag{4.53}$$

where

$$f_j^0 := f_j(\theta, \mathbf{r}^0), \qquad \bigtriangledown f_j^0 := \left( \frac{\partial f_j}{\partial r_1}, ..., \frac{\partial f_j}{\partial r_q} \right) (\theta, \mathbf{r}^0),$$

$$g^0 := g(\theta, \mathbf{r}^0), \qquad G^0 := \begin{bmatrix} \bigtriangledown g_1^0 \\ \vdots \\ \bigtriangledown g_q^0 \end{bmatrix} \text{ and } \bigtriangledown g_j^0 := \left( \frac{\partial g_j}{\partial r_1}, ..., \frac{\partial g_j}{\partial r_q} \right) (\theta, \mathbf{r}^0).$$

Rearranging, we get the linear first order hyperbolic system

$$L(\mathbf{r}^1(\theta)) := \sum_{j=1}^{p} f_j^0 \frac{\partial \mathbf{r}^1}{\partial \theta_j} + c^0(\theta)\mathbf{r}^1 = b^0(\theta) \tag{4.54}$$

where

$$c^0(\theta) = \{ \sum_{j}^{p} \frac{\partial \mathbf{r}^0}{\partial \theta_j} \bigtriangledown f_j^0 - G^0 \} \text{ and } b^0(\theta) = \{ \sum_{j=1}^{p} \frac{\partial \mathbf{r}^0}{\partial \theta_j} \bigtriangledown f_j^0 \} \mathbf{r}^0 + g^0 - G^0 \mathbf{r}^0. \tag{4.55}$$

In the case of a single two-torus ($p = 2$, $q = 1$), this further reduces to

$$L(r^1(\theta)) := \sum_{j=1}^{2} f_j^0 \frac{\partial r^1}{\partial \theta_j} + c^0(\theta) r^1 = b^0(\theta) \tag{4.56}$$

where

$$c^0(\theta) = -g_r^0 + f_{1r} r_{\theta_1}^0 + f_{2r} r_{\theta_2}^0 \quad \text{and} \quad b^0(\theta) = g^0 + [-g_r^0 + f_{1r} r_{\theta_1}^0 + f_{2r} r_{\theta_2}^0] r^0.$$

We shall discretize these equations using orthogonal collocation.

### 4.2.1 Orthogonal collocation discretization

In this section we give a basic formulation of orthogonal collocation method for solving hyperbolic partial differential equations of the form (4.54) with periodic boundary conditions. In particular, we consider a p-dimensional Hermite cubic collocation discretization. Given a mesh

$$\Pi : 0 = \theta_j^1 < \theta_j^2 < \ldots < \theta_j^{N_j+1} = 2\pi, \quad j = 1, ..., p,$$

with $h_j^i = \theta_j^{i+1} - \theta_j^i$ and $\theta = (\theta_1, \theta_2, \ldots, \theta_p)$, a Hermite p-cubic collocation approximation to $\mathbf{r}(\theta)$ defined on the mesh is given by

$$\mathbf{r}_c(\theta) := \sum_{k_1}^{2N_1+2} \sum_{k_2}^{2N_2+2} \cdots \sum_{k_p}^{2N_p+2} r_{k_1 k_2 \cdots k_p} \phi^{k_1}(\theta_1) \cdots \phi^{k_p}(\theta_p). \tag{4.57}$$

The standard cubic Hermite basis functions are given by

$$\phi^{2i-1}(\theta_j) = \begin{cases} \left(\frac{\theta_j - \theta_j^{i-1}}{h_j^{i-1}}\right)^2 \left(3 - \frac{2(\theta_j - \theta_j^{i-1})}{h_j^{i-1}}\right), & \theta_j \in [\theta_j^{i-1}, \theta_j^i], \\ \left(1 - \frac{\theta_j - \theta_j^i}{h_j^i}\right)^2 \left(1 - \frac{2(\theta_j - \theta_j^i)}{h_j^i}\right), & \theta_j \in [\theta_j^i, \theta_j^{i+1}], \\ 0, & \textit{other}, \end{cases} \tag{4.58}$$

$$\phi^{2i}(\theta_j) = \begin{cases} -h_j^{i-1} \left(\frac{\theta_j - \theta_j^{i-1}}{h_j^{i-1}}\right)^2 \left(1 - \frac{(\theta_j - \theta_j^{i-1})}{h_j^{i-1}}\right), & \theta_j \in [\theta_j^{i-1}, \theta_j^i], \\ h_j^i \left(1 - \frac{\theta_j - \theta_j^i}{h_j^i}\right)^2 \left(\frac{(\theta_j - \theta_j^i)}{h_j^i}\right), & \theta_j \in [\theta_j^i, \theta_j^{i+1}], \\ 0, & \textit{other}. \end{cases} \tag{4.59}$$

Differentiating (4.57) gives

$$\frac{\partial \mathbf{r}_c(\theta)}{\partial \theta_j} = \sum_{k_1}^{2N_1+2} \cdots \sum_{k_p}^{2N_2+2} r_{k_1 \cdots k_p} \phi^{k_1}(\theta_1) \cdots \phi^{k_{j-1}}(\theta_{j-1}) \frac{\partial \phi^{k_j}(\theta_j)}{\partial \theta_j} \phi^{k_{j+1}}(\theta_{j+1}) \cdots \phi^{k_p}(\theta_p). \tag{4.60}$$

Using collocation points $(\epsilon_1^{i_1}, \epsilon_2^{i_2}, \ldots, \epsilon_p^{i_p})$ defined by

$$\epsilon_j^{2i-1} := \frac{1}{2}(\theta_j^{i-1} + \theta_j^i) - \frac{h_j^i}{2\sqrt{3}}, \qquad \epsilon_j^{2i} := \frac{1}{2}(\theta_j^{i-1} + \theta_j^i) + \frac{h_j^i}{2\sqrt{3}},$$

we obtain the collocation equations

$$L(\mathbf{r}^1(\epsilon_j^i)) = b^0(\epsilon_j^i), \qquad j = 1, \ldots, p, \qquad i = 1, \cdots, N_j. \tag{4.61}$$

In order to write this in matrix form, define the $2N_j \times 2N_j$ matrices $C_j$ and $B_j$, $j = 1, \ldots, p$, by

$$(C_j)_{im} := \phi^m(\epsilon_j^i), \qquad (B_j)_{im} := \frac{\partial \phi^m(\epsilon_j^i)}{\partial \theta_j}, \tag{4.62}$$

and let

$$M_j = 2N_j, \quad M = \Pi_{j=1}^p M_j$$

and $(\mathbf{r}_c)_{mesh} \in \mathbf{R}^M$ be the coefficients of $\mathbf{r}_c$ in (4.57) and $(\mathbf{r}_c)_{coll} \in \mathbf{R}^M$ be the solution values at the collocation points. From (4.57)

$$(\mathbf{r}_c)_{coll} = [C_1 \otimes C_2 \otimes \cdots \otimes C_p](\mathbf{r}_c)_{mesh}. \tag{4.63}$$

From (4.60)

$$\left(\frac{\partial \mathbf{r}_c}{\partial \theta_j}\right)_{coll} = [C_1 \otimes C_2 \otimes \cdots \otimes C_{j-1} \otimes B_j \otimes C_{j+1} \otimes \cdots \otimes C_p](\mathbf{r}_c)_{mesh}. \tag{4.64}$$

For the special case $p = 2$ and $q = 1$, (4.63) becomes

$$(\mathbf{r}_c)_{coll} = [C_1 \otimes C_2](\mathbf{r}_c)_{mesh}.$$

From (4.64),

$$\left(\frac{\partial \mathbf{r}_c}{\partial \theta_1}\right)_{coll} = [B_1 \otimes C_2](\mathbf{r}_c)_{mesh} \quad \text{and} \quad \left(\frac{\partial \mathbf{r}_c}{\partial \theta_2}\right)_{coll} = [C_1 \otimes B_2](\mathbf{r}_c)_{mesh}.$$

Defining $F_i, G \in \mathbf{R}^{M \times M}, i = 1, 2$ and $b_c \in \mathbf{R}^M$, by

$$F_i := diag(f_i(\epsilon_1^1, \epsilon_2^1, r^0(\epsilon_1^1, \epsilon_2^1)), f_i(\epsilon_1^1, \epsilon_2^2, r^0(\epsilon_1^1, \epsilon_2^2)), \ldots, f_i(\epsilon_1^{M_1}, \epsilon_2^{M_2}, r^0(\epsilon_1^{M_1}, \epsilon_2^{M_2}))),$$

$$G := diag(c^0(\epsilon_1^1, \epsilon_2^1, r^0(\epsilon_1^1, \epsilon_2^1)), c^0(\epsilon_1^1, \epsilon_2^2, r^0(\epsilon_1^1, \epsilon_2^2)), \ldots, c^0(\epsilon_1^{M_1}, \epsilon_2^{M_2}, r^0(\epsilon_1^{M_1}, \epsilon_2^{M_2}))),$$

$$b_c := (b^0(\epsilon_1^1, \epsilon_2^1, r^0(\epsilon_1^1, \epsilon_2^1)), b^0(\epsilon_1^1, \epsilon_2^2, r^0(\epsilon_1^1, \epsilon_2^2)), \ldots, b^0(\epsilon_1^{M_1}, \epsilon_2^{M_2}, r^0(\epsilon_1^{M_1}, \epsilon_2^{M_2})))^T,$$

and substituting these into (4.61), we obtain the linear system of equations

$$[F_1 \cdot (B_1 \otimes C_2) + F_2 \cdot (C_1 \otimes B_2) - G \cdot (C_1 \otimes C_2)](\mathbf{r}_c)_{mesh} = b_c.$$

The coefficient matrix has the sparse structure

$$\begin{bmatrix}
x & x & x & x & & & & \\
x & x & x & x & & & & \\
 & & x & x & x & x & & \\
 & & x & x & x & x & & \\
 & & & \ddots & \ddots & \ddots & \ddots & \\
 & & & & x & x & x & x \\
 & & & & x & x & x & x \\
x & x & & & & & x & x \\
x & x & & & & & x & x
\end{bmatrix}. \tag{4.65}$$

### 4.2.2 Stability and convergence analysis

In this section we study the accuracy and numerical stability of the collocation algorithm for the linear case

$$\begin{aligned} &\dot{\theta}_j = \omega_j, \qquad j = 1, 2, \ldots, p, \\ &\dot{\mathbf{r}} = -A\mathbf{r} + \Phi(\theta) \end{aligned} \tag{4.66}$$

where $A$ is a $q \times q$ constant matrix and we assume that $\Phi$ is a smooth function. The corresponding PDE system of (4.54) is

$$\omega_1 \frac{\partial \mathbf{r}}{\partial \theta_1} + \omega_2 \frac{\partial \mathbf{r}}{\partial \theta_2} + \cdots + \omega_p \frac{\partial \mathbf{r}}{\partial \theta_p} + A\mathbf{r} = \Phi(\theta), \qquad \theta \in S^p \tag{4.67}$$

with periodic boundary conditions.

This case is analyzed in [DLR] for a finite difference scheme, where it is shown that (4.67) has a unique solution if

$$a_m := min\{Re[\lambda(A)]\} \neq 0, \tag{4.68}$$

where $\lambda(A)$ denote the eigenvalues of $A$. The analysis in this case follows [ERS].

The collocation system now has the form

$$\begin{aligned} I_q \otimes \left(\textstyle\sum_{i=1}^{p} \omega_i (C_1 \otimes \cdots \otimes C_{j-1} \otimes B_j \otimes C_{j+1} \cdots \otimes C_p)\right)(\mathbf{r}_c)_{mesh} + \\ A \otimes (C_1 \otimes \cdots \otimes C_p)(\mathbf{r}_c)_{mesh} = \Phi_c. \end{aligned} \tag{4.69}$$

Here, $I_q$ denotes the $q \times q$ identity matrix and $\mathcal{C}_j$ and $B_j$, $j = 1, 2, \ldots, p$, are defined in (4.62). We rewrite (4.69) as

$$A_c(\mathbf{r}_c)_{mesh} = \Phi_c. \tag{4.70}$$

Some basic properties of tensor products are summarized below.

**Lemma 4.1.** *The tensor product $\otimes$ satisfies*

$$\begin{aligned}
&(U_1 + U_2) \otimes V = U_1 \otimes V + U_2 \otimes V;\\
&U \otimes (V_1 + V_2) = U \otimes V_1 + U \otimes V_2;\\
&(U_1 \otimes U_2)(V_1 \otimes V_2) = (U_1 V_1) \otimes (U_2 V_2).
\end{aligned}$$

Let $\|u\|_2$ denote the Euclidean norm for $u \in \mathbf{R}^M$. The following Lemma, whose proof parallels that in [RS], gives the eigen structure of $B_j C_j^{-1}$.

**Lemma 4.2.** *Let $B_j$ and $C_j$ be defined in (4.62). Then*

*(i) for each pair $B_j$ and $C_j$ there exists a nonsingular matrix $Q_j$ such that*

$$Q_j \Lambda_j Q_j^{-1} = B_j C_j^{-1}, \qquad \Lambda_j = diag(\lambda_{j1}, \lambda_{j2}, \ldots, \lambda_{jN_j});$$

*(ii) the eigenvalues of $B_j C_j^{-1}$ are purely imaginary;*

*(iii) there exists a constant $a_0$ independent of the partition $\Pi$ such that*

$$\|Q_j\|_2 \cdot \|Q_j^{-1}\|_2 \le a_0, \qquad j = 1, 2, \ldots, p.$$

**Theorem 4.1.** *If (4.68) holds and (4.70) is a Hermite cubic collocation system of equations for (4.67) using a uniform mesh in each coordinate direction, then*

*(i) (4.69) has a unique solution and*

*(ii) the collocation algorithm is stable in the sense*

$$\|(\mathbf{r}_c)_{mesh}\|_2 \le a_1 \|\Phi_c\|_2 \tag{4.71}$$

*where $a_1$ is a constant independent of the partition $\Pi$.*

**Proof.** We rewrite (4.69) as

$$\begin{aligned}
I_q \otimes \left(\textstyle\sum_{j=1}^{p} \omega_j (I^{(1)} \otimes \cdots \otimes I^{(j-1)} \otimes B_j C_j^{-1} \otimes I^{(j+1)} \otimes \cdots \otimes I^{(p)})\right) (\mathbf{r}_c)_{coll}\\
+ A \otimes \left(I^{(1)} \otimes \cdots \otimes I^{(p)}\right) (\mathbf{r}_c)_{coll} \;=\; \Phi_c
\end{aligned} \tag{4.72}$$

where $I^{(j)}$ denotes the $M_j \times M_j$ identity matrix, $j = 1, 2, \ldots, p$ and $(\mathbf{r}_c)_{coll}$ is defined in (4.63). Using a similarity transform with $T = I_q \otimes (Q_1 \otimes Q_2 \otimes \cdots \otimes Q_p)$, (4.72) becomes

$$\begin{array}{c} I_q \otimes \left( \sum_{j=1}^{p} \omega_j (I^{(1)} \otimes \cdots \otimes I^{(j-1)} \otimes \Lambda_j \otimes I^{(j+1)} \otimes \cdots \otimes I^{(p)}) \right) \tilde{\mathbf{r}}_c \\ + A \otimes \left( I^{(1)} \otimes \cdots \otimes I^{(p)} \right) \tilde{\mathbf{r}}_c = \tilde{\Phi}_c \end{array} \tag{4.73}$$

where

$$\tilde{\mathbf{r}}_c := T(\mathbf{r}_c)_{coll}, \qquad \tilde{\Phi}_c := T\Phi_c. \tag{4.74}$$

The system (4.73) is block diagonal with $q \times q$ diagonal blocks given by

$$D_{k_1,k_2,\ldots,k_p} := \sum_{j=1}^{p} (\omega_j \lambda_{jk_j}) I_q + A, \qquad k_j = 1, 2, \ldots, M_j;\ j = 1, 2, \ldots, p. \tag{4.75}$$

The eigenvalues of $D_{k_1,k_2,\ldots,k_p}$ can be expressed as

$$\lambda(D_{k_1,k_2,\ldots,k_p}) = \left( \sum_{j=1}^{p} \omega_j \lambda_{jk_j} \right) + \lambda(A).$$

By Lemma 4.2 $Re[\lambda_{jk_j}] = 0$, and

$$|Re[\lambda(A_c)]| = |Re[\lambda(A)]| \geq |a_m| > 0. \tag{4.76}$$

Thus $A_c$ is nonsingular, and (i) follows.

In order to prove (ii), let

$$\begin{cases} C = C_1 \otimes \cdots \otimes C_p, \\ Q = Q_1 \otimes Q_2 \otimes \cdots \otimes Q_p, \\ D = \sum_{j=1}^{p} \left( I^{(1)} \otimes \cdots \otimes I^{(j-1)} \otimes \Lambda_j \otimes I^{(j+1)} \otimes \cdots \otimes I^{(p)} \right), \\ \tilde{I} = I^{(1)} \otimes \cdots \otimes I^{(p)}, \end{cases} \tag{4.77}$$

where $D$ has the simple form

$$D := diag(d_1, d_2, \ldots, d_M).$$

We rewrite $A_c$ as

$$A_c = (I_q \otimes Q)^{-1} \cdot \left( I_q \otimes D + A \otimes \tilde{I} \right) \cdot (I_q \otimes Q) \cdot (I_q \otimes C). \tag{4.78}$$

Since $A_c$ is nonsingular, from (4.70)

$$\|(\mathbf{r}_c)_{mesh}\|_2 \leq \|A_c^{-1}\|_2 . \|\Phi_c\|_2 \tag{4.79}$$

and therefore,

$$\|(r_c)_{mesh}\|_2 \leq \|(I_q \otimes C)^{-1}\|_2 \cdot \|(I_q \otimes Q)^{-1}\|_2 \cdot \| \left(I_q \otimes D + A \otimes \tilde{I}\right)^{-1} \|_2 \cdot \|(I_q \otimes Q)\|_2 \cdot \|\Phi_c\|_2. \tag{4.80}$$

Using (4.77) and Lemma 4.2, we have

$$\begin{aligned} \|I_q \otimes Q\|_2 \cdot \|(I_q \otimes Q)^{-1}\|_2 &= \|Q\|_2 \cdot \|Q^{-1}\|_2 \\ &= \left(\prod_{j=1}^{p} \|Q_j\|_2\right) \cdot \left(\prod_{j=1}^{p} \|Q_j^{-1}\|_2\right) \leq K_1, \end{aligned} \tag{4.81}$$

and

$$\begin{aligned} \| \left(I_q \otimes D + A \otimes \tilde{I}\right)^{-1} \|_2 &= \|(D \otimes I_q + \tilde{I} \otimes A)^{-1}\|_2 \\ &= \max_l \|(d_l I_q + A)^{-1}\|_2 \leq K_2 \end{aligned} \tag{4.82}$$

for suitable constants $K_1$ and $K_2$ independent of the partition $\Pi$. Now (ii) is proved by substituting equations (4.81)-(4.82) into (4.80) and noting that for a suitable constant $K_3$

$$\|I \otimes C\|_2 \leq \max_i\{\|C_i\|_2\} \leq K_3. \quad \blacksquare$$

To analyze the accuracy of the orthogonal collocation approximation to (4.67), we assume that the mesh is uniform, the step size $h$ is the same in any coordinate direction and the eigenvalues of the matrix $A$ satisfies the condition $Re(\lambda(A)) > 0$ such that

$$a_0\|\mathbf{u}\|_{L^2}^2 \leq \int_{S^p} \mathbf{u}^T A \mathbf{u} d\Omega, \qquad \text{for any } \mathbf{u}(\theta) \in \mathbf{R}^q, \tag{4.83}$$

where $a^0$ is a constant and $\|\mathbf{u}\|_{L^2}^2 = \int_{S^p} \mathbf{u}^T \mathbf{u} d\Omega$.

**Theorem 4.2.** *Suppose that (4.83) holds and that* $\mathbf{r}(\theta)$ *and* $\mathbf{r}_c(\theta)$ *are the solution of (4.67) and the corresponding collocation system (4.70), respectively. Then there exists a constant* $a_1$ *independent of the partition* $\Pi$ *such that*

$$\|\mathbf{r} - \mathbf{r}_c\|_{L^2} \leq a_1 h^4 \tag{4.84}$$

**Proof.** If $\mathbf{e}(\theta) := \mathbf{r}(\theta) - \mathbf{r}_c(\theta)$, then from (4.67)

$$\omega_1 \frac{\partial \mathbf{e}}{\partial \theta_1} + \omega_2 \frac{\partial \mathbf{e}}{\partial \theta_2} + \cdots + \omega_p \frac{\partial \mathbf{e}}{\partial \theta_p} + A\mathbf{e} = \Psi \tag{4.85}$$

where $\Psi(\theta) = 0$ at the Gauss points.

Multiplying (4.85) by $\mathbf{e}^T(\theta)$ and integrating it gives

$$\omega_1 \int_{S^p} \mathbf{e}^T \frac{\partial \mathbf{e}}{\partial \theta_1} d\Omega + \cdots + \omega_p \int_{S^p} \mathbf{e}^T \frac{\partial \mathbf{e}}{\partial \theta_p} d\Omega + \int_{S^p} \mathbf{e}^T A \mathbf{e} d\Omega = \int_{S^p} \mathbf{e}^T \Psi d\Omega. \tag{4.86}$$

The error $\mathbf{e}(\theta)$ satisfies periodic boundary conditions, and we have

$$\int_{S^p} \mathbf{e}^T \frac{\partial \mathbf{e}}{\partial \theta_j} d\Omega = 0, \qquad j = 1, 2, \ldots, p,$$

so (4.86) gives

$$\int_{S^p} \mathbf{e}^T A \mathbf{e} d\Omega = \int_{S^p} \mathbf{e}^T \Psi d\Omega. \tag{4.87}$$

By Hölder's inequality, we have

$$\int_{S^p} \mathbf{e}^T \Psi d\Omega \leq \|\mathbf{e}\|_{L^2} \cdot \|\Psi\|_{L^2}. \tag{4.88}$$

Since $\mathbf{r}(\theta)$ is the unique solution of (4.67) and is smooth enough, standard arguments show (*e.g.*, see [PR]) that

$$\|\Psi\|_{L^2} = O(h^4), \tag{4.89}$$

and thus, from (4.83), (4.87) - (4.89),

$$a_0 \|\mathbf{e}\|_{L^2}^2 \leq \int_{S^p} \mathbf{e}^T A \mathbf{e} d\Omega \leq \|\mathbf{e}\|_{L^2} O(h^4). \tag{4.90}$$

which implies that

$$a_0 \|\mathbf{e}\|_{L^2} \leq O(h^4). \quad \blacksquare \tag{4.91}$$

*Remarks*

(i) Although the proof of Theorem 4.2 is given for the case of a uniform mesh and Hermite cubic splines, it also holds for non-uniform meshes where $h$ represents the maximal step size. For orthogonal collocation method with $k$th order splines, the argument generalizes to give $O(h^{2k})$ accuracy. Also, recall that the leap-frog algorithm [DLR] gives $O(h^2)$ accuracy for a uniform mesh and $O(h)$ for non-uniform meshes.

(ii) It has been noted that when the solution is sufficiently smooth Hermite cubic collocation has fourth-order accuracy in the norm $\|\cdot\|_\infty$ for two-point boundary value problems [DS] and in the norm $\|\cdot\|_{L^2}$ for two-dimensional elliptic problems [PR]. Theorem 4.2 shows that the accuracy for this hyperbolic problem is the same as for two-dimensional elliptic problems. Numerical experiments indicate that this is an optimal estimate.

(iii) The proof of stability is given under the assumption (4.83), which implies attractivity of the invariant manifold.

## 4.3 Numerical Results

In this section, we apply the collocation scheme described above to two problems. While the numerical algorithm can in principle be used to compute an $n$-dimensional torus, we restrict our examples to a 2-torus. The first example is chosen as an artificial linear hyperbolic partial differential equation with a known analytic solution in order to illustrate the high order accuracy of the algorithm. The second is a system of two-coupled oscillators. The solution set displays rich behavior [ADO] and is a challenging numerical problem [DLR]. The third example is the van der Pol equation. The collocation matrix (4.65) has a block structure for which we use the LU codes provided by [W] Wright. This considerably reduces the matrix storage requirements. The computations were done on a SUN Sparc 20 workstation and the figures were produced on an SGI Indigo 2 Extreme.

### 4.3.1 A linear problem

Consider the hyperbolic partial differential equation

$$\frac{\partial r}{\partial \theta_1} + \frac{\partial r}{\partial \theta_2} + r = -sin(\theta_1)sin(\theta_2) + cos(\theta_1)cos(\theta_2) + cos(\theta_1)sin(\theta_2), \tag{4.92}$$

with analytic solution $r = cos(\theta_1)sin(\theta_2)$. This corresponds to the case $p = 2$ and $q = 1$ in (4.53). Errors for orthogonal collocation with cubic Hermites and for the leap frog method are given in table 1 where the maximum error is taken over the mesh points. Here $r_c$ is the numerical solution for the collocation method and $r_{lf}$ is the numerical solution for the leap frog method.

| *Mesh Points* | *Orthogonal Collocation* $\|r - r_c\|_\infty$ | *Leap Frog* $\|r - r_{lf}\|_\infty$ |
|---|---|---|
| 20 | 1.76840D-05 | 7.56372D-03 |
| 30 | 3.51505D-06 | 3.27613D-03 |
| 40 | 1.12094D-06 | 1.91729D-03 |
| 50 | | 1.17820D-03 |
| 100 | | 3.01426D-04 |
| 200 | | 7.43552D-05 |

Table 4.1: A comparison of the error for the orthogonal collocation and the leap frog schemes.

The results in table 1 indicate that the orthogonal collocation and leap frog algorithms have convergence rates roughly $O(h^4)$ and $O(h^2)$, respectively.

### 4.3.2 Coupled oscillators

While a substantial amount of work has been done toward understanding free and forced dynamical behaviour of a single nonlinear oscillator, there has been recent interest in understanding the dynamics of coupled oscillators. Coupled oscillators arise in models of oscillating organic reactions, neural networks, intestinal waves and in numerous other problems in biology, physiology and chemistry.

Our second numerical example is a system of two-coupled nonlinear oscillators

$$\begin{pmatrix} \dot{x_1} \\ \dot{y_1} \\ \dot{x_2} \\ \dot{y_2} \end{pmatrix} = \begin{pmatrix} \alpha_1 x_1 + \beta_1 y_1 - (x_1^2 + y_1^2)x_1 - \delta(x_1 + y_1 - x_2 - y_2) \\ \alpha_1 y_1 - \beta_1 x_1 - (x_1^2 + y_1^2)y_1 - \delta(x_1 + y_1 - x_2 - y_2) \\ \alpha_2 x_2 + \beta_2 y_2 - (x_2^2 + y_2^2)x_2 + \delta(x_1 + y_1 - x_2 - y_2) \\ \alpha_2 y_2 - \beta_2 x_2 - (x_2^2 + y_2^2)y_2 + \delta(x_1 + y_1 - x_2 - y_2) \end{pmatrix}, \tag{4.93}$$

where $\delta \geq 0, \beta_1 > 0, \beta_2 > 0, \alpha_1 > 0$ and $\alpha_2 > 0$. Introducing the parametrization $x_i = r_i cos(\theta_i)$ and $y_i = -r_i sin(\theta_i)$, $i = 1, 2$ we get

$$\begin{pmatrix} \dot{\theta_1} \\ \dot{\theta_2} \\ \dot{r_1} \\ \dot{r_2} \end{pmatrix} = \begin{pmatrix} \beta_1 + \delta\{cos2\theta_1 - \frac{r_2}{r_1}[sin(\theta_1 - \theta_2) + cos(\theta_1 + \theta_2)]\} \\ \beta_2 + \delta\{cos2\theta_2 - \frac{r_1}{r_2}[sin(\theta_2 - \theta_1) + cos(\theta_1 + \theta_2)]\} \\ r_1(\alpha_1 - r_1^2) - \delta\{r_1(1 - sin2\theta_1) + r_2[sin(\theta_1 + \theta_2) - cos(\theta_1 - \theta_2)]\} \\ r_2(\alpha_1 - r_2^2) - \delta\{r_2(1 - sin2\theta_2) + r_1[sin(\theta_1 + \theta_2) - cos(\theta_1 - \theta_2)]\} \end{pmatrix}. \tag{4.94}$$

Each oscillator has a unique attracting periodic solution, and the uncoupled product system has a unique attracting invariant torus. The torus persists for a weak coupling and contains two periodic solutions when the coupling is linear and conservative. One of them occurs when the oscillators synchronize. It is stable and persists for all coupling strength. The other occurs when $\beta_1 = \beta_2$ and the oscillators are $\pi$ radians out of phase. It is unstable except on an open set in the frequency-coupling-strength plane and has a torus bifurcation. We refer to [ADO] for a motivation for the form of the coupling used in this example. We choose $\alpha_1 = \alpha_2 = 1.0$ and let $\delta$ be the bifurcation parameter. If the manifold $M = (\theta_1, \theta_2, r_1(\theta_1, \theta_2), r_2(\theta_1, \theta_2))$ denotes an invariant torus for the system then the uncoupled system has an invariant torus defined by $M_1 := (\theta_1, \theta_2, 1, 1)$. The stable periodic solution is defined by the sub-manifold $M_2 = (\theta, \theta, 1, 1)$ where $\theta = \theta_1 = \theta_2$. We will focus visually on the representation of the projections $r_1(\theta_1, \theta_2)$ and $r_2(\theta_1, \theta_2)$.

In our computations we use simple continuation in $\delta$. We use 40 equi-spaced mesh points in each direction and stop the Newton iteration when the maximum norm of the difference

between the two successive iterates is less than $10^{-8}$.

**case 1** $\beta_1 \neq \beta_2$.

The torus is computed using continuation from $\delta = 0$ using the known solution $M_1$ as the initial value. We choose $\beta_1 = 0.5$, $\beta_2 = 0.4$. The first continuation step size from $\lambda = 0$ is $\triangle\delta = 0.20$. We then take continuation steps with $\triangle\delta = 0.010$ until reaching $\delta = 0.220$. The resulting cross-sections $r_1(0, \theta_2)$ and $r_2(0, \theta_2)$ are shown in figures 4.1 and 4.2, respectively. We also show the results for some intermediate values of $\delta$ between 0 and the first continuation step mentioned above.

**case 2** $\beta_1 = \beta_2$.

In this case, the following symmetries on the torus can be directly verified from equation (4.93):

- $r_1(\theta_1, \theta_2) = r_2(\theta_2, \theta_1)$;
- $r_1(\theta_1, \theta_2) = r_1(\theta_1 + \pi, \theta_2 + \pi)$;
- $r_2(\theta_1, \theta_2) = r_2(\theta_1 + \pi, \theta_2 + \pi)$.

Given $r_1^0(\theta_1, \theta_2)$, we use the first symmetry condition above to get $r_2^0(\theta_1, \theta_2)$ and solve the equation

$$\sum_{i=1}^{2} f_i(r_1^0, r_2^0, \theta_1, \theta_2)\frac{\partial r_1^1}{\partial \theta_i} + c^0(r_1^0, r_2^0, \theta_1, \theta_2) = b^0(r_1^0, r_2^0, \theta_1, \theta_2), \tag{4.95}$$

for $r_1^1(\theta_1, \theta_2)$ and then obtain $r_2$ from the symmetry condition. We choose the parameter value $\beta_1 = \beta_2 = 0.55$ which is the one used in [DB] [DLR]. The first continuation step from $\lambda = 0$ is $\triangle\delta = 0.255$, and subsequent continuation steps $\triangle\delta = 0.001$ are used until $\delta = 0.258$. The cross-sections $\mathbf{r}_1(0, \theta_2)$ and $\mathbf{r}_2(0, \theta_2)$ are shown in figures 4.3 and 4.4, respectively. For this example, the unstable periodic solution lies on the sub-manifold $M_3 = (\theta, \theta + \pi, r, r)$, where $r = r_1 = r_2$. These computations are very sensitive to the distribution of the mesh. An important feature is that the torus begins to lose smoothness and $r_1(\theta_1, \theta_2)$ and $r_2(\theta_1, \theta_2)$ start to develop cusp on them as the parameter $\delta$ increases (see figures 4.5, 4.6,4.13, 4.14, 4.15 and 4.16). Indeed, it is easy to obtain spurious solution behaviour when one considers a non-equal mesh distribution on a fixed grid. In one case, the tori were calculated up to $\delta = 0.264$ with apparent success until it is observed that key intrinsic properties of the tori are not satisfied.

### 4.3.3 Adaptive method

In this section we introduce an adaptive scheme which refines the mesh around the cusp for case 2 ($\beta_1 = \beta_2$), allowing us to follow the branch of the tori close to the torus breakdown. The idea is to map the trace of the cusp to the $\theta_1$-axis and then redefine the mesh in the $\theta_2$ direction, refining near $\theta_2 = 0$ and $2\pi$. To illustrate the method, consider the equation

$$f_1(\theta_1,\theta_2)\frac{\partial r}{\partial \theta_1} + f_2(\theta_1,\theta_2)\frac{\partial r}{\partial \theta_2} = g(\theta_1,\theta_2), \tag{4.96}$$

$$(\theta_1,\theta_2) \in S^2 := [0,2\pi]\times[0,2\pi].$$

Let the function $\theta_2 = p(\theta_1)$ be the trace of the cusp in $(\theta_1,\theta_2)$-plane and $\Omega$ be defined as

$$\Omega := \{(\theta_1,\theta_2) \mid p(\theta_1) \le \theta_2 \le 2\pi + p(\theta_1);\ 0 \le \theta_1 \le 2\pi\}.$$

The mapping $H : S^2 \longrightarrow \Omega$ is defined by

$$\begin{aligned} \psi &= \theta_1 \\ \xi &= \theta_2 - p(\theta_1), \end{aligned} \tag{4.97}$$

and we have

$$\begin{aligned} \frac{\partial r}{\partial \theta_1} &= \frac{\partial r}{\partial \psi}\frac{\partial \psi}{\partial \theta_1} + \frac{\partial r}{\partial \xi}\frac{\partial \xi}{\partial \theta_1} = r_\psi - r_\xi p'(\theta_1), \\ \frac{\partial r}{\partial \theta_2} &= \frac{\partial r}{\partial \psi}\frac{\partial \psi}{\partial \theta_2} + \frac{\partial r}{\partial \xi}\frac{\partial \xi}{\partial \theta_2} = r_\xi. \end{aligned}$$

The PDE (4.96) in terms of the new variables $(\psi,\xi)$ is rewritten as

$$f_1\frac{\partial r}{\partial \psi} + [f_2 - f_1 p'(\psi)]\frac{\partial r}{\partial \xi} = g. \tag{4.98}$$

The construction of the trace $\theta_2 = p(\theta_1)$ is done as follows: We choose a constant $E_0 > 0$ such that if

$$max_{\{\theta_1^i,\theta_2^j\}}|\frac{\partial r}{\partial \theta_2}| > E_0 \quad i = 1,\ldots,N_1, \quad j = 1,\ldots,N_2, \tag{4.99}$$

then we need to construct the trace of the cusp; otherwise, we can assume the torus is smooth and the construction is unnecessary. To construct the trace, we only need to define $p(\theta_1^i)$ for $i = 1,\ldots N_1$. For some fixed $\theta_1^i$, let $\bar{\theta}_1^i$ be an extreme point satisfying

$$|\frac{\partial r}{\partial \theta_2}(\theta_1^i,\bar{\theta}_2^i)| = \max_j |\frac{\partial r}{\partial \theta_2}(\theta_1^i,\theta_2^j)| \tag{4.100}$$

and

$$p(\theta_1^i) = \bar{\theta}_2^i \text{ if } |\frac{\partial r}{\partial \theta_2}(\theta_1^i, \bar{\theta}_2)| > E_0, \text{ else } p(\theta_1^i) \text{ is undefined.} \quad (4.101)$$

We define $p(\theta_1)$ as the smooth periodic spline interpolation of the defined values of $p(\theta_1^i)$ in (4.101). Equation (4.99) is tested at each continuation step to check the smoothness of the torus. The torus is nonsmooth or the cusp occurs only when (4.99) is satisfied. In this case, the mesh is redistributed such that more points are near the cusp.

With a $40 \times 40$ mesh we are able to reach $\delta = 0.2601$ with this strategy for $\beta_1 = \beta_2 = 0.55$ (see figure 4.5 and 4.6). For the same values Moore [M] get results up to $\delta = 0.255$ using the continuation step $\triangle\delta \geq 0.001$. His approach uses the fact that the projection of the vector field at any point on the torus in the normal direction is zero. His results are close to our results. Again our results are the same as the results of Hadamard graph transform method of Edoh and Russell [ER2] (see figures 4.5, 4.6, 4.9 and 4.10). Dieci and Bader [DB] get results up to $\delta = 0.2627734375$ using multigrid methods with $320 \times 320$ mesh. However, it is noted that for higher values of $\delta$ our results differ from those of Dieci [BD]. Our results seems to be reliable since they satisfy some properties of the differential equation for all values of $\delta$. In figures 4.7 and 4.8 we see that our results for the final two values of $\delta$ for the adaptive scheme satisfy the conditions that the radii $r_1$ and $r_2$ of the stable and unstable periodic solutions on the torus are the same at $\theta_2 = 0$ and $\pi$ on the cross-section $\theta_1 = 0$. *i.e.*

- $r_1(0,0) = r_2(0,0)$,
- $r_1(0,\pi) = r_2(0,\pi)$.

In figures 4.11 and 4.12 we show the cross-sections $r_1(0,\theta_2)$ and $r_2(0,\theta_2)$, respectively, for different values of $\delta$ and $\beta_1 = \beta_2 = 0.50$. The bifurcation diagram for this parameter value is shown in [ADO]. At $\delta = 0.245$ a third periodic solutions which is not on the torus begins to bounce back and forth from the torus. The influence of this periodic solution might have caused the invariant circles to begin to cross one another at $\delta \approx 0.24$. In [HDER] simulations with AUTO shows that there is a saddle-node like bifurcation between the unstable orbit on the torus and two other periodic solutions that were off the torus at $\delta \approx 0.2605$. This may well explain why the invariant circles begin to cross one another at around $\delta \approx 0.255$ (see figures 4.5 and figure 4.6. Figures 4.13-4.16 show how far the torus has deformed at $\delta = 0.2601$.

### 4.3.4 van der Pol equation

When the PDE approach was tried on this problem as in the HGT method we were only able to compute the torus for the parameter value $\kappa = 0.38$.

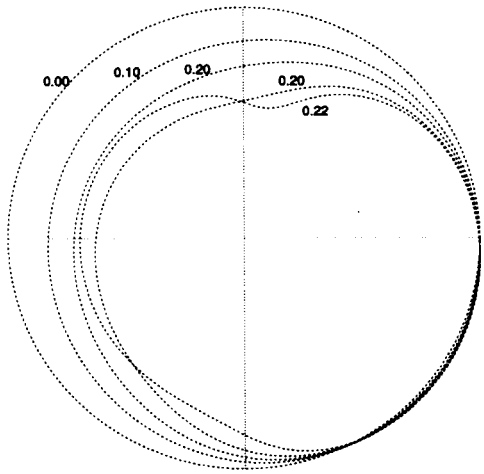


Figure 4.1: The cross-section $r_1(0, \theta_2)$ with $\delta$ as shown above for $\beta_1 = 0.50$, $\beta_2 = 0.4$ and $\alpha_1 = \alpha_2 = 1.0$ using 40 mesh points.

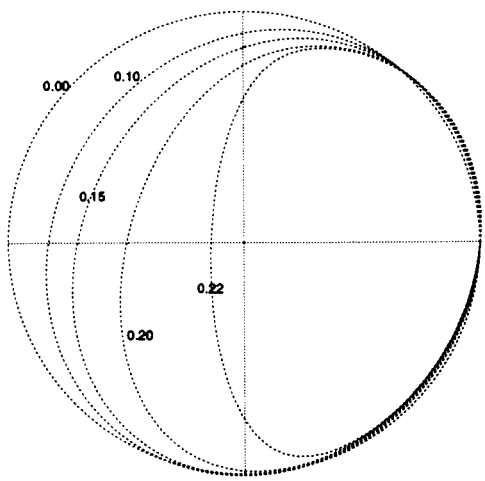


Figure 4.2: The cross-section $r_2(0, \theta_2)$ with $\delta$ as shown above for $\beta_1 = 0.50$, $\beta_2 = 0.4$ and $\alpha_1 = \alpha_2 = 1.0$ using 40 mesh points.

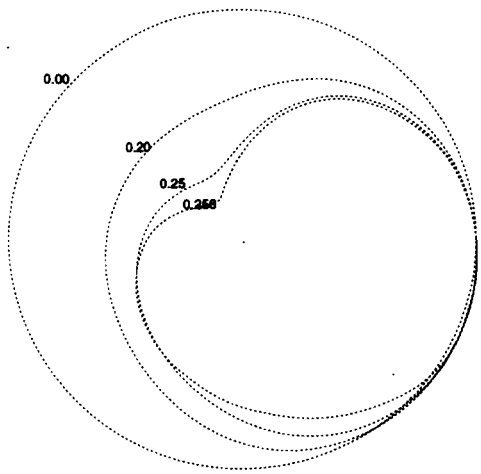


Figure 4.3: The cross-section $r_1(0, \theta_2)$ with $\delta$ as shown above for $\beta_1 = \beta_2 = 0.55$ *and* $\alpha_1 = \alpha_2 = 1.0$ using 40 mesh points.

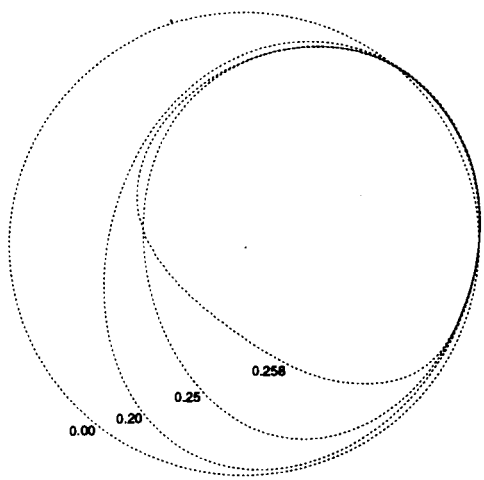


Figure 4.4: The cross-section $r_2(0, \theta_2)$ with $\delta$ as shown above for $\beta_1 = \beta_2 = 0.55$ *and* $\alpha_1 = \alpha_2 = 1.0$ using 40 mesh points.

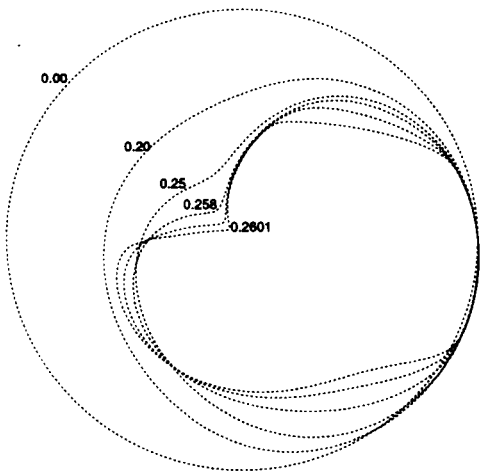


Figure 4.5: The cross-section $r_1(0, \theta_2)$ with $\delta$ as shown above for $\beta_1 = \beta_2 = 0.55$ *and* $\alpha_1 = \alpha_2 = 1.0$ using 40 mesh points with the adaptive scheme.

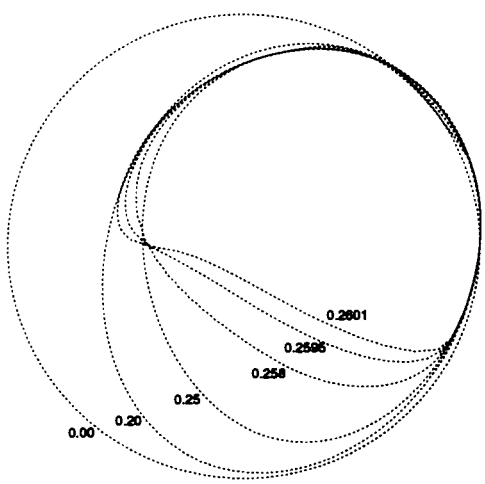


Figure 4.6: The cross-section $r_2(0, \theta_2)$ with $\delta$ as shown above for $\beta_1 = \beta_2 = 0.55$ *and* $\alpha_1 = \alpha_2 = 1.0$ using 40 mesh points with the adaptive scheme.

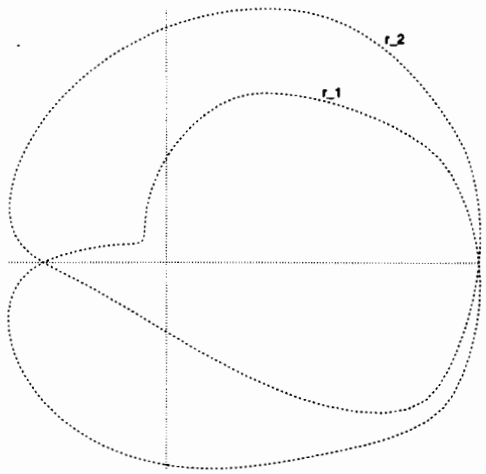


Figure 4.7: The cross-section $r_1(0,\theta_2)$ and $r_2(0,\theta_2)$ with $\beta_1 = \beta_2 = 0.55$ $\delta = 0.2595$ and $\alpha_1 = \alpha_2 = 1.0$ using 40 mesh points with the adaptive scheme.

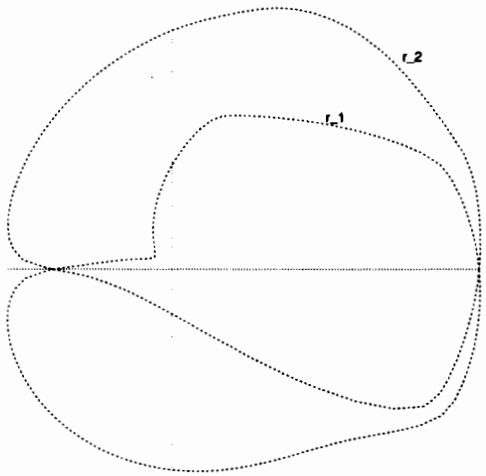


Figure 4.8: The cross-section $r_1(0,\theta_2)$ and $r_2(0,\theta_2)$ with $\beta_1 = \beta_2 = 0.55$, $\delta = 0.2601$ and $\alpha_1 = \alpha_2 = 1.0$ using 40 mesh points with the adaptive scheme.

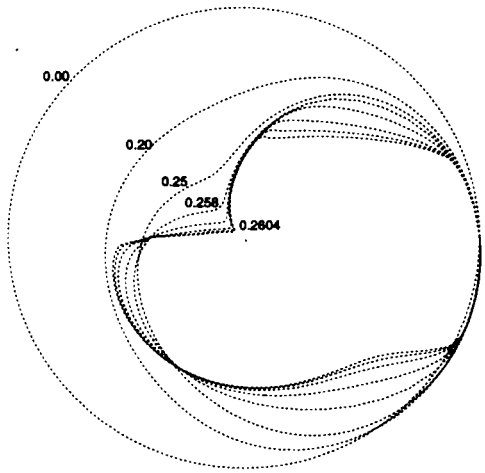


Figure 4.9: The cross-section $r_1(0, \theta_2)$ with $\delta$ as shown above for $\beta_1 = \beta_2 = 0.55$ and $\alpha_1 = \alpha_2 = 1.0$ using 40 mesh points with the method in [ER2].

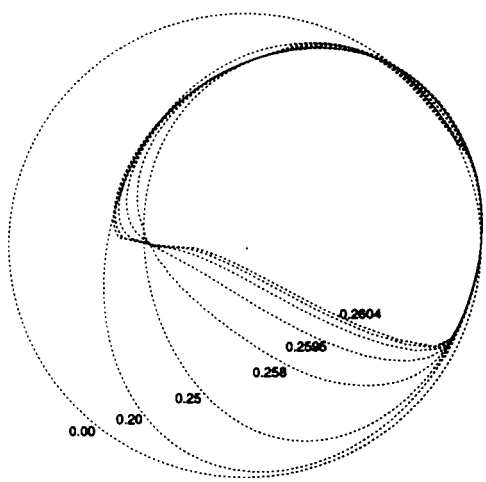


Figure 4.10: The cross-section $r_2(0, \theta_2)$ with $\delta$ as shown above for $\beta_1 = \beta_2 = 0.55$ and $\alpha_1 = \alpha_2 = 1.0$ using 40 mesh points with the method in [ER2].

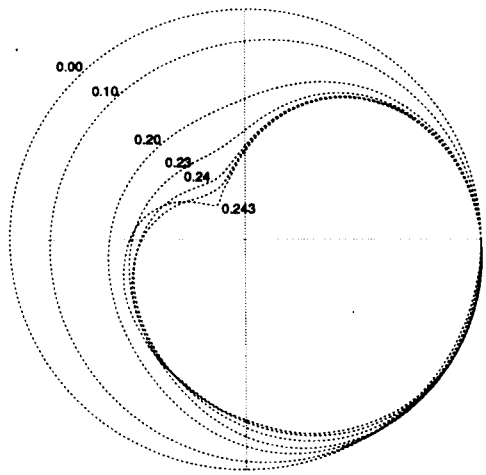


Figure 4.11: The cross-section $r_1(0, \theta_2)$ with $\delta$ as shown above for $\beta_1 = \beta_2 = 0.50$ and $\alpha_1 = \alpha_2 = 1.0$ using 40 mesh points with the adaptive scheme.

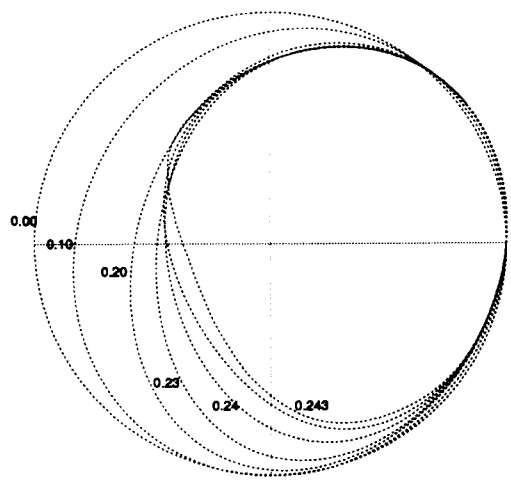


Figure 4.12: The cross-section $r_2(0, \theta_2)$ with $\delta$ as shown above for $\beta_1 = \beta_2 = 0.50$ and $\alpha_1 = \alpha_2 = 1.0$ using 40 mesh points with the adaptive scheme.

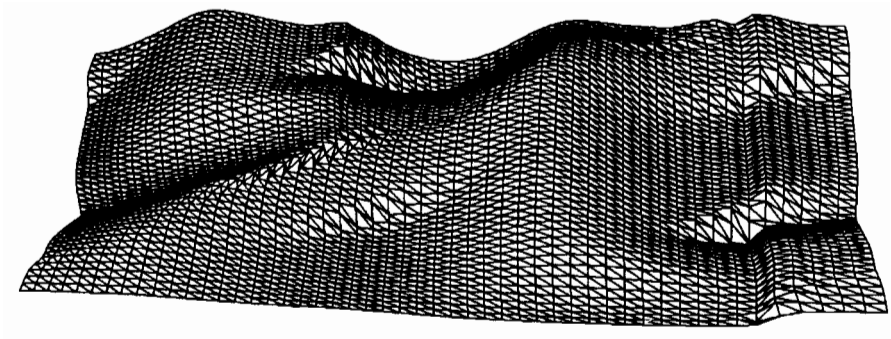

Figure 4.13: The flat surface of the torus $r_1(\theta_1, \theta_2)$ for $\delta = 0.2601$ with $\beta_1 = \beta_2 = 0.55$ and $\alpha_1 = \alpha_2 = 1.0$. where $\theta_1$ is in the horizontal direction and $\theta_2$ in the vetical direction.

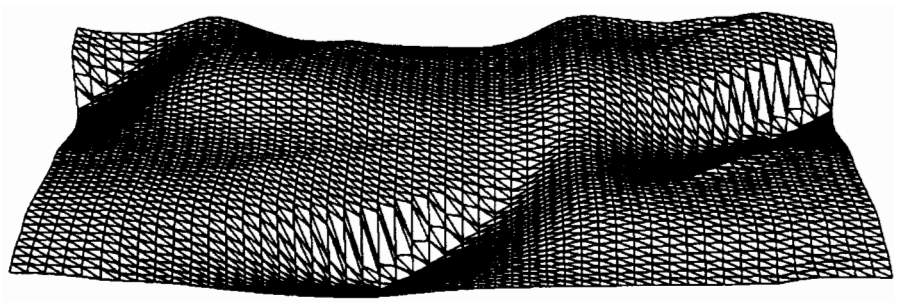

Figure 4.14: The flat surface of the torus $r_2(\theta_1, \theta_2)$ for $\delta = 0.2601$ with $\beta_1 = \beta_2 = 0.55$ and $\alpha_1 = \alpha_2 = 1.0$. where $\theta_1$ is in the horizontal direction and $\theta_2$ in the vetical direction.

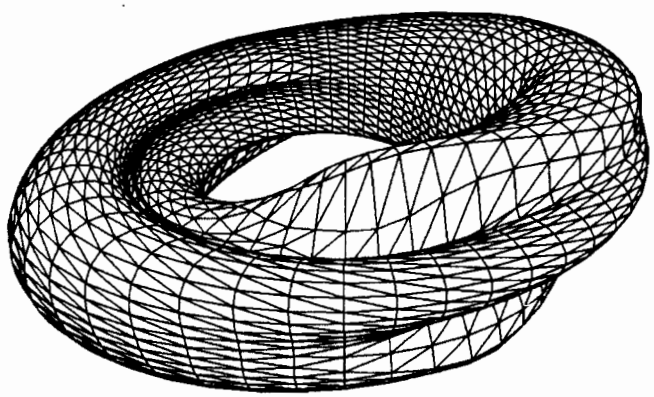

Figure 4.15: The torus $r_1(\theta_1, \theta_2)$ for $\delta = 0.2601$ with $\beta_1 = \beta_2 = 0.55$ and $\alpha_1 = \alpha_2 = 1.0$.

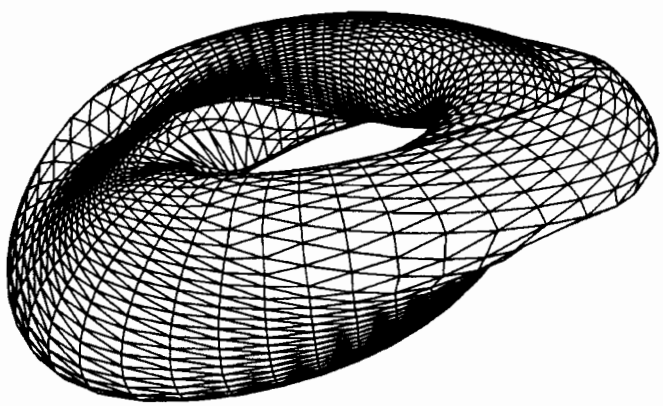

Figure 4.16: The torus $r_2(\theta_1, \theta_2)$ for $\delta = 0.2601$ with $\beta_1 = \beta_2 = 0.55$. and $\alpha_1 = \alpha_2 = 1.0$.

# Chapter 5

# Comparison of the HGT and PDE methods and torus visualization

In this chapter we make a comparison between the HGT method and the PDE method. We also give a review of recent developments in the application of visualization to mathematics. We show how visualization can be used to help explain the breakdown mechanism of an invariant torus.

## 5.1 Comparison of the methods

In this section we compare the Hadamard graph transform approach with the Partial differential equation approach. We make a comparison of their speed, the errors, the robustness, and some special features of each of the methods.

In the computation of invariant tori, most numerical schemes depends on the attractivity of the torus. The HGT scheme has this dependence too. It only works for attracting and repelling invariant tori. However, the numerical scheme of the PDE approach for example, the collocation scheme does not depend on the attractivity of the torus. So the collocation scheme is applicable to a wider class of invariant tori in this sence than the HGT scheme.

The collocation scheme is be easily modified to determine the solution at any point on the torus once the solution at the mesh points and their derivatives have been computed. On the other hand, one will have to find an interpolation scheme to determine the solution at a point on the torus from the computed solution at the mesh points when using the

Hadamard graph transform approach.

The collocation scheme has $O(h^4)$ convergence rate as compared to the HGT method whose convergence depend on the attractivity of the torus and the interpolations scheme. Both numerical schemes are parallelizable. The boundary value problems of the HGT method can be solved simultaneously while the linear system in the PDE method also can be solved by parallel solvers.

Invariant submanifolds on the torus do influence the computations of the torus. It is easier to modify the HGT program to adaptively distribute mesh points around the invariant submanifold than the collocation method.

Both methods can be extended to compute a higher dimesional torus. iA bad choice of the crosssection to be computed in the HGT method can lead to singularities.

| *Number of points* | *The collocation method* | *HGT method* |
|---|---|---|
| 10 | 229.240 | 43.0 |
| 15 | 1211.170 | 85.8 |
| 20 | 5084.110 | 140.3 |
| 25 | 10593.700 | 207.3 |
| 30 | 20910.800 | 283.6 |
| 35 | 38153.300 | 368.1 |
| 40 | 68778.300 | 460.1 |
| 45 | | 470.4 |
| 50 | | 691.9 |
| 100 | | 2550.8 |

Table 5.1: The cpu for the HGT and the PDE methods for a system of coupled oscillators

The results in table (5.1) show that the HGT method uses less cpu than the PDE method. In some cases when the torus is exponentially attracting the HGT method takes far lesser cpu time to converge than PDE scheme.

## 5.2 Visualization

Visualization is basically trying to give some meaning in a set of data. It can be defined as the study, the development, and the use of graphic representations and supporting techniques that facilitate the visual communication of knowledge - that make computer images speak to us [KK1]. Those who benefit from the construction and viewing of an image of data include:

geologists, physicists, engineers, medical doctors, physiologists, mathematicians etc. And visualization specialists include among others computer scientists, system analysts, artists, computer graphics programmers and designers. In the past, commercial advertising has used graphics representation to sell out products and now scientists are beginning to use it to support their research.

A general approach for doing visualization work on a data set is to have a goal and then find a visualization techniques to achieve that goal. Sometimes the goal can be misleading or it can used to carry false information.

### 5.2.1 Visualization in dynamical systems

Analysis and numerical simulation have been the usual tools in understanding dynamical systems. For example, numerical computations have provided inspiration for many significant discoveries about dynamical systems. Nonetheless, it is often difficult to directly compute and understand interesting aspects of the dynamics of the dynamical system. In recent years numerical analysis, symbolic computations, visualization, and the design interface that facilitate interactive exploration of the behavior of a system all have contributed to the study of dynamical systems. One can thus say that computer graphics has proven to have the potential to be an effective tool in the qualitative development of dynamical systems. Powerful desktops facilitate the development of more sophisticated tools in the exploration of more complex systems.

The power of visualization in dynamical systems theory is dated as far back to Poincaré when he introduced geometry into the study of differential equations. Some recent developments are in the theory of fractals, where the complexities of fractals objects are explained using computer graphics. Observers and researchers in this area have become excited over similarities between the properties of such sets and those of naturally occurring phenomena, such as growing plants, clouds, and coastlines. One application of fractals with computer graphics is in roadways where it has been used to analyze and compress images of roadway cracks. Further development in this area could lead to ways of, enabling highway authorities to schedule repair programs more efficiently and to smoother travel for us all.

In general, one can see that analysis alone is not sufficient to explain the intricate behavior of dynamical systems. With the presence of "cheap" computer power one can use numerical simulations, computations and computer graphics to formulate new hypotheses and conjectures.

Some recent mathematical software that have been used in the study of dynamical systems are DYNPAQ, KAOS, AUTO [DK], DSTOOL and XPPAUT. AUTO is a software for the continuation and bifurcation problems in ODEs. DSTOOL finds solutions of dynamical systems and computes properties of solutions of dynamical systems like the Lyapunov exponents etc. XPPAUT is a tool for modeling dynamical phenomena. These software packages are capable of handling systems with simple invariant manifolds like fixed points, periodic solutions, and connecting orbits (homo/heteroclinic) etc.

We now focus our attention on the computation and visualization of invariant manifolds. Much work has been done on the study of fractals, connecting orbits and fixed points (the trivial case). The rich mathematics of invariant tori is yet to be observed, using numerics and graphics tools. In our study of invariant tori we realised that numerical results are not sufficient to gain a full understanding of the behavior. In this case, visualization is essential to gain a qualitative understanding and to generate hypotheses which can be scrutinized by other methods (analysis, numerics). An early example of the application of computer graphics to the study of invariant tori is the work by Baxter et al [BES]. A much more sophisticated application of computer graphics is given by Kocak et al [KBBL].

We have seen that there is a need to develop a software that can simulate an invariant torus and bridge the gap in the bifurcation sequence from a fixed point through a periodic solution and then to an invariant torus and finally to a chaotic attractor (possibility). Our aim thus is to develop a package that can be used to follow a bifurcation sequence up to an invariant tori and then compute its essential features and properties. This package will include a graphical tool that can be used to visualize projections of the torus in two and three dimensions. We hope to help researchers to study and to understand the breakdown process of the invariant tori.

So far we have used visualization to gain a qualitative understanding of the breakdown of an invariant torus in some specific examples. It has allowed some key features of the torus to be determined. An example is the invariant torus in a system of two coupled oscillators by Hepting et al. [HDER1], [HDER2], [EHR]. Computer graphics have been very useful in this case. The 3-dimensional projections of the 4-dimensional torus has helped us to partly understand the breakdown process. We hope to follow the torus to complete breakdown.

Below are some diagrams of a 3-dimensional projections of an invariant tori of 2-coupled oscillators using Computer Graphics.

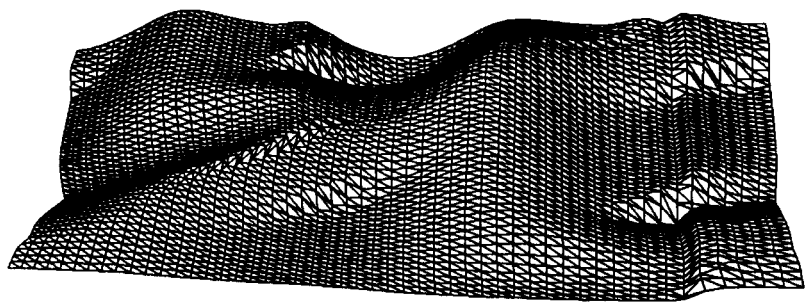

Figure 5.1: The flat surface of the torus $r_1(\theta_1, \theta_2)$ for $\delta = 0.2601$ and $\beta_1 = \beta_2 = 0.55$. where $\theta_1$ is in the horizontal direction and $\theta_2$ in the vetical direction.

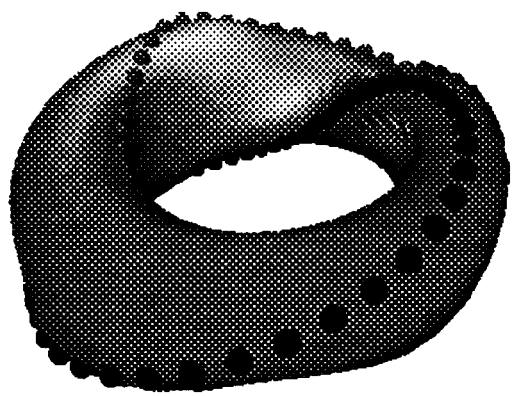

Figure 5.2: The torus $r_2(\theta_1, \theta_2)$ for $\delta = 0.2601$ and $\beta_1 = \beta_2 = 0.55$.
The black and light dots on the torus indicate the stable and unstable periodic solutions respectively.

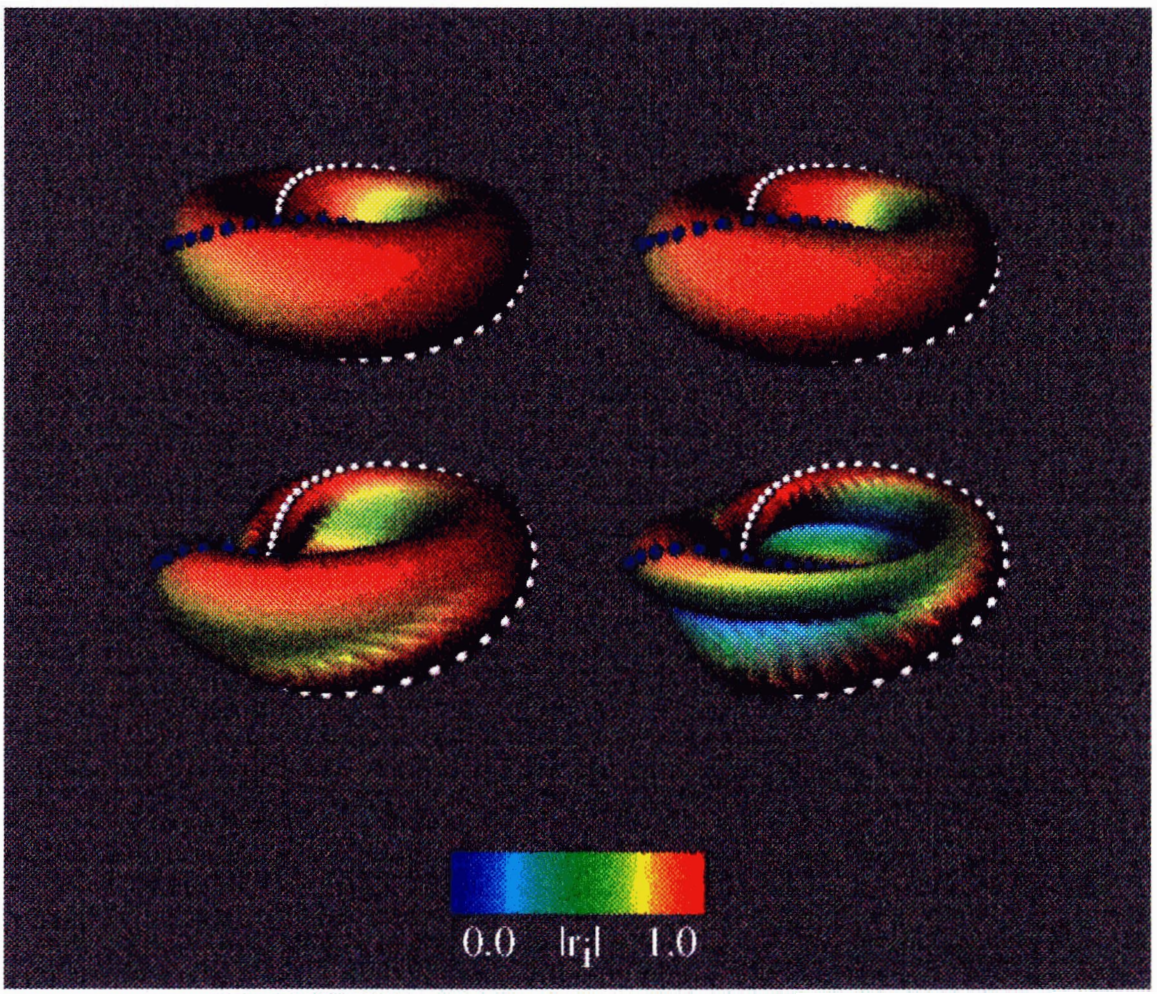


Figure 5.3: The two tori, $r_1(\theta_1, \theta_2)$ and $r_2(\theta_1, \theta_2)$, for $\beta = 0.55$. At the top are displayed the tori representing the invariant torus for $\delta = 0.20$ and at the bottom are the tori representing the invariant torus for $\delta = 0.26$.

# Chapter 6

# Conclusions

In this thesis, we have been concerned with the analytical and the computational study of invariant manifolds in dissipative dynamical systems in both finite and infinite dimensional systems. Much of the work is on the computation of these manifolds and on the convergence of the numerical schemes in finite dimensional systems. The eventual goal is to obtain algorithms for computing invariant manifolds in both finite and infinite systems. We want to include these algorithms in existing software for the determination of solutions and bifurcations of dynamical systems. We also looked at the smoothness and the invariance of the calculated invariant manifolds and studied the structural stability of our system under variation of a bifurcation parameter.

The invariant manifolds that we considered are invariant circles and tori. We did not study the computations of these invariant manifolds in Hamiltonian systems since the behavior of quasi-periodic solutions in this case is well understood. We did some theoretical work on the integral representation of invariant manifolds. Three methods are discussed, two of which we investigated numerically in this thesis. We look at the center manifold theory and realised that the graph of the center manifold and of the stable (unstable) manifolds all solve a first order quasi-linear PDE. Since the graph of the invariant circles and tori also solves a first order quasi-linear PDE, we hope to extend the numerical algorithms for the computation of invariant circles and tori to that of center (stable and unstable) manifolds.

We considered two algorithms for computing invariant circles and tori. The first is the PDE approach for the computation of invariant manifolds of autonomous finite dimensional systems ODEs. In this approach these PDEs arise because the invariant surface can be described as a graph of a function which has to satisfy the ODE system. The PDEs that

we obtained are first order hyperbolic systems with the same principal part. We focussed attention on the discretization schemes for the PDEs and solved these discretized equations by using orthogonal collocation. This high order scheme have improved our results as we compare it to the results of some low order schemes. We prove convergence and stability of the collocation scheme for a model problem with constant coefficients. We show that our method is independent of the attractivity of the torus. The high order convergence of our method depends on the smoothness of the torus (geometry). We introduce an adaptive grid refinement scheme in some of the problems to allow for continuation close to the actual point of torus bifurcation.

In the second approach we introduce a method based on the Hadamard graph transform technique of Fenichel. We use the fact that the torus can be defined implicitly by an invariant circle under the Poincaré map. We use this method to compute the invariant circle for maps as well as the Poincaré map of an invariant torus. This reduces the complexity of computing the torus in the regions of parameter values for which the torus begins to break down and where things also begin to be interesting. We show how this method relates to the Poincaré map approach of van Veldhuizen. This method can be easily parallelized.

For my future work, I plan to improve upon these numerical issues and hope to:

1. remove the restriction we have on the parametrization in the PDE approach,
2. apply these programs to a large variety of problems to see how robust they are,
3. find better ways to solve the sparse linear system in the PDE approach,
4. compute some three dimensional tori,
5. extend our programs to systems in infinite dimension,
6. modify the programs to compute center, stable and unstable invariant
7. use collocation to solve the BVP in the HGT method. manifolds.

# Bibliography


[ACHM] Aronson D.G., Chory M.A., Hall G.R. and McGehee R.P., *Bifurcation from an invariant circle for two parameter families of maps of the plane: a computer-assisted study, Comm. Math. Phys., 83, pp. 303-354, 1982.*

[ADO] Aronson D.G., Doedel E.J. and Othmer, H.G., *An analytical and numerical study of the bifurcations in a system of linearly-coupled oscillators, Physica 25D, pp. 20-104, 1987.*

[AMR] Ascher U.M., Mattheij R.M.M. and Russell R.D., *Numerical Solution of Boundary Value Problems for Ordinary Differential Equations, Prentice Hall, New Jersey, 1988.*

[BES] Baxter R., Eiserike H. and Stokes A., *A pictorial study of an invariant torus in phase space of four dimensions. In Weiss L., editor, Ordinary Differential Equations, 1971 NRL-MRC Conference, Academic press, pp. 331-349, 1972.*

[BV] Babin A.V. and Vishik M.I., *Attractors of evolution equations, Studies in mathematics and its applications, editors Lions J.L., Papanicolaou G., Fujita H. and Keller H.B. Elsevier science publishers, Netherlands, 1989.*

[C] Carr J., *Application of Center Manifold Theory. Springer- Verlag, New York, 1981.*

[CH] Chow S.N. and Hale J.K., *Methods of Bifucation Theory, Springer-Verlag, New York, 1982.*

[DB] Dieci L. and Bader G., *Solution of the system associated with to invariant tori approximation. II: multigrid methods, SIAM J. Sci. Comp. 15, pp 1375-1400, 1994.*

[DK] Doedel E.J, and Kernevez J.P., *AUTO : Software for the Continuation and Bifurcation Problems in ODEs, Applied Math. Technical Report, Cal. Inst. of Technology, 1986.*

[DL1] Dieci L. and Lorenz J., *Block M-matrices and computation of invariant tori, SIAM Journal Sci. Stat. Comp., 13, pp. 885-903, 1992.*

[DL2] Dieci L. and Lorenz J., *Computation of invariant tori by the method of characteristics, to appear in SIAM J. Numer. Anal., 32, 1995.*

[DLR1] Dieci L., Lorenz J. and Russell R.D., *Numerical calculation of invariant tori. SIAM J Sci. Stat. Comp. 12, pp. 607-647, 1991.*

[DLR2] Dieci L., Lorenz J. and Russell R.D., *Decoupling of dynamical systems using boundary value techniques. LCCR Technical Report.*

[DS] de Boor C. and Swartz B., *Collocation at Gaussian points, SIAM J. Numer. Anal. 10, pp. 582-606, 1973.*

[ER] Edoh K.D. and Russell R.D., *Numerical approximation of and invariant circles. Proceeding of the fifth International Conference on Scientific Computing, Ada Jane Press Nigeria (ltd) pp 27-31 1994.*

[ER1] Edoh K.D. and Russell R.D., *An Algorithm for Computing Invariant Circles. In preparation.*

[EHR] Edoh K.D., Hepting D. and Russell R.D., *Visualization as a qualitative tool for the computation of invariant tori. Presented at '3rd SIAM Conf. on Application of Dynamical Systems, Utah, may 21-24, 1995.*

[ERS] Edoh K.D. Russell R.D. and Sun W., *Numerical Approximation of Invariant Tori Using Orthogonal Collocation, submitted SIAM Jour. Sci. Comp.*

[F] Fenichel N., *Persistence and smoothness of invariant manifolds for flows, Indiana Univ. Math. J. 21, pp. 193-226, 1971.*

[F1] Finlayson B.A., *The method of weighted residuals and variational principles, Academic press, New York, 1972.*

[GH] Guckenheimer J. and Holmes P., *Nonlinear Oscillations, Dynamical Systems and Bifurcation of Vector Fields, Springer Verlag, New York, 1983.*

[HJ] Hale J.K., *Ordinary differential equations. Wiley-Interscience John Wiley and Sons, New York, 1969.*

[HDER1] Hepting D.H., Derks G., Edoh K.D. and Russell R.D., *A visual Analysis of Invariant Tori. Western Computer Graphics Symposium, Banff, Canada, March 1995.*

[HDER2] Hepting D.H., Derks G., Edoh K.D. and Russell R.D., *Case Study: Qualitative Analysis of Invariant Tori as Qualitative Tool in a Dynamical Systems. To be presented at "Visualization 1995".*

[HKW] Hassard B.B., Kazarinoff N.B. and Wan Y.H., *Theory and applications of Hopf bifurcationi, Cambridge University Press, Cambridge, New York, 1981.*

[IO] Iooss G., *Bifurcation of maps and applications. Math studies, 36, North-Holland, 1979.*

[KASP] Kevrekidis I.G., Aris R., Schmidt L.D. and Pelican S., *Numerical computation of invariant circles of maps. Physica 16D, pp. 243 - 251, 1985.*

[KK1] Keller P.R. and Keller M.M., *Visual Cues: Practical Data Visualization, Manning Publications Co., Greenwich, 1993.*

[KUW] Karlheinz G., Ulrich P. and Werner L., *Comparison of Different Methods for Computing Lyapunov Exponents, Progress of Theoretical Physics, 83, no 5, 1990.*

[L] Langford W.F., *Numerical Studies of Torus Bifurcations, International Series of Numer. Maths, Vol 70, Birkhauser Verlag Basel, 1984.*

[LP] Lapidus L. and Pinder G., *Numerical solutions of partial differential equations in science and engineering, Wiley, New York, 1982.*

[M] Moore G., *Computation and parametrization of invariant curves and tori, submitted to SIAM. J. Numer. Anal. 1994.*

[MCT] Matsumoto T., Chua L.O. and Tokunaga R., *Choas Via Torus Breakdown, IEEE Transactions On Circuits and Systems, Vol CAS-34, No 3, pp. 240- 253, 1987.*

[MM] Marsden J.E. and McCracken M., *The Hopf Bifurcation and Its Applications, Applied Mathematical Science, 19, Spring-Verlag New York Inc, 1976.*

[PR] Prenter P.M. and Russell R.D., *Orthogonal Collocation for Elliptic Partial Differential Equations, SIAM J., Numer. Anal. 13, No. 6, pp 923-939, 1976.*

[PW] Percell P. and Wheeler M.F., *A $C^1$ finite element collocation method for elliptic equations, SIAM J. Numer. Anal. 17, pp. 605-622, 1980.*

[S] Sacker R., *A new approach to the perturbation theory of invariant surfaces, Comm. Pure Applied Math., 18, pp. 717-732, 1965.*

[Sc] Schumaker L.L., *Spline Functions: Basic Theory, John Wiley & Sons, New York, etc., 1981.*

[SM] Scheurle J. and Marsden J., *Bifurcation to quasiperiodic tori in the interaction of steady-state and Hopf bifurcation. Preprint, Berkeley, Calif. 1982.*

[RS] Russell R.D. and Sun W., *Spline collocation differentiation matrices, Department of Mathematics and Statistics, Reseach Report No. 94-08, Simon Fraser University.*

[RT] Ruelle D. and Takens F., *On the nature of turbulence. Comm. Math. Phys., 20, pp. 167-192, 1971.*

[SG] Swinney H.L. and Gollub J.P., (ED) *Hydrodynamic Instabilities and the Transition to Turbulence, Springer-Verlag, 1985.*

[TR] Temam R., *Some Recent Results on Infinite Dimensional Dynamical Systems in "Turbulence in Fluid Flows A Dynamical System Approach" by Sell R.G., Foias C., and Temam R., The IMA voluems in Mathematics and its Applications, vol 55, Springer-Verlag, 1993.*

[VV1] Van Veldhuizen M., *A new algorithm for the numerical approximation of an invariant curve, SIAM J. Sci. Stat. Comp. 8, pp. 951-962, 1987.*

[VV2] Van Veldhuizen M., *Convergence results for invariant curve algorithms, Math. Comp. 51, pp. 677-697, 1987.*

[Wi] Wiggins S., *Introduction to Applied Nonlinear Dynamical System and Chaos, Springer-Verlag, New York Inc, 1990.*

[W] Wright S J., *Stable parallel algorithms for two-point boundary value problems, SIAM J. Sci Stat. Comput., 13, pp. 742-746, 1992.*